Development of a Coating Formulation Procedure for Ni-base Shielded Metal Arc Electrodes with Varying Core Wire Composition

THESIS

Presented in Partial Fulfillment of the Requirements for the Degree Master of Science in the Graduate School of The Ohio State University

By

Brian Gaal

Graduate Program in Welding Engineering

The Ohio State University

2012

Master's Examination Committee:

John Lippold, Advisor and Stanislav Rokhlin

Abstract

In order for manufacturers of shielded metal arc welding (SMAW) electrodes to stay competitive, they must be able to have flexibility in the performance of their products, as well as flexibility in the manufacturing process. Nickel base welding consumables often require specialized chemical compositions which are more stringent than the requirements for the base material on which they are welded. To complicate this problem further, the core wire chemistry often has a target which is a different chemical composition, and different manufacturers may not have the same target composition. To compensate for these variances, alloying elements are often added through the flux coating to adjust the weld deposit composition. Understanding how these additions to the flux coating will affect the weld deposit is critical to the manufacturing process.

This work examines two common types of nickel base SMAW electrodes, ENiCrMo-4 and ENiMo-10. Both were manufactured with a baseline coating which did not contain any alloying elements. Then using the same heat of core wire and flux formulation, electrodes were manufactured with multiple iterations of that coating with a single additional alloying element. The electrodes were then welded using a specially designed mechanized SMAW machine. The mechanized SMAW repeated each weld bead as closely as possible in order to minimize any variation in arc length, which may interfere with evaluation of the results. The effects of the various coatings were evaluated to prove the addition's effectiveness. The tests used in this work are the cast pin tear test, SS DTA measurements, and tensile testing.

The effects of each coating addition on all of the alloying element's recovery rates were compared to find that addition's overall impact on the weld deposit. The solidification range was measured using single sensor DTA to evaluate the effect of the altered weld metal composition on the solidification range. This was then compared to

the solidification range predicted by modeling software. The cracking susceptibility of the altered weld metal was also evaluated using the cast pin tear test.

This work demonstrates the first step in creating a logical, methodical process for the determination of the amount of the addition of the alloying elements to the weld deposit through the flux coating. Alloying through the flux allows the manufacturer to compensate for core wires of varying chemical composition. This work also outlined tests which are necessary to verify that the alloying additions did not compromise the integrity of the welding electrode.

Dedication

This document is dedicated to my family and friends; I would not have been able to accomplish this without their support.

ACKNOWLEDGMENTS

I would like to acknowledge and thank all the professors in the welding engineering department for helping me with any problems or questions which arose during this thesis work. I would like to extend special thanks to Boian Alexandrov for helping and guiding me along the way and allowing me the opportunity to do a thesis in the distance learning program. I would also like to thank John Lippold and Stanislav Rokhlin for being my committee members and for all of the insight from their years of experience.

I would also like to thank Bill Newell and Roger Swain from Euroweld for their help in initiating this work as well as their sharing many years of experience in working with all varieties of welding consumables. I would like to thank all the guys at Specialty Welding & Machining expressly James "Buster" Hales for all the help with the mechanized SMAW machine, as well as providing me with all of my experience in mechanized welding. Last, but certainly not least, I would like to thank James "Franklin" Turner and EEI for providing me with all of my background knowledge of welding flux and sharing all of his vast knowledge about shielded metal arc welding.

Vita

Born September 15, 1982 ……..Warren Ohio USA

June 2001……Westerville North High School

June 2006……...B.S. Welding Engineering, The Ohio State University

2008 to present……..M.S, The Ohio State University

Fields of Study

Major Field: Welding Engineering

Table of Contents

List of Figures

List of Tables

Chapter 1: Introduction

Shielded metal welding electrodes are made up of two major components, the core wire and the flux coating. In iron base welding electrodes, the core wire is common and inexpensive. The carbon steel and low alloy SMAW electrodes, with a few exceptions, generally do not have large amounts of alloying elements added to them. Therefore, these electrodes are somewhat tolerant of some variation in the electrode composition while still meeting the basic mechanical requirements of that electrode.

Nickel based electrodes often have additional requirements requested by the customer which are above the general requirement set forth by the American Welding Society. This requires the electrodes to be manufactured to produce a weld deposit with tighter constraint of the chemical composition than the standard range. This range may not always be the same composition that is targeted by the manufacturer of the core wire. For example, core wire which is manufactured of the standard alloy C-276 will not be used to create an ENiCrMo-4 electrode with a non-alloyed flux coating. To make that electrode using any acceptable C-276 core wire, some alloying elements must be added through flux coating.

A problem occurs when multiple suppliers of a single alloy are used to produce the same electrode. Nickel base welding electrodes use core wire which is very expensive. In order to stay competitive, the manufacturers must shop around for the best price. This can lead to core wire which is the same alloy, but has enough variation in the chemical composition that it cannot use the same amount of alloying additions to the flux coating in order to meet the standard and customer requested mechanical properties.

Adjusting the flux coating for each different heat of core can be very difficult and expensive. This is can be even more difficult when customers request that the electrode meet additional mechanical properties which require different targeted weld deposit

compositions. Understanding how the alloying elements which are added to the weld deposit through the flux coating effect the weld deposit composition is the only way it is possible to manufacture these dynamic products. Therefore, a method must be developed which allows the manufacturer to adjust the flux coating for different targeted weld deposit compositions. This method can then also be used to allow the manufacturer more freedom in the purchasing of the core wire for the electrodes.

Chapter 2: Literature Review

2.1 Introduction

Shielded metal arc welding SMAW is the oldest form of arc welding and the most commonly used around the world. (1) It has been adapted to all varieties of alloys including nickel base alloys. Shielded metal arc welding uses a metallic core wire which is coated with flux. A current is then applied through the wire as an arc is struck between the core wire, which is now an electrode, and the work piece. The heat from this arc melts the metallic core wire and the surrounding flux. Once the flux is molten, it is then referred to as slag and once the wire has melted it is referred to as weld metal.

The core wire conducts the current and supplies it to the arc. The core wire is important to the function of all shielded metal electrodes, but is much more simplistic in nature. It has tight processing requirements; it must be of the correct chemical composition and it must not contain excessive amounts of undesirable elements. The wire needs to be cut and straightened to high standards. The standards are all very easily controlled and not a subject of this work. The second component is the welding flux which will be discussed in detail in this chapter.

There are two major components of SMAW electrodes. The first is the core wire and the second is the welding flux. The main function of the core wire is to supply the bulk material that will be deposited as weld metal. In the case of most electrodes, it is desirable to have a core wire that is of matching composition to the desired deposit. This helps to keep the flux system simple without additional alloying elements. A simple flux system helps to keep the coating thickness to a minimum, a benefit when welding out of position. With low alloyed steel electrodes, this works well when the core wire is abundant and easy to obtain. The resistivity of most low alloy steel wire is also low, which provides benefits to the electrode by reducing the amount of resistance heating.

The challenge with higher alloyed steel and nickel based electrodes is that the wire tends to have higher electrical resistance, which can cause excessive heating of the electrode and results in poor welding operability. In some nickel base electrodes it can be desirable to add alloying additions through the flux and use a core wire with low resistivity and still obtain a high alloy deposit. Simple low alloyed core wire allows for multiple electrodes to be made from the same wire. Alloying through the coating also makes it possible to make small batches of electrodes without a making a new heat of material.

Varying the flux coating can have major implication on the weld metal's mechanical properties. The addition of one element to the flux coating can have an impact on the transferred amount of another alloying element.(2) When manufactures adjust the flux coating they often test to see how that change will affect the weld deposit and its mechanical properties. Common properties which may be of concern are ultimate tensile strength, elongation and resistance to solidification cracking which is important in nickel base alloys and austenitic steels. Alloying through the flux can also cause anomalies in the weld metal microstructure which can have a detrimental effect on mechanical properties as well. The weld deposit microstructure is often examined for segregation of alloying elements, inclusions, and discontinuities.

The flexibility of the SMAW electrode can have advantages in development, but can cause major difficulties in manufacturing. Procurement specifications must be written so that enough raw materials can be obtained to meet demand, but tightly controlled in order to maintain the targeted weld deposit. Core wire can often have large enough variation in the chemical composition that the flux coating must be altered to achieve the targeted weld deposit. The addition of alloying elements to the flux coating is not a new concept; it has been done for many years. (3) However, due to the complicated nature of the interactions between the molten metal and molten flux as they pass through the welding arc, predicting the weld deposit chemistry can be extremely difficult. Causing additional testing, rework and scrap in the manufacturing process all costing the manufacturer money. This work will look at how different alloying elements added through the flux coating impact the weld deposit's mechanical properties and

chemistry. Based on the results of this work recommendations can be made to assist in the development of flux coatings for selected nickel base alloys. The welding consumables that will be used for this work are: ENiCrMo-4 and ENiMo-10.

ENiCrMo-4 is a welding consumable which was originally designed for use on C-276 base material. The nominal compositional requirements set forth by AWS for an ENiCrMo-4 are listed in Table 2.1. (4)

C	Mn	Fe	P	S	Si	Cu	Ni	Co	Cr	Mo	V	W
.02	1.0	4-7	0.04	0.03	0.2	0.05	rem	2.5	14.5-16.5	15-17	0.35	3.0-4.5

Table 2.1 The AWS compositional requirements for ENiCrMo-4, single values are a max

ENiCrMo-4 has found uses for multiple applications such as: welding of other nickel based alloys containing chromium and molybdenum, overlay surfacing of steel, and the welding of a wide variety of dissimilar metals. The amount of molybdenum 15wt% to 17wt% gives this weld deposit excellent resistance to pitting corrosion.

ENiMo-10 Is a welding consumable which was designed to be a SMAW consumable for use on Hastelloy® B-3® material, B-2 and other high molybdenum containing nickel based alloys as well as cladding of carbon steel. The nominal requirements set forth by AWS for an ENiMo-10 are listed in Table 2.2. (4)

C	Mn	Fe	P	S	Si	Cu	Ni	Co	Cr	Mo	W
.02	2.0	1-3	0.04	0.03	0.2	0.05	rem	3.0	1.0-3.0	27-32	3.0

Table 2.2 The AWS compositional requirements for ENiMo-10

This alloy's primary purpose was for service in hydrochloric acid and other non-oxidizing environments in a wide range of temperatures. ENiMo-10 electrodes have high yield strength of about 68 ksi (5) which make them an excellent choice for high strength corrosion applications. It has also been used in service environments which contain high amounts of hydrogen chloride, sulfuric, acetic and hydrofluoric acid. Through a tighter control of the chemistry this consumable has improved thermal stability which gives it superior resistance to stress corrosion cracking when compared to previous electrodes used for the B series of nickel alloys.

2.1.1 Nickel Based Alloys: C Series

The C series of alloys are all based upon the original alloy C which was developed in the 1930's, the nominal composition is listed in Table 2.3.(6)

C	Fe	Mo	W	Ni	Cr
0.1	6.0	17	5.0	bal	17

Table 2.3 The nominal composition of alloy C

Alloy C is now obsolete because the modern melting techniques argon oxygen decarburization and vacuum oxygen decarburization are able to control trace or unwanted elements to much lower levels. Alloy C was based on the compatibility of nickel and chromium and nickel and molybdenum. By optimizing the levels of chromium and molybdenum Alloy C was created. Ternary phase diagrams of the Ni – Cr – Mo system can be very useful when working with any C type alloys to predict the phases which may be present at a given temperature. There are additional alloying elements in the C type alloys, but a nickel, molybdenum and chromium equivalency formula has been developed. (7)

$$\text{Ni}\,eq = wt\,\%\,\text{Ni} + wt\,\%\,Fe + wt\,\sum X \text{ where } X \text{ is all remaining alloying elements.}$$

$$Moeq. = wt\%Mo + wf\%W$$

$$Cr\ eq. = wt\ Cr$$

Equation 2.1 Ni, Cr, and Mo equivalency equations

Figure 2.1 illustrates the Ni-Cr-Mo ternary phase diagram at 300 °C, the red cross is the approximate location of C-276 using equation 2.1.(8)

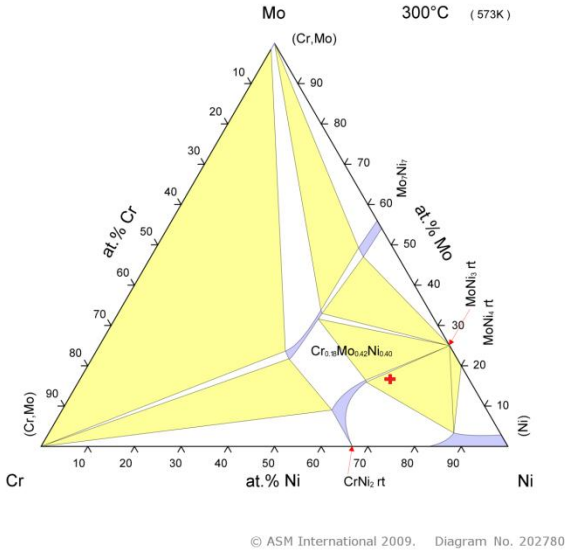

Figure 2.1 Ternary phase diagram of Ni-Cr-Mo system @ 300 °C

Alloy C had some major drawbacks from a welding stand point. In the heat affected zone, the formation of precipitates would lead to intergranular corrosion attack. This was a particular problem in oxidizing caustic, halide-containing environments. The

only way a welded vessel could be used in these environments was for the vessel to be solution annealed which dissolved all of the detrimental precipitates. (9) This is not a simple task with large components and limited the use of Alloy C in situations requiring welding.

C	Mn	Fe	Mo	W	Si	Ni	Co	Cr	V
0.01	1.0	5.5	16	4.0	0.08	bal	2.5	15.5	0.35

Table 2.4 Nominal composition of C-276

Alloy C-276 UNS # (N10276) was developed in 1965 and is still used today. It was specifically designed to overcome the weldabilty issues of alloy C. The US patent number 3203792 was issued to the German company, BASF.(10) They modified the chemical composition of alloy C by dramatically reducing the levels of carbon and silicon typically to 50 ppm for carbon and 400 ppm for silicon, (9) Table 2.4 lists the maximums for these elements

Although most C series nickel base alloys are considered to have low cracking susceptibility,(11) C-276 has the poorest resistance to hot cracking when compared to C-22 and C-4. This is illustrated in Figure 2.2 by varestraint work done by Ceislak *et al.* (7)

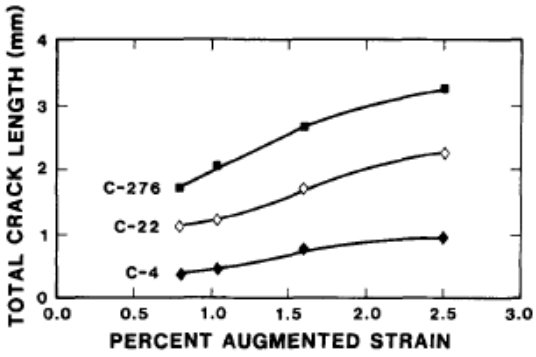

Figure 2.2 varestraint rankings of alloys C-4, C-22, and C-276

The continuous cooling transformation curve and time temperature transformation curve (12) for C-276 has the time scale in hours. The continuous cooling transformation curve has been generated using JMatPro Software and is illustrated in Figures 2.3. This means that fast cooling will not affect the weld properties and it is actually beneficial. Quickly cooling the weld to under 650ºC will keep the grain size small and may help to minimize any detrimental phases.

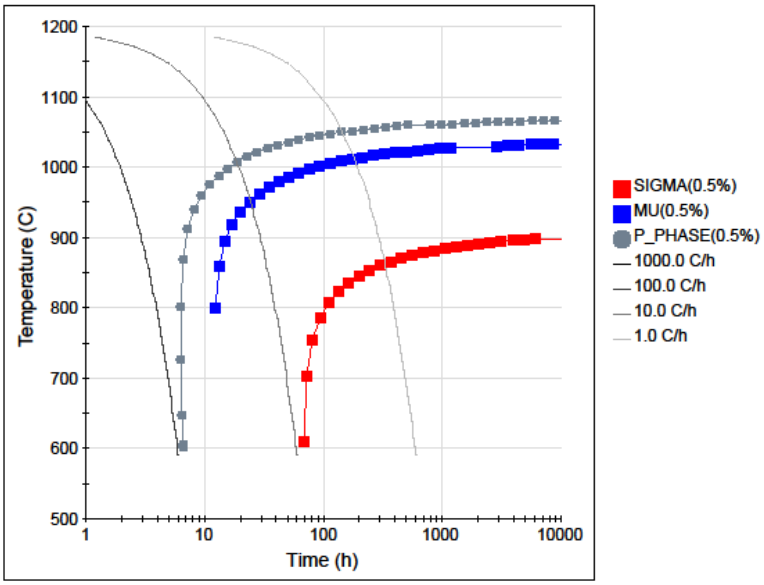

Figure 2.3 Continuous Cooling Curve for C-276

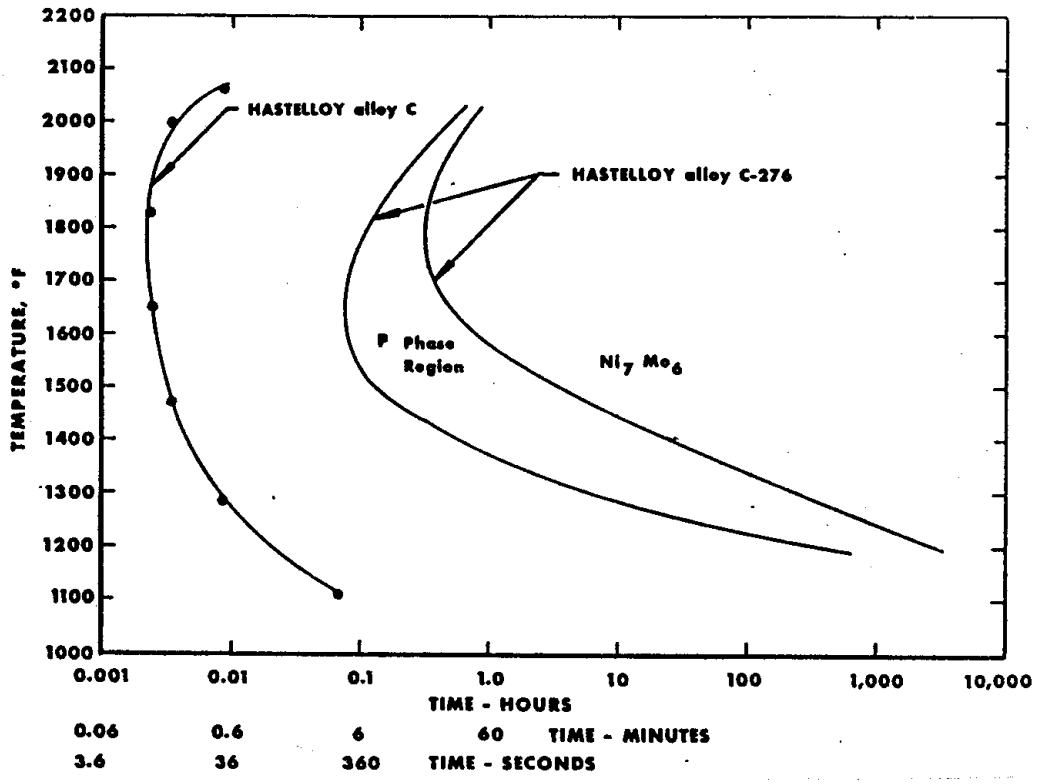

Figure 2.4 Time Temperature Transformation Curve for C-276

Alloy C-276 is a solid solution strengthened alloy. Which means that the primary phase is a face centered cubic structure called gamma. The alloying elements are used to strengthen the gamma matrix primarily, chromium and molybdenum, replace a nickel atom at the lattice site. The atomic radii mismatch puts a strain on the matrix and makes it harder for dislocations to move or slip planes to become active. (13) The large amount of solid solution strengtheners which are added to the matrix allows other phases to precipitate if the conditions are right or upon non-equilibrium solidification. The phases which can often cause problems are topological close packed phases or TCP's. These phases can be beneficial in small amounts and in the correct ratios they can give these alloys their high tensile strengths.(14) The most common TCP's in nickel alloys are P, μ, σ, and gamma prime. In alloy C-276 the TCP phases which occur are P and μ phases.

Sigma is not as likely to form due to low chromium (6) however, it is commonly found in alloy C-22 which is similar composition to C-276, but it contains higher chromium. Gamma prime is not likely to form in C-276 base metal due to the typically low levels of titanium and aluminum.

C-276 has a fairly short solidification range between 1370 and 1325 °C. The solidification sequence of C-276 is $L \rightarrow L + \gamma \rightarrow L + P + \gamma \rightarrow \gamma + P + \mu$. (6) The solidification begins with gamma, but ends with the terminal solidification of P phase. There is always some P phase because it solidifies while there is liquid present and this means there is no cooling rate that can avoid it. P phase is the nucleation site for the μ phase. They are often both found in weld metal although a rapid cooling rate can minimize the μ phase.

2.1.2 Nickel Based Alloys: B Series

The B series alloys are nickel based materials with the major alloying element being molybdenum. The nickel-molybdenum phase diagram can be very useful in determining the structure and phases in the final weld deposit. The NiMo phase diagram is illustrated in Figure 2.5.(15) The red line on the diagram is the target molybdenum level for all B series alloys, alloy B 28 wt% Mo, alloy B-2 26-30 wt% Mo, controlled composition B-2 27-30 wt% Mo, and Hastelloy® B-3® 27- 30 wt% Mo. Most of the development work with the B series of nickel alloys has been with adjusting the levels of carbon, silicon, and iron.

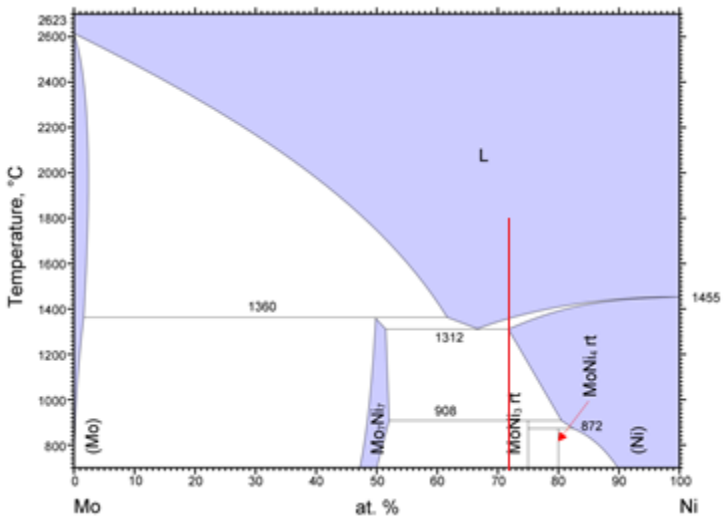

Figure 2.5 Nickel and Molybdenum Phase Diagram

The nickel molybdenum system is a peritectic system with three peritectic reactions, two of which are of interest, which can take place with varying concentrations of molybdenum. The peritectic reaction that is of most interest is the reaction which results in Ni_4Mo. The Ni_4Mo phase is a very fine Widmanstatten type precipitation in the weld metal which can causes age hardening. (16) The Ni_4Mo phase can also provide very high tensile strengths in excess of 120 ksi; however these strengths come with a loss of ductility. The face centered cubic, gamma phase, can have elongation up to 40% while the Ni_4Mo phase has a typical elongation of only 1 %! (17) For this reason control of the amount of molybdenum is critical for obtaining a weld deposit that can meet the mechanical property requirements of AWS A5.11 ENiMo-10 which are tensile strength of 100 ksi and an elongation of 25%.(3)

In the Ni Mo system, there are three stable phases: Ni_4Mo, Ni_3Mo, and NiMo. At elevated temperatures there are two metastable phases that have the DO22 structure.(18) Ni_2Mo is an unstable intermetallic phase which can occur in some ordered reactions. With molybdenum levels between 29 and 29.6 the Ni_4Mo phase can form, this is a hard

and brittle phase which often leads to cracking. Higher levels of iron will inhibit the formation of the Ni_4Mo phase during slow cooling or aging between 500 and 850 °C.(16)

The alloy B is age hardenable and has very good tensile and rupture strength at elevated temperatures. The aging temperature needs to be above 705º C to achieve maximum hardness (16); however this leads to a drastic loss in elongation which can lead to premature failure of a part in service. Therefore the ageing temperature and time must be controlled to achieve desired properties.

In the 1920's alloy B UNS # (N10001) was developed, the composition is listed below in Table 2.5. (6)

C	Mn	Fe	Si	Ni	Co	Cr	Mo	V
0.1	0.80	5.5	0.7	bal	1.25	0.6	28	0.3

Table 2.5 the composition of alloy B

This alloy was based on the nickel molybdenum system and it was developed primarily to be used in highly corrosive environments like hydrochloric acid. This alloy had problems in the heat affected zone when welded. The heat of welding causes M_6C, to form because of the high levels of carbon.(19) These precipitates lead to corrosion problems in the HAZ, which limited the use of alloy B in the welded condition unless it was solution heat treated after welding.

In 1975 alloy B-2 UNS # (N10665) was developed, the composition is listed below in Table 2.6(6) The major difference in alloy B-2 was the dramatic reduction the in the levels of carbon and silicon. Which was not possible at the time of the development of alloy B, but with new melting techniques, argon oxygen decarburization and vacuum oxygen decarburization these lower levels became possible.

C	Mn	Fe	Si	Ni	Co	Cr	Mo
.02	1.0	2	0.10	bal	1.0	1.0	26 -30

Table 2.6 composition of alloy B-2

This allowed the B-2 alloy to be used in the as-welded condition with no corrosion problems in the heat affected zone.(19) This also made alloy B-2 the material of choice for non-oxidizing acid environments. The B-2 alloy had the lower limit removed on the iron which lead to problems with cracking during fabrication. The cracking was related to rapid formation of intermetallic phase Ni_4Mo. These problems lead Thyssen Krupp VDM to develop tighter chemistry restrictions which lead to a controlled chemistry B-2. (18)

The annealed and quenched structure of alloy B-2 is a gamma phase FCC solid solution. The solidification sequence for alloy B-2 is $L \rightarrow L + \gamma \rightarrow L + \gamma + M_6C \rightarrow \gamma + M_6C$. (19) The gamma phase undergoes a solid state transition transformation to the Ni_4Mo phase between the 860 and 600°C. In alloy B-2 the Ni_4Mo phase causes a dramatic increase in hardness and loss of ductility. Iron and chromium can retard this transformation and lower the critical temperature range. Additions of 4 wt% iron can completely suppress the formation of the Ni_4Mo phase. The controlled chemistry of the B-2 alloy had an iron content of 1.6 to 2 wt% and chromium content from .5 to 1 wt%. (18)

The alloy which is now known as Hastelloy® B-3® UNS # (N10675) was developed by Haynes International. The nominal composition of Hastelloy® B-3® is listed in Table 2.7, (6) note the addition of tungsten, aluminum and titanium.

C	Mn	Fe	Al	Ti	Si	Ni	Co	Cr	Mo	W
.01	3	1.5	0.5	0.2	0.1	65	3.0	1.5	28.5	3.0

Table 2.7 the nominal composition of Hastelloy® B-3®

Hastelloy® B-3® has very good corrosion properties in a wide range of non-oxidizing media.(20) Due to the addition of tungsten and control of iron, it has a level of thermal stability greatly superior to earlier B series alloys by retarding the formation and growth of the Ni_4Mo and Ni_3Mo phases. (18)

2.1.3 Weldability of Nickel Based Alloys

Nickel base weld metal behaves very differently from iron base alloys which are much more commonly welded. Nickel base weld metal is much more viscous and does not flow and wet out as easily as iron based weld metal. It is traditionally welded at much lower amperages or "colder" than iron base alloys. All of these differences can create a whole new set of welding challenges for the operator. Some weldability problems are similar to those found in iron base welding and the solutions are same. However, there are also some weldability issues which are exclusive to the nickel base filler metals.

2.1.3.1 Solidification cracking

The most common problem in welding nickel base alloys is solidification cracking. Solidification cracking is a well understood phenomenon which has been the subject of inquiry as long as austenitic materials have been welded. The general consensus is that it is caused by liquid films which are present at the end of solidification.

(11) These films wet out along the solidification grain boundaries which are illustrated in Figure 2.6.(21) The solidification grain boundaries are formed as the dendrites grow

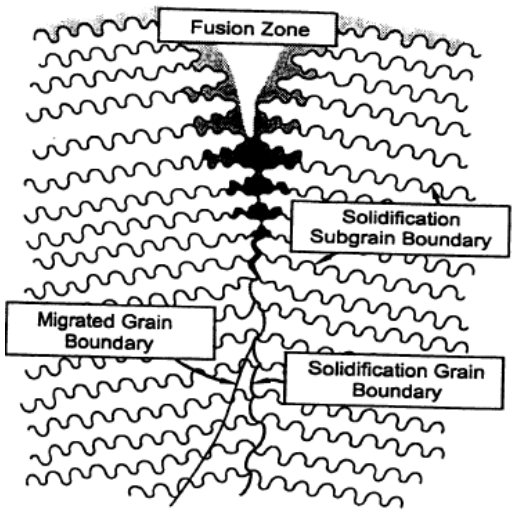

Figure 2.6 Illustration of the solidification grain boundary and fusion zone

into each other and form a relatively straight solidification front which runs along the center of the weld bead. The liquid film which is present at the end of solidification is of a lower melting point eutectic liquid. (22) The liquid film may not be able to support the strain which is caused by solidification and the liquid cannot maintain continuity and voids or cracks are formed. The composition of the weld metal can have a large influence on the amount of liquid which is present at the end of solidification. Niobium is an alloying element which is added to nickel alloys to increase mechanical properties; niobium forms a low melting eutectic with carbon. The work done by Cieslak *et al.*(23) demonstrated that the even within the compositional limits of an alloy that variation of niobium can have a large effect on the amount of eutectic liquid at the end of solidification.

The bulk composition and amount of solute play a large role in the susceptibility to solidification cracking. However, there are also several other elements

which can have an adverse effect on cracking susceptibility. Additions of boron and zirconium, even though they are typically added in parts per billion, must be added very carefully due to their large tendency for segregation. (24) This is very problematic because boron forms a M_3B_2 boride and zirconium forms ZrS both of which have low melting temperatures and tend to wet out along the grain boundaries. Liquid films along the grain boundaries reduce the amount of stress which the metal is capable of sustaining increasing the risk of solidification cracking.

Niobium carbides can increase the tensile strength, (25) but niobium is another element which exhibits a large tendency for segregation. (26) When niobium is added to the weld metal the amount of carbon must be closely monitored because of the formation of niobium carbides. Niobium carbide forms a low melting temperature eutectic which can form liquid films which are unable transfer any significant amount of stress. This increases the total solidification time which thereby enhances the susceptibility to solidification cracking. Even with tight control of the chemical composition of the filler metal solidification cracking may still occur because any solidifying metal will crack if there is enough strain applied to it.

In a situation such as this the welding parameters and weld bead geometry must be examined. When welding with nickel based alloys a round weld pool is preferred to a teardrop shaped weld pool. The teardrop shape creates additional stresses at the solidification front which can increase the chance of cracking. (27) If this phenomenon is observed it can be corrected by simply slowing down the travel speed. The weld bead geometry can be another problematic source for solidification cracking. In nickel base welding a convex weld bead is preferred to a concave weld bead. A concave weld bead will have tensile stresses across the surface of the weld bead. This increase in stress will increase the susceptibility for solidification cracking. To avoid this problem a convex weld bead is preferred because this causes compressive stresses on the surface of the weld bead which minimizes the susceptibility to solidification cracking. In order to change the weld bead profile the welding parameters need to be adjusted. The travel speed can be slowed down or more filler metal can be added. However, caution must be

used when changing these parameters which can modify the weld microstructure leading to other problems which are outside the scope of this thesis work.

2.1.3.2 Ductility Dip Cracking

Ductility dip cracking (DDC) is a solid state phenomenon that typically occurs in reheated weld metal or the base metal HAZ at temperatures between 50 to 80 percent of the melting temperature. In those temperature ranges, some nickel alloys have a severe drop in ductility. With sufficient strain, the metal can crack and fail. (28) There have been multiple theories as to the mechanism for DDC. The first focused on grain boundary shearing, sulfur segregation and embrittlement, these are listed out by DuPont *et al*. (11) The more recent theories focus on the grain boundary morphology, grain boundary sliding, and carbide distribution. (11) In the work done by Lippold and Ramirez, (29) they developed a simple but informative diagram illustrated below in Figure 2.7

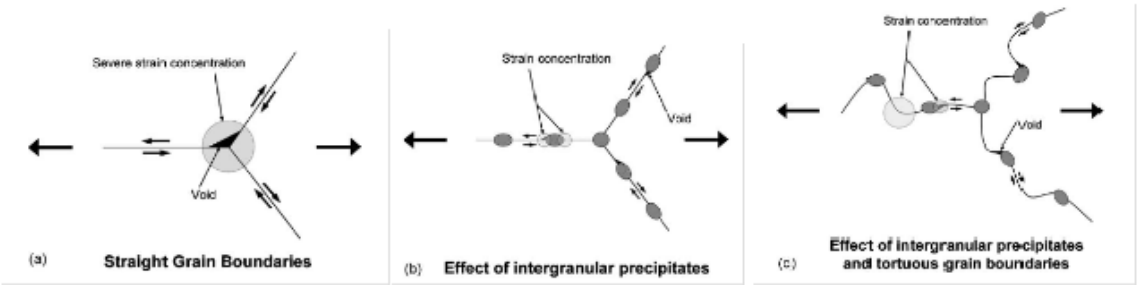

Figure 2.7 Effect of grain boundary precipitates and tortuosity at triple points

This simple figure clearly illustrates how the strain is concentrated at the triple points when the grain boundaries are smooth. Additions of precipitates which prevent grain boundary sliding relocate the voids to a more tolerant location. The most favorable

situation is a tortuous path which relocates the stress to a region where the grains can mechanically lock to prevent sliding.

The mechanism for DDC according to Young *et al* (30) is that DDC is caused by the combination of macroscopic thermal and solidification stresses induced during grain boundary precipitation of partially coherent $(Cr, Fe)_{23}C_6$ carbides. The strong correlation between the time/temperature dependence of DDC with precipitation, but not with grain boundary impurity segregation, such as sulfur, indicates that for some compositions, segregation is not a significant factor. This type of cracking can be mitigated by alloying to minimize the $(Cr, Fe)_{23}C_6$ carbide precipitation. (30)

Research done by Nissley and Lippold (31) on the ENiCrFe-7 weld metal found that molybdenum additions can help reduce the risk of DDC. The high levels of molybdenum could be why DDC is not commonly found in weld metal from an ENiCrMo-4 or ENiMo-10 electrodes. These electrodes are commonly used in the as-welded condition and this phenomenon has not been readily reported in the weld metal from these electrodes.

There are other ways minimize the risk of DDC, additions of niobium and titanium can help control the formation $(Cr, Fe)_{23}C_6$ carbides. Lowering the overall levels of chromium and iron in an alloy and using a welding procedure that minimizes the stresses induced by welding will reduce the risk of DDC. (31) The grain boundary microstructure can also play a role in the susceptibility to DDC. Long straight grains are more susceptible to DDC. Additions of niobium can create tortuous grain boundaries which are much less susceptible to DDC.

The strain-to-fracture test was developed by Nissley *et al* in order to evaluate ductility dip cracking austenitic stainless steels and nickel alloys. (32) This test uses a dog bone type sample on which GTA spot weld is made in the center. A programmed down slope at the termination of the weld leaves the weld microstructure with a radial aliment of the migrated grain boundaries. The samples is then heated and strained with a Gleeble testing machine and then it is examined for cracks.

2.1.3.3 Strain Age Cracking

Strain age cracking is a term which is used to describe cracking in nickel based super alloys which are post weld heat treated with an aging process. Alloys which are susceptible to strain age cracking contain additions of aluminum and titanium. In most nickel based super alloys the ratio of aluminum to titanium is targeted at a one to one. (14) These alloying elements form with nickel to create gamma prime, $Ni_3(Ti,Al)$ precipitate. In the correct ratios this precipitate can give nickel based super alloys very high strength even at elevated temperatures. The ratio of gamma to gamma prime is also very important to getting good mechanical properties in nickel based super alloys. According to the literature the ratio for gamma to gamma prime is also targeted at one to one.(14) Gamma prime has very high strength but is very brittle if there is too much in the matrix the alloy will have low ductility. The ratio is easy to control in manufacturing of new material, but can cause problems when it comes to welding.

The common aging temperature is between 700 and 900 ºC for most nickel based super alloys. This temperature range is experienced the HAZ of welded components. In this temperature range the gamma prime forms and coarsens. Nickel base super alloys are commonly given a solutionizing PWHT which is over 1000 ºC. If the heat treatment remains in the range between 700 ºC and 900 ºC the gamma prime will coarsen, building up stress in the HAZ. If the stress becomes too larger strain age cracking may occur

2.1.3.4 HAZ Liquation Cracking

HAZ liquation cracking is traditionally found in precipitation strengthened alloys such as 718. This phenomenon occurs due to small pockets of low melting temperature regions which upon the rapid heating associated with welding can melt before the surrounding base metal. Typically this occurs in the partially melted region in the HAZ. When strain is applied from welding these small pockets of molten metal wet out along the grain boundaries and creates micro voids and lowers the ability for stress to be

supported across the grain boundaries. Thompson et al.(33) have proposed a mechanism for HAZ liquation cracking the in the 718 alloy, it is illustrated in Figure 2.8. In the case of 718 the low melting "pocket" is niobium carbide.

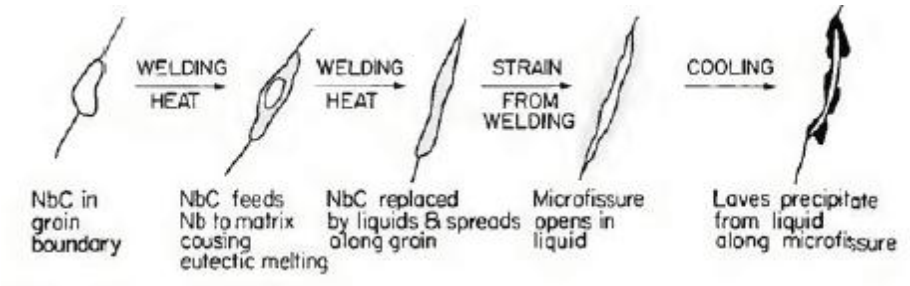

Figure 2.8 The liquation cracking sequence in alloy 718

The composition of an alloy can as have an effect on the susceptibility of HAZ liquation cracking. Sulfur and phosphorus are typically held as low as possible in all nickel base weld metal. However, they can be problematic even when they are held under the limits which are allowed by the AWS code A5.14. Sulfur and phosphorous form low melting constituents which wet out along the grain boundaries, similarly to the niobium carbide in alloy 718. According to Morrison *et al*, (34) additions of silicon, magnesium and manganese can reduce the susceptibility to HAZ liquation cracking because they will tie up the sulfur and minimize its ability to segregate to the grain boundaries.

The size of the grains controls the area of the grain boundaries and can also have an effect on HAZ liquation cracking. The grain boundary area effects the liquation cracking susceptibility in three ways.(11) First as the grain sizes decreases the grain boundary area increases which reduces the amount of strain on localized regions of the grain boundary. Secondly, the large grain boundary areas reduce the stress concentrations at triple points which are the locations in which voids are first likely to form. Finally, the grain boundary area dictates the thickness of the liquid layer that may

be formed. The thickness of the layer has an effect on how long the liquid takes to solidify, which allows for more stain to amass thereby increasing crack susceptibility.

2.1.3.5 Sensitization

Sensitization is a problem which is common to austenitic stainless steels (35) and some chromium-containing nickel base alloys such as C-276. (6) Sensitization occurs when the chromium atoms which would normally protect the surface combine and are effectively removed from the matrix. These phases do not allow the chromium on the surface to react with oxygen. This oxide film that is normally formed from surface chromium is very tenacious and protects the alloy. High levels of chromium create a protective oxide film; this is what makes stainless steels "stainless".

When welding on alloy C-276 sensitization can occur in the range of 650° to 1040° C. This is due to the formation of μ phase and other secondary carbides. The μ phase transforms from the P phase which is inherent to alloy C-276 because it forms when the metal is still molten. (6) This sensitization limits service temperature of alloy C-276, because of the sensitizing effects of the μ phase.

2.1.3.6 Porosity

Porosity is a common problem with most nickel base alloys. Porosity is caused by gas that is trapped in the molten weld metal as it solidifies. This happens because the solubility for most gasses is much higher in liquid metal than in solid. There are several gases that can be trapped in this way: Hydrogen, Oxygen, Nitrogen, Carbon Dioxide, Carbon Monoxide, Helium, and Argon. Hydrogen, Helium, and Argon are used in the gas tungsten or gas metal arc welding processes. Therefore, they are not a consideration in SMAW.

In nickel base welding electrodes the main cause for porosity is nitrogen, which is introduced to the weld metal from the atmosphere. This is the primary porosity former in all nickel base weld metal, because of the low solubility of nitrogen in solid nickel alloys. The lower the chromium content in the weld metal, the greater the risk of porosity from nitrogen. (36)

Another gas which can cause gross porosity is oxygen. Oxygen also enters the weld metal from the atmosphere and from the decomposition of oxides which may be contained in the flux. When it enters the weld pool, it first reacts with nickel to form nickel oxide. The stirring action of the molten metal from the extreme heat and arc forces, the nickel oxide will have the oxygen stripped by carbon because carbon monoxide will have lower energy. For this reason, the carbon content of the base metal and weld metal can have an effect on the susceptibility to porosity in nickel-based welds. (37) However, if adequate time is present the carbon monoxide will boil up out of the weld pool and act as an efficient deoxidizer. (37)

Fluxes for nickel base electrodes contain compounds that decompose to carbon dioxide and carbon monoxide. These gasses are used to protect the weld pool from the atmosphere. They do not enter the weld pool easily, even though they are heavier and fall, displacing any nitrogen or oxygen. However, they cannot protect the weld from porosity which can be caused by excessive moisture. If a SMAW electrode has not been stored properly or baked at a high enough temperature the weld metal from that electrode can be full of porosity. (37) In reality, this is the leading cause of porosity in any SMAW electrode which is commercially available.

2.1.3.7 Weld Cleanliness

One of the biggest problems in welding with nickel base electrodes is not related to the electrode at all, but the shop environment itself. All nickel based welding requires very clean base material and clean welding practices. The smallest amount of shop dirt, grease, oil, or other contaminants can cause major welding problems. The weld area

must be cleaned, commonly with acetone, prior to welding. The mill scale should be ground back two inches from the weld joint on both sides if it is full penetration weld. (38) Temperature indicating are commonly used to measure inter-pass temperature should be avoided, but if necessary should not be used near the welding area.

Nickel is very sensitive to contamination from residual elements. Bismuth, tin, antimony, lead, sulfur, zinc, boron, and phosphorus all form low melting temperature eutectics which can lead to liquation in the HAZ and weld metal. (38) These low melting temperature compounds can flow out along the gain boundaries and cause liquation cracking.

Iron contamination can also cause major problems, not only from liquation, but, a small increase of iron can have a devastating effect on corrosion resistance, particularly when it is in a localized concentration which is commonly caused from a tool strike. This is often the case in cladding where multiple layers of weld metal are used. Iron can be left on the surface of the previous bead from wire brushes and other tools, when the next weld bead is made, the level of iron in the weld metal increases. The final weld deposit will then have iron levels which will be susceptible to corrosion. It is common practice to use clean stainless wire brushes. However, caution must still be used; even stainless steel wire brushes have been found to leave trace amounts of iron behind. (38) In some extreme cases wire brushes and other jigs and tools have been made up of nickel 200 to avoid the possibility of iron contamination.

2.1.3.8 Welding Practice

One of the most common weldability issues are welders that are not experienced with using nickel base welding electrodes. Molten nickel weld metal is viscous and does not flow well compared to molten iron weld metal. (27) When an iron base electrode is not flowing and wetting out well the problem is often solved by increasing the welding amperage. Increasing the power and the iron weld metal becomes more fluid. However, that is not the case for nickel base welding consumables. Nickel base welding electrodes

have much higher electrical resistance and when the amperage is increased beyond the manufacturers' recommendation the electrode quickly overheats and the flux coating degrades which causes additional welding problems.

The weld bead shape of a nickel base welding electrodes is much more important that in iron base electrodes because of the previously mentioned weldability problems. These can be controlled, but excessive stresses due to poor bead shape such as a concave weld surface will cause excessive strain during solidification which can result in cracking. A convex weld bead is always recommended to help avoid solidification cracking. (27)

The welding technique is also different when welding with a nickel base welding consumable. Due to the lower welding amperages nickel base welding electrodes have less arc force and therefore get less penetration. To compensate for the lack of penetration it is desirable to oscillate the welding electrode. Making it necessary to use a wider included angle and then when welding with an iron base electrode. This also helps the weld metal tie in to the side wall of a weld groove avoiding slag inclusions which are visible upon radiographic inspection, sometimes referred to a wagon tracks. (27)

2.2 Mechanical Testing

The only tests which are required by the AWS code A5.11(4) are tensile and bend testing and an X-ray of the test assembly for weld metal soundness. However, in order to compare and evaluate the coating modifications and weld metal deposits, many different tests have been developed and used. The X-ray for soundness and the bend tests are mainly tests to determine the weldability and operability of an electrode. An experienced welder can determine if an electrode is capable of passing these tests simply by welding a few beads. Therefore, these tests have been removed from this work. The tensile test measures how strong and ductile a weld metal is. This is one of the first requirements of a qualified weld metal and can be greatly influence by the flux coating of an SMAW electrode. The most basic requirement for a shielded metal arc welding electrode is that

it welds and the slag is easily removed. Whether or not that will happen is greatly dependent on the solidification range of the weld metal compared to that of the slag and their respective coefficients of thermal expansion.

2.2.1 Liquids and Solidus temperature measurement using the Single Sensor Differential Thermal Analysis Method or SS DTA

Differential thermal analysis (DTA) is a process in which the sample is heated in a crucible with a thermocouple measuring the temperature of the sample and a second thermocouple measuring the crucible temperature or some point to get a reference temperature. The two streams of data are then compared and when sample data varies from the reference data either an exothermic or endothermic process is occurring. Depending on whether the sample is being heated or cooled this variation in the data can be used to predict a phase change. (39) The DTA process was used extensively to measure the solidification behavior of alloy 625. (23, 39) However, this process requires specific lab equipment and destructive sampling techniques.

The single sensor thermal analysis was developed at The Ohio State University by Alexandrov *et al.*(40) This process using a single thermocouple and math based software to achieve similar results. This process is typically set up in a controlled laboratory environment, but it also can be made portable to measure phase transformations on full sized mock-ups which may have slightly different results due to different cooling rates. (41) This process has also been used in combination with solidification cracking tests in order to compare the solidification range to the cracking susceptibility ranking. (42)

2.2.2 Susceptibility to solidification cracking

There are multiple tests which have been used to study an alloy's susceptibility to solidification cracking. Some of the more common tests are the varestraint and the hot ductility. Gallagher *et al* used that test along with the varestraint and hot ductility test to

evaluate the solidification cracking susceptibility of alloy C-22. (43) However, these tests require the use of matching compositional base metal which is then machined and autogenously welded. Those tests are actually testing the weldability of a consumable and base metal combination which may impact the results. In the case of a SMAW electrode the targeted weld deposit composition may not be the same as the base metal. Often it has a different target composition than the base metal or has additional alloying elements to avoid problems like solidification cracking. From the stand point of an electrode developer the cast pin tear test is the best choice because the required samples can be obtain directly from a small amount of the electrode's weld metal.

The cast pin tear test was first developed by F.C. Hull, but a modified version of this test has been developed at The Ohio State University by The Welding Metallurgy Group. (44) The version used for this work melted the test sample in an argon chamber above the pin mold with a TIG torch; the entire apparatus is illustrated in Figure 2.9. The pressure of the argon chamber and the pin mold are controlled which allows the molten charge to be dropped into the pin mold. The mold is illustrated in figure 2.10.(44) The pins range in length from a half inch up to two inches. An example of the pin molds is illustrated in Figure 2.11.(44) As the length increases the longitudinal stress also increases.

Figure 2.9 Cast pin testing apparatus

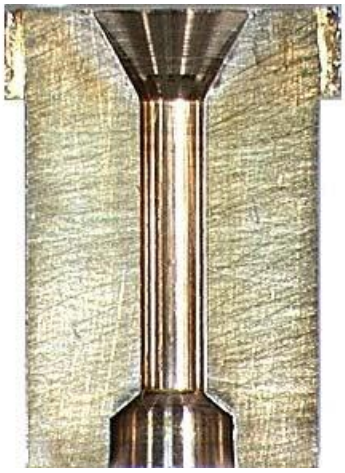

Figure 2.10 cross section of the cast pin mold

Figure 2.11 example of cast pins

This test is very useful in comparing and ranking similar filler metals susceptibly to solidification or “hot” cracking. Once the pins have been cast they are examined for cracking under a stereo scope. The equation for calculating the total percent cracking is written below in equation 2.2.

$$\%Cracking = \frac{L_T^{\,0}}{360^0} \times 100 \quad ,\%,$$

Equation 2.2

From this data collected the important values are the minimum pin length with 100% cracking, the maximum pin length with no cracking. The region between these points is the cracking response curve, this is illustrated in Figure 2.12.(44)

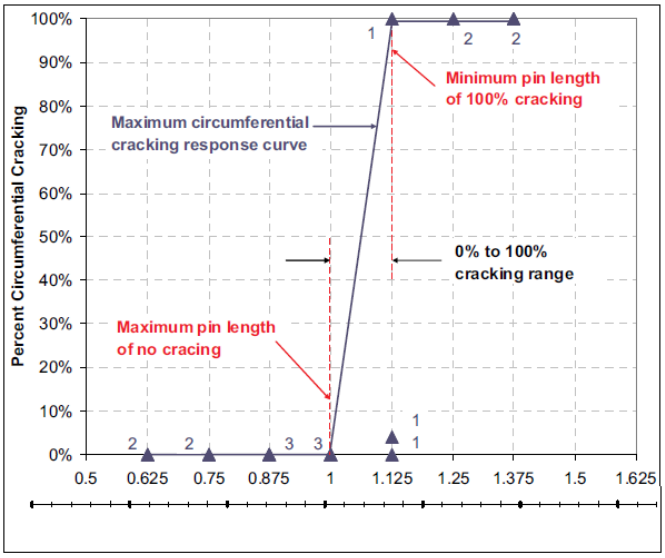

Figure 2.12 Graph of maximum circumferential cracking response curve for René 77.

Multiple alloys can easily be compared by plotting these points on the same graph making this an excellent comparative test. The cracking response curve for several nickel base alloys are illustrated in Figure 2.13.(44)

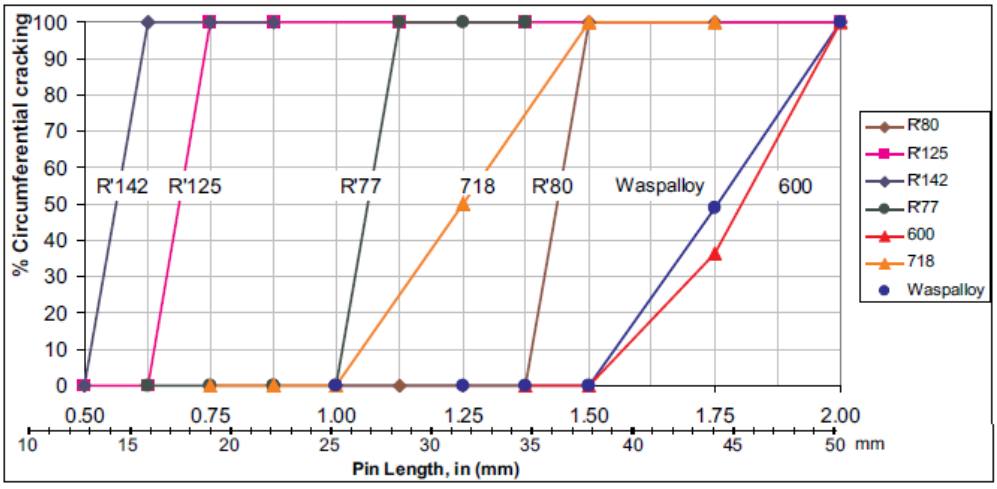

Figure 2.13 Cracking response curve for several nickel base alloys

2.3 Flux Coating

Shielded metal electrodes contain both core wire which provides the majority of the filler metal and a flux coating. The flux coating is made up of minerals, metal oxides, halides and metal powders as well as constituents which aid in the manufacturing process. The interactions of these ingredients for fluxes have been well documented by Chia *et al*. (45) and Tanaka (46) in the submerged arc welding of steel. The reactions which take place in SMAW of nickel coated electrodes has been studied VanBemsta. (47) The most notable point of his work is that the recovery of alloying elements which are introduced to the weld deposit via the flux coating are not as effective as alloying elements which are present in the core wire. The flux coating becomes a type of composite ceramic after it has been cured and its function is to transform a normal piece of wire into a welding electrode.

2.3.1 Fundamentals of Welding Flux

C.E. Jackson's, WRC Bulletin, Fluxes and Slags in Welding, describes eleven fundamental functions of welding flux for shielded metal electrodes. The functions of welding flux include: (3)

1) Stabilize the arc; ionize the arc gap by releasing electrons
2) Control arc resistivity
3) Provide a gas to shield the arc and prevent excessive atmospheric contamination of the molten filler metal
4) Provide a slag protection layer with the proper melting temperature to protect the molten metal from the air and improve the mechanical properties, bead shape, and surface cleanliness of the weld metal
5) Provide scavengers, deoxidizers, and fluxing agents to cleanse and refine the weld pool
6) Add alloying elements

7) Provide proper viscosity for out-of-position welding

8) Produce a low density slag

9) Promote slag detachability

10) Produce a smooth weld contour with good wetting

11) Reduce spatter and fume

The functions of welding flux for SMAW electrodes are the same regardless of the type of core wire that is used to make the electrode. The different compositions of the core wire may require special components be added or removed from the coating. But, all fluxes for coated electrodes must perform these eleven functions.

2.3.2 The Ellingham Diagram and the Role of Deoxidizers

Functions five and six on the formerly mentioned list work together and are extremely important when altering the weld deposit composition via the flux coating. Metallic powders are added to the flux coating in order to alter the weld deposit or to remove oxygen from the weld pool. The metallic powders can react with oxygen which is present from the atmosphere or from oxides in the flux coating. The problem is to determine which elements and how much of them will end up in the weld deposit and in the slag. In order to answer this question the Ellingham Diagram (48) has been generated and is a very complex thermodynamic tool. The diagram is a graph which illustrates the temperature dependency of many different compounds using the second law of thermodynamics. In welding, the primary compound of interest is oxide formation. The Ellingham diagram plots the change in the Gibbs free energy of oxide reactions of a range of temperatures. The Ellingham diagram for oxides of common metals is illustrated in Figure 2.14.

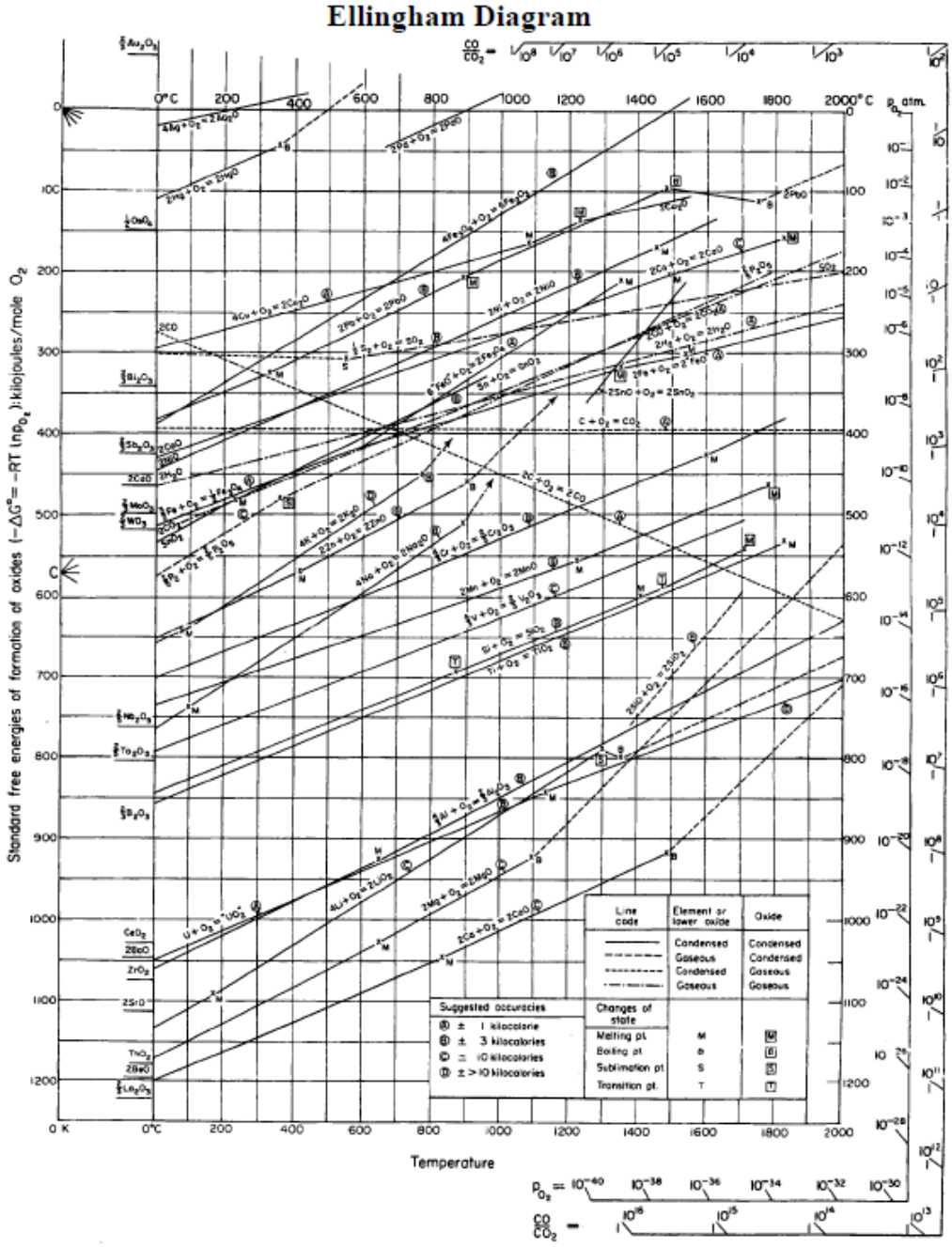

Figure 2.14 Ellingham diagram for many common metal oxides

The exact temperatures and pressures of a welding arc are very dynamic and it is extremely difficult isolate them to a single value. If the temperature and pressure are removed from the discussion the Ellingham Diagram really becomes a chart which ranks a metals affinity for oxygen. When looking at the chart with that method it becomes much less complicated. The elements of interest to welding can then be ranked:

Cu – Ni – Co – Fe – W – Mo – Cr – Mn – V - Nb – Si – Ti – Al – Mg – Zr

Where copper is the least likely to combine with oxygen and zirconium the most likely to combine with oxygen. An elements affinity for oxygen explains why additions of iron and cobalt typically recover in larger percentage than silicon or niobium. The elements to the far right are added to the flux coating in order to remove oxygen from the weld pool. These elements are traditionally known as deoxidizers, the most common deoxidizers used in nickel based fluxes are Ti, Al, and Mg. Silicon is a very effective deoxidizer in steel base electrodes, but it is not commonly added to nickel base electrodes due to solidification cracking problems it tends to cause. These elements can be extremely difficult to add to the weld deposit via the flux coating.

2.3.2 Types of Welding Flux

All fluxes for coated electrodes or submerged arc welding can be classified under four general categories: (49,50)

Acid Fluxes: Acid type fluxes which were primarily used for submerged arc welding fluxes, but have been adapted to covered electrodes. These types of flux contain large amounts of MnO and SiO_2 and may also contain fluoride bearing compounds. These compounds help to stabilize the arc, but can be detrimental to the arc force of an electrode. The low arc force can result in weld with lower penetration and which can lead to slag inclusions. The acid slag system produces a reducing atmosphere in which metal oxides may be reduced to the pure metal in the weld deposit. They are mainly used when the retention of alloying elements which have a high affinity for oxygen is required. An example of a typical composition of an acid type flux is listed below in Table 2.8 (41)

Fluorides	Carbonates	Silica and silicates	Alloying additions	Arc Stabilizers	Extrusion Aids
0-30%	20 - 40%	0 – 35%	0 – 20%	0 - 5%	5%

Table 2.8 Typical composition of an acid flux

Rutile Fluxes: Rutile type fluxes contain up to 50 percent rutile or TiO_2. The other major ingredient is calcium carbonate or $CaCO_3$. This compound can come in the form of limestone or crushed marble. This type of coating generally has higher levels of oxygen than basic coatings. An example of a typical composition of a rutile flux coating is listed below in Table 2.9 (41)

TiO_2	Carbonates	Alloying additions	Arc Stabilizers	Extrusion Aids
25-50%	25 - 50%	0 – 25%	0 - 5%	5%

Table 2.9 Typical composition of a rutile flux

Cellulosic Fluxes: Cellulosic type fluxes contain organic materials, the most common of which is a form of cellulose. When these fluxes decompose, they produce hydrogen, which not only protects the molten metal, but produces a hotter arc and tends to help wetting in iron base electrodes. An example of a typical composition of a cellulose based flux coating is listed below in Table 2.10 (41)

Cellulose	Carbonates	Alloying additions	ZrO_2, Al_2O_3, SiO_2, MgO	Arc Stabilizers	Extrusion Aids
20 - 40%	20 - 40%	0 – 10%	0 – 15%	0 - 5%	10%

Table 2.10 typical composition of a cellulosic flux

Basic Fluxes: Basic fluxes are used in situations which require high quality welds with low amounts of hydrogen. Basic fluxes do not have as good operability as other types of fluxes and they tend to form a deep cup on the electrode end. The deep cup of a basic electrode shields the conductive metal resulting in restarting problems. An example of a typical composition of a basic flux coating is listed below in Table 2.11 (41)

Carbonates	Alloying additions	CaO, MgO, Na_2O, K_2O	Arc Stabilizers	Extrusion Aids
20 - 50%	0 – 30%	0 – 35%	0 - 5%	5%

Table 2.11 typical composition of a basic flux

Extrusion aids will vary by manufacturer, but are always required in order to product high quality electrodes. Extrusion aids are generally various type of clays and other organic compounds which decrease the flow stresses of the wet flux coating mixture during the extrusion process.(41) These ingredients are often not stable and burn out at arc temperatures and rarely effect the weld deposit.

Arc stabilizers will also vary by manufacturer and electrode type. They generally contain sodium and potassium which have very low ionization potential.(41) Alloying additions are commonly pure metal powders or alloy powders. In a reducing system, such as an acid slag system, the additions can be metal oxides. Caution must be taken

with selecting some alloying additions such as aluminum and magnesium. These elements can create reactions (51) which will affect the operability of the electrode.

Most flux coatings that are used today are hybrids of these four general categories. Manufacturers have chosen different raw materials from each type of these coatings to maximize different properties in their SMAW electrodes. In some cases the same type of electrode can be made with different slag systems which are tailored for special applications.

2.3.3 Slag Removal

The thermal expansion of the slag crust is very important and must be much lower than that of the weld metal which it protects. Then, as the hot metal cools, it shrinks and pulls away from the slag crust. The main components, which are typically a ternary system of oxides from the flux, form the matrix of the slag. The ternary system of these ingredients dictates the thermal expansion of the slag. For example, in the ternary system of MgO, SiO_2, and Al2O_3 a flux system used for C-276 varying the amount of Al_2O_3 by only 10 wt% can change the matrix from Cordierite, which has very low thermal expansion, to Fosterite, which has a thermal expansion very close to the alloy C-276. (52) The slag system which is primarily made up of Cordierite will have very good slag removal. A slag system that is primarily made up of Fosterite will need a chipping hammer or grinder to remove the slag.

2.3.4 Slag Viscosity

The viscosity of the slag significantly influences the operability of the welding electrode. The slag viscosity can also affect the adhesion of the slag to the metal. (53) The slag must be fluid enough so that it wets out and covers the molten metal. However, if it becomes too fluid, it can flow in front of the weld pool and cause operability problems. The most common problem which can be traced back to slag viscosity or

fluidity are islands in the slag. These are pockets of weld metal with have been exposed because the molten slag was so fluid that it ran off the top of the weld bead.

When out of position welding, the fluidity and the solidification range of the slag is critical. The molten flux must be stiff enough to support the molten metal as in the case of most nickel based welding electrodes. The other option when welding out of position is to reduce the solidification range of the molten flux and use what is referred to as a fast freeze flux system. This type of flux coating is more commonly found among the steel electrodes because of their lower melting temperatures.

There are compounds which can affect the viscosity of the slag. The molten flux forms a type of composite ceramic glass due to its high solidification rate. Since the slag is actually a glass, the way to control the solidification rate is to use glass modifiers. These are typically to non-bridging oxides which break up and modify the glass structure, one of the most potent of which is alumina. (54) Silicon dioxide is another compound which commonly affects the viscosity of the slag. However, silicon must be used with caution in nickel based alloys, as many nickel based alloy have very low tolerance for it.

2.4 Flux Coating Used in Nickel Based Electrodes

Nickel based SMAW electrodes typically use a basic flux coating or a hybrid basic and rutile. The basic coating help minimizes unwanted elements such as sulfur and silicon. The basic coating, along with the typically sluggish nature of nickel base weld metals, causes the operability of nickel based electrodes to be lower than many iron base electrodes. Special welder skill and care must be taken with nickel based electrodes in order to produce a quality weld deposit.

Modified halide fluxes contain large percentages of fluorides and chlorides. These often contain other active elements that have a high affinity for oxygen. These fluxes have been primarily used for submerged arc welding of high temperature nickel based alloys. These compounds are not often used in large quantities in shielded metal arc welding with the exception of calcium fluoride and Na_3AlF_6 or cryolite. These elements

can provide some benefits when welding nickel based alloys. Increasing the CaO, Al_2O_3 and the SiO_2 will decrease the transfer efficiency of alloying elements. (55) As weld metal becomes contaminated with silicon, the susceptibility to solidification cracking increases. The addition of sodium fluoride in the flux can lead to an increase in transfer efficiency of aluminum and titanium. Sodium and strontium, along with additions of tungsten, significantly improve hot cracking resistance. (55) The ionization potential of halide elements in nickel based alloys is quite low. Low potential is the reason the reactions between the halide elements occur more easily than many other reactions, this low potential also helps to smooth the welding arc. These reactions not only occur in the molten metal, but also at the liquid gas interface. (55)

2.5 Mechanized SMAW

In order to produce high quality welds which where repeatable the shielded metal arc welding process had to be mechanized. Automatic SMAW welding has been explored with widely varying results. Most of the equipment has been designed for laboratory trials to increase the repeatability and standardization of the SMAW welding. The majority of these systems operated in straight polarity and did not represent a real world welding situation.

The majority of industrial use of automatic SMAW has been in under water welding, particularly for pipelines. Kang's thesis work (56) looked into the design of an arc voltage controller which would operate in DCEP in order to weld with SMAW electrodes automatically under water. Lima *et al* (57) took a different approach and programed a six axis robot to perform the same task. These trials all used an E6010 or E7018 steel electrode. These consumables are some of the most forgiving and simple electrodes for welding. Nickel base consumables are much less forgiving and often have issues such as excessive resistance heating. To combat these challenges a special piece of equipment was designed and built which could produce a sound weldment using nickel

base electrodes. This equipment utilized both a modified arc voltage controller and programmable slides in order to accomplish this task.

Chapter 3: Objective and Tasks

The objective of this work is to demonstrate the first step in creating a logical, methodical process for the determination of the amount of the addition of alloying elements to the weld deposit through the flux coating. This will allow the manufacturer to compensate for core wires of varying chemical composition. It will also outline tests which may be necessary to verify that the alloying additions did not compromise the integrity of the welding electrode.

In order to understand how alloying additions will affect the weld deposit, shielded metal electrodes were manufactured with varying alloying additions in the flux coating. Once the weld deposits of these electrodes have been analyzed, a procedure can be generated to adjust the flux coating in order to create a weld deposit with desired weld deposit chemistry. This procedure will be applicable to shielded metal electrodes which fall under the AWS designation of ENiCrMo-4 and ENiMo-10. To achieve this objective, nine tasks have been determined to be critical to the success of this project. The individual tasks are listed below:

1. Development of a device for mechanized SMAW that provides reproducible weldments.
2. Modification of electrode coatings with variable content of Al, Ti, Nb, Mo, Ni, and Zr for welding consumables ENiCrMo-4 and ENiMo-10 using alloyed core wires of C-276 and Hastelloy® B-3® respectively.
3. Use of the ENiCrMo-4 and ENiMo-10 electrodes to create multi-pass weldments from which undiluted weld metal samples can be taken for testing.
4. Use of statistical analytical tools to study the effect of coating composition on the arc stability utilizing data collected from an independent data acquisition system.

5. Use of the known amounts of selected alloying elements in the flux coating and the amount of each alloying element in the weld deposit to calculate the percent recovery of selected alloying elements.
6. Study of the effect of coating composition on the weld metal solidification behavior by thermodynamic simulations (JMatPro, Thermocalc) and experimental measurements (SS DTA).
7. Evaluation of the susceptibility to solidification cracking of each heat by the Cast Pin Tear Test, and compare the effect of each alloy addition as well as comparing the results of the ENiCrMo-4 to the results of the ENiMo-10 electrodes.
8. Use of characterization techniques such as: optical metallography, scanning electron microscopy, and energy dispersive spectroscopy to identify and classify the typical weld metal microstructure of each welding consumable. Also, identify any metallurgical anomalies which may be caused by the alloying additions in the flux coating.
9. Performance of tensile testing to determine which alloying elements may be beneficial to tensile strength and elongation of the weld metal.

Chapter 4: Materials and Procedures

4.1 Core Wire for ENiCrMo-4 and ENiMo-10 Electrodes

The electrodes used for this work were manufactured using materials which have passed the quality standards of Electrode Engineering, a small company that specializes in made to order welding electrodes. The core wire used for these electrodes was C-276 for the ENiCrMo-4 and Hastelloy® B3 ® for the ENiMo-10. The core wire compositions are listed below in Table 4.1.

ENiCrMo-4	C	Mn	Si	S	P	Fe	Ni	Mo	
	0.012	0.52	0.06	0.007	0.01	6.08	54.17	16.33	
	Cu	Co	Ti	Cr	V	W	Zr	Al	Nb
	0.14	1.19	0.02	17.18	0.127	3.89	0.005	0.273	0.03
ENiMo-10	C	Mn	Si	S	P	Fe	Ni	Mo	
	0.001	0.63	0.01	0.002	0.004	1.53	66.39	28.3	
	Cu	Co	Ti	Cr	V	W	Zr	Al	Nb
	0.1	0.07	0.01	1.8	0.01	0.1	0.01	0.4	0.06

Table 4.1 Chemical composition of the core wire used for the experimental electrodes

The same lot of each ingredient in the flux coating was used to make the experimental electrodes. Therefore, the only difference in composition and particle size distribution resulted from the addition of alloying elements. All of the metallic alloying elements were a -60 to +325 mesh size. The particle size can have some effect on the amount of that element recovered in the weld deposit.(58) Using the same metallic particle size will help to minimize this effect.

4.2 Mechanized Shielded Metal Arc Welding

Developing a method to create repeatable weld beads was critical to this work. To achieve this task, the SMAW process had to be mechanized in a method which simulated a human welder as closely as possible. The mechanized SMAW machine was designed to perform the following tasks:

1) Initiation of the welding arc without high frequency assist
2) Weld with a SMAW electrode
3) Function with a power source operating in reverse polarity
4) Control the travel speed in a range that would be comparable to that used by a human welding operator
5) Control the electrode feed rate in order to maintain a constant arc length
6) Synchronize all functions in order to be completely repeatable

The mechanized SMAW machine used a Thermal Arc 300 GMS power source and an Arc Products AVC-5 arc voltage controller. A custom built controller was used to synchronize all components with the movement of the electrode. The power source was set up for electrode positive, constant current at 110 amps and the AVC was set to control the arc length at 25 volts. The travel speed was held at nine inches per minute. These

parameters were the maintained for all tests. The machine ay out is illustrated in Figure 4.1.

Figure 4.1 Mechanized SMAW machine

A SMAW electrode's straightness does not affect its operability unless the electrode is bent to a degree where it cannot reach the weld joint or if the coating has been damaged. A human welder will accommodate for a slight bend in an electrode without even realizing it. However, a machine with fixed slides cannot make those miniscule adjustments which result in a straight weld bead. If the electrode is bent or held at a skew, the machine will weld at an angle to the desired straight line path. This is a problem when making multi-pass welds. For this work, this problem was overcome by mounting the test plates into a cross slide vise which could be manually adjusted as the machine was welding, thereby correcting any lateral movement due to a bent electrode. Note this cross slide vise is not pictured in Figure 4.1

The concentricity of an electrode is a measurement of how consistent the coating thickness is around the core wire. The acceptable limit is determined by the manufacturer, but most will default to the military specification MIL-E- 22000 (59) which states: "covering on all sizes of electrodes shall be concentric to the extent that the

maximum core-plus-one covering dimension shall not exceed the minimum core-plus-one dimension by more than the following percent" Table 4.2 presents the core wire diameter specific percent.

3/32" and smaller	7%
1/8" and 5/32"	5%
3/16" and larger	4%

Table 4.2 percent of variation allowable by Mil-E-22200

Most manufacturers will used this calculation to determine the result in thousandths of an inch for their thinnest coating at each diameter and create a blanket standard for all sizes.

If the core wire is not concentric with the core wire, it will not melt evenly, which will form an uneven cup, commonly called a "fingernail", or the welding is referred to as "finger nailing". With manual welders, a small amount of finger nailing can be controlled, depending on the welding position. However, a larger amount of eccentricity requires the electrode to be scrapped. In mechanized SMAW, finger nailing causes the electrode to drag and skip, producing welds that are unacceptable.

4.3 Coating Development and Modification

The electrode coatings which were used in this project were based on proprietary coatings which are used for standard versions of ENiCrMo-4 and ENiMo-10 SMAW electrodes. The coatings were then modified by adding alloying elements according to Table 4.3. To create these formulations, the production formulation was proportionally scaled back to allow for the measured amount of alloying elements. This was done to minimize the effects of the alloying elements on the slag system. In order to analyze how a single alloying element affected the coating, all alloying elements were removed from the baseline formulation. Each iteration had a single alloying element or

combination of elements added into the coating. Note that iron was an unintentional addition in mixes 9, 12, and 21. Due to the cost and slow disillusion of pure niobium, it was necessary to use a ferro-niobium alloy. Zirconium is not stable in the pure form, especially when it will interact with water from the binder this element was added as a stable alloy of zirconium, silicon, and iron.

The alloying additions and rationale are listed in Table 4.3. Each alloying element was added because of a specific function that it performs in the flux coating. Aluminum and titanium are called deoxidizers because the remove oxygen from the weld deposit. They are effective because of their high affinity for oxygen, see section 2.3.2. Additions of niobium were added because niobium interacts with carbon to form niobium carbide a lower meting temperature eutectic. Which causes problems with slag removal, but is a common alloying addition because it can increase the mechanical prosperities of the weld metal. Molybdenum and nickel in the B series of nickel base alloys and just nickel in the C series of nickel base alloys are added because they can be used to lower the amount of other alloying elements in the weld deposit. Molybdenum also has a low affinity for oxygen which results in one of the highest recovery rates of commonly added alloying elements which makes it good for a baseline comparison.

Mix Number	Electrode Type	Alloying Elements	Rationale
1	ENiCrMo-4	0%	Baseline
7	ENiCrMo-4	5% Al	Deoxidizer
8	ENiCrMo-4	5% Ti	Deoxidizer
9	ENiCrMo-4	3% Nb + 2 % Fe	Modification of Solidification Range
10	ENiCrMo-4	5% Mo	Recovery Rate
11	ENiCrMo-4	18% Ni	Dilution Effects
12	ENiCrMo-4	2.45% Zr + 3.15% Si + 1.26% Fe	Modification of Solidification Range
13	ENiMo-10	0%	Baseline
19	ENiMo-10	5% Al	Deoxidizer
20	ENiMo-10	5% Ti	Deoxidizer
21	ENiMo-10	3% Nb + 2 % Fe	Modification of Solidification Range
22	ENiMo-10	15% Mo	Recovery Rate/ Dilution Effects
23	ENiMo-10	18% Ni	Dilution Effects

Table 4.3 Alloying additions and mix number

4.4 Electrode Production

The shielded metal electrodes for this work were produced by Electrode Engineering located near Chattanooga, Tennessee. The electrodes for this project were made according to their quality control procedures. The manufacturing process can best be described in four steps: dry mixing, wet mixing, extrusion, and drying /curing.

The first step in electrode manufacturing is the dry mixing. In this step, all of the dry ingredients of the electrode coating are added to a mixer. For this work, a V type, 4 quart Patterson Kelly twin shell mixer with liquids bar was used, which was sized for a dry mix of about 4.4 pounds.

The second step in the production of shielded metal electrodes is commonly referred to as the wet mixing. In the wet mixing step, the dry power has a binder added to it which turns it into a usable paste or mud. This is done with the aid of a mixer which is capable of injecting the binder into the powder as it is mixing. The same mixer that

was used to do the dry mixing also did the wet mixing. The binder was pumped using a Made In The USA peristaltic metering pump, the entire mixing system is illustrated in Figure 4.2

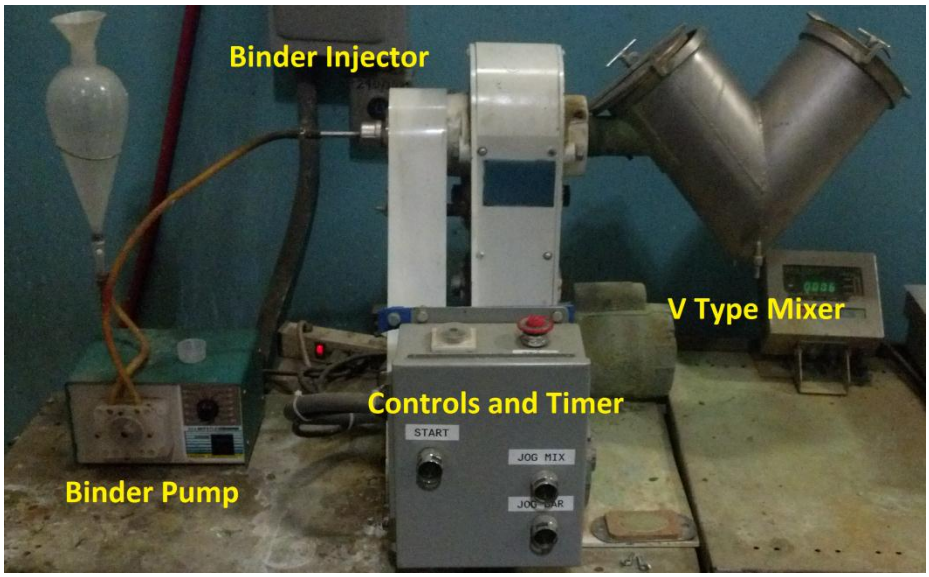

Figure 4.2 Flux mixing system, dry and wet mixing

The two main ingredients in the binder which was used for the electrodes were sodium and potassium silicates. The binder was mixed in specific ratios with a few other proprietary ingredients in order to create a binder with a Baumé of 35° heavy. Baumé is a measurement of specific gravity which is commonly used in industry; it is called heavy or light, with the specific gravity of water being zero for both scales going to 100. Binder is then pumped into a small twin shell mixer which evenly blends the dry and wet ingredients into a paste or mud.

The extrusions of the electrodes for this project were produced on an Oerlikon EP12 extruder. The extruder is illustrated in Figure 4.3 and the red arrow indicates the direction of the wire feed. In this figure the barrel is open and ready to be loaded.

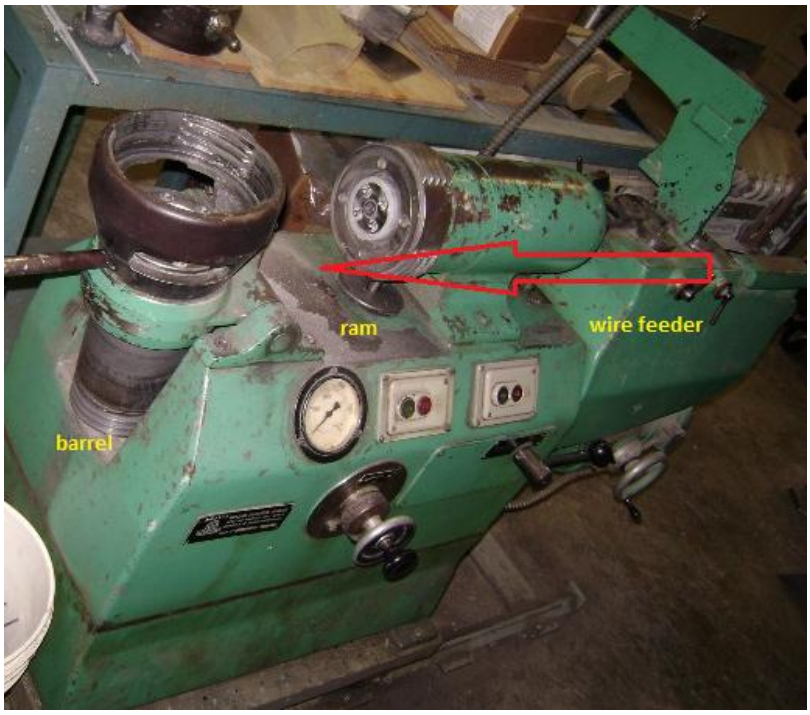

Figure 4.3 The extruder used to manufacture the electrodes for this work

This is an inline type extruder suitable for doing test batches of about 10 pounds. With the wire speed and pressure adjusted correctly, the extruder will discharge a smooth concentric electrode. The extrusion is the step where many problems can arise in the manufacturing process. A short list of defects which are pertinent to this project can be found below in Table 4.4.

The final step in the manufacturing of shielded metal electrodes is the drying and curing stage. A large portion of sodium and potassium silicate is water, which can cause problems if the electrodes are baked immediately after extrusion. The electrodes were air dried a then baked at a 650°F for a period of two hours. These electrodes were for lab tests only, so they were packaged in vacuum sealed containers which were not opened until testing was to be performed.

Hydraulic ram pressure too low / wire moving too fast	The electrode coating will be cracked and inconsistent core wire may be visible	The overall volume of the coating will be less per electrode, if alloying elements are added via the flux; the amount will be incorrect resulting in a weld deposit with a lower chemical composition.
Hydraulic ram pressure is too high or wire is moving too slow	The coating will have a rough appearance and a larger than desired outer diameter	The overall volume of the coating will be more per electrode, if alloying elements are added via the flux; the amount will be incorrect resulting in a weld deposit with a higher chemical composition.
Mud is not flowing evenly through the web or the wire nib has too much clearance	Can be very difficult to tell by the appearance unless grossly out of center. However, when welding, the electrode cup will be oval instead of circular	When the concentricity is bad, the electrode will finger nail which can make the operability difficult; often results in a long arc length which can affect the recovery rate of an alloying element

Table 4.4 Common problems during extrusion which affect the weld deposit composition

Electrode Manufacturing Parameters	
Dry coating mixture	4.4 lbs. / 2000g
Binder used	25% sodium silicate 75% potassium silicate
Binder amount	1.3 lbs. / 590g
extrusion parameters	5000 psi
coating diameter	0.200"
Air dry time	24 hours
Baking Time	2 hours @ temperature
Baking Temperature	650° F

Table 4.5 Electrode manufacturing parameters

4.5 Undiluted Multi-Pass Weld Metal Deposits

This project required many different samples in a variety of shapes and weights. The common denominator was that all of the samples needed to be undiluted weld metal. To obtain the amount of undiluted weld metal that was necessary, multi-pass weld metal deposits were made. These deposits were welded on carbon steel inside a fixture made of copper and aluminum held together with clamps. The first layer of the deposit was four beads wide because nickel based electrodes don't wet out well on the steel. The subsequent layers were three beads wide. This resulted in a deposit which was one inch wide and about five and a half inches in length. The height of the deposit was dependent on how many samples needed to be taken from it. All samples were taken a minimum of 0.375 inches from the base metal to ensure the metal was non-diluted

The amperage setting for each multi-pass undiluted weld metal deposit was fixed at 110 amps as set on the welding power source and the AVC was set to 25 volts. The interpass temperature was held at 300° F, checked using Tempilsticks® of 250°F and 300°F on the area of the weld buildup that was scrapped. The interpass temperature was not a major issue because of the large heat sink of the base plate and fixture as well as the somewhat extended reset time. The slag was removed by a handheld chipping hammer, and a pneumatic wire brush was used to clean the surface after every weld pass.

The deposits were welded with the mechanized SMAW machine in the "semiautomatic feed mode". What this means is that the arc start, travel speed, and length of weld time were controlled by the machine. The feed rate was preprogramed and the AVC was maintaining the arc length, but the operator was able to make fine adjustments. This resulted in a typical feed rate which closely follows an exponential curve with an exponent of about 0.02. This mode was successful because the operator had adjustable control of the feed rate, allowing compensation for irregularities in the welding electrodes. When finger nailing caused the electrode to begin to drag, the operator had the ability to slow the feed rate slightly until the arc stabilized, avoiding an

unacceptable weld bead. These small adjustments are identical to those which would be made by a human welder.

Once the multi-pass non-diluted weld metal deposits were completed, multiple samples needed to be cut from the deposit. The location where samples were taken from the deposit can be seen in Figure 4.4. The first sample removed was a slice approximately 0.375 inch in thickness taken from the bottom. This sample was cut cold with a band saw and was then machined into a 0.25 inch reduced section tensile sample commonly referred to as a 252 or a T3, all weld metal tensile sample. With the exception of the metallography samples, the other samples were cut with an abrasive saw because the microstructure was irrelevant. The samples which were used for chemical analysis were cut from the top surface of the deposit at a height of 0.625 inches above the base metal. This cutting is beyond what is required by ASW Code A5.11. Traditionally, this is done for chemical composition samples which will be tested at an outside lab in order to avoid analysis of the wrong surface.

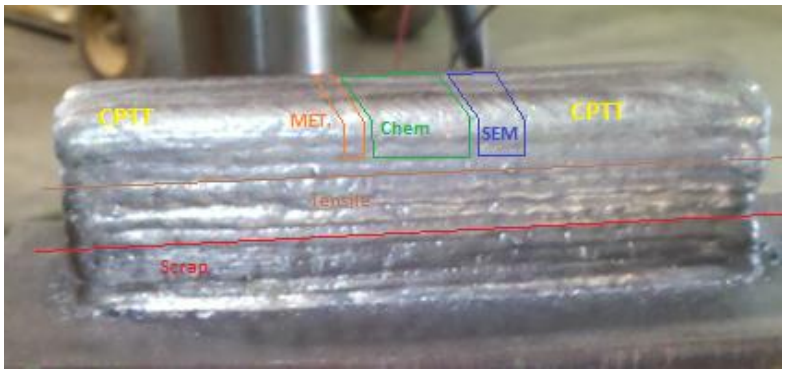

Figure 4.4 Sample locations in multi-pass weld build up

4.6 Arc Stability

The data collected to study the arc stability was taken from two independent data acquisition systems. Both systems were made by Dataq Instruments. The data was recorded using both systems for the multiple pass all weld metal deposits as well as the test welds used to measure the solidification temperature range. The reason for using two independent systems was to first compare the readings to ensure correct operation. These systems were used for many different functions and had to be set up and taken down multiple times throughout the testing period. The second reason is that each system operated at different sample rates. The system that was used to monitor the mechanized SMAW machine was a DI 718B multi-channel data logger which operated at a sample rate of 100 Hz per channel. This was slow enough to actually read the values in real time to ensure the settings of the machine were correct. The travel speed and electrode feed speed were measured with a tachometer. If the voltage output of the tachometer is measured at too high of a sample rate, the ripple from the armatures on the motor becomes visible. This is not necessarily a problem, but is does require the system to do calculations to generate a single value for the speeds. The data acquisition system's software did not have the capability to do this in real time. Therefore, the slow sample rate allowed for the machine to be adjusted and monitored in real time as is was operating.

The second data acquisition system that was used measured only the welding voltage and the welding current. This system used a DI 158U data logger which sampled at a much higher rate of 7.2 kHz per channel. The data collected from this system was processed using Matlab® software to produce histograms of the voltage and current, and then create three dimensional plots of the entire weld. This methodology was first used *by* Carter *et al.* (60) to determine the effect of the power source type on E9015-B9 SAMW electrodes.

Monitoring the welding voltage and amperage in real time has become a necessity when welding with new inverter type power sources in any situation where heat input is critical. This technique was adapted to the mechanized SMAW in order to insure that

each electrode was welded with identical conditions. Any variation in the welding parameters could affect the amount of alloying elements transferred across the welding arc.

4.7 Percent Recovery of a Specific Alloying Element

The amount of an alloying element which is present in the weld deposit compared to the total amount of that element which available in the consumed electrode is known as that element's percent recovery. This is not yet a standardized method; many manufacturers refer to percent recovery of SMAW consumables in different ways. In the scope of this work, percent recovery of a given alloying element shall be defined as: the total amount of an alloying element which exists in the electrode, calculated by the total amount, by weight percent, in the core wire plus the amount in the flux coating, divided into the amount, in weight percent, of the same alloying element which is present in the weld deposit. For example, if the amount of a specific alloying element (X) is known in the core wire, the coating and in weld deposit, the percent of recovery can be determined by Equation 4.1(41) written below.

$$\frac{(wt\%\ X(deposit))}{[(wt\%\ X(coating) + (wt\%\ X(wire)]}$$

Equation 4.1 Percent recovery of element X

The recovery rates for selected alloying elements were calculated using this method to observe how recovery rates changed when the alloying elements in the flux coating are varied.

The core wire composition was taken from the wires' certified material test report or CMTR and is listed in Table 4.1. The amount of the alloying elements was taken from the weight percent that was added in the dry mix, not the percent of dry mix plus binder. It was calculated in this manner because the amount of binder that is required is dependent on the temperature humidity level, and type of extrusion equipment. The majority of the binder is water which is removed when the electrode is dried and baked. The final composition of the non-diluted weld deposit was analyzed by optical emission spectroscopy.

4.8 SS DTA Solidification Range Measurements

Single Sensor Differential Thermal Analysis Method or SS DTA was developed at The Ohio State University. This process uses a single thermocouple to measure the temperature of the liquid metal as it solidifies. There are a few variations of this test, it can be performed with a weld metal button all of one alloy or a variation is to use a second smaller button of a differing alloy to simulate a weld. For this work the process was modified from the traditional set up which involved using a GTAW system to form a puddle of molten metal and then plunging the thermocouple into the puddle as it solidifies. The basic schematic is illustrated in Figure 4.5 (40)

The focus of this work was to measure solidification of a SMAW weld puddle. Therefore the thermocouple was mounted to an air solenoid which was wired to a limit switch. As the welding electrode passed the limit switch the solenoid plunged the thermocouple into the weld puddle. Once the thermo couple data was collected it was analyzed using SS DTA software. This software is able to fit a regression curve to the data. When the data varies from the regression curve it implies that there is a change in energy which is not resulting in a temperature change. This phenomenon can only be the result of a phase change within the system.

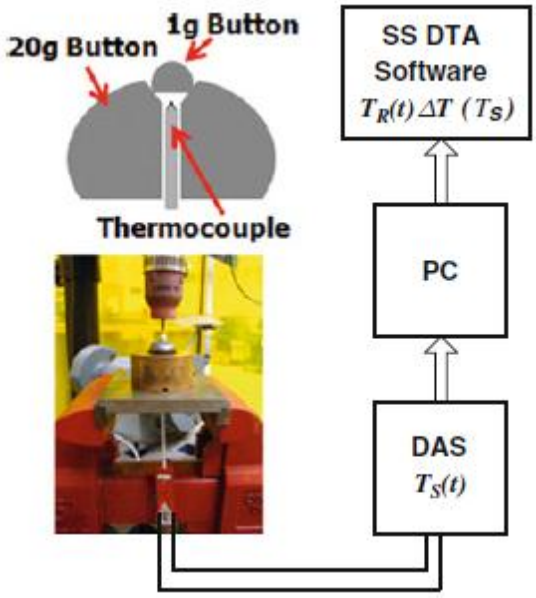

Figure 4.5 Schematic of the SSDTA GTAW and button method

The solidification range and solid state transformations were measured using single sensor differential thermal analysis. The procedure for these tests was modified from the traditional TIG and button procedure which was referenced in the section 2.2.1 and illustrated in Figure 4.5. In order to capture the solidification range of the weld pool from a SMAW electrode the weld needed to be made on base metal. The base metal used was C-276 for the ENiCrMo-4 and Hastelloy® B3® for the ENiMo-10. The coupon size was the same for each alloy to ensure that the cooling rate would be the same for all samples. To assure that all welding was done under identical conditions, the mechanized SMAW machine was set with a fixed electrode feed rate and travel speed. This allowed each electrode to be welded with the same conditions ensuring complete repeatability; it also standardized the size and shape of the weld pool. As the welding electrode passed the limit switch, the solenoid plunged the thermocouple into the weld puddle at a standardized depth. The solenoid was mounted in the same location for all tests and the coupon was also held in the same place by a fixture. The thermocouple data was

collected using Lab View® software and these processed using the SS DTA software in an attempt to determine the liquidus and solidus temperatures. The data was then processed using the same methodology as a sample prepared using the GTAW and button method.

4.9 Solidification Modeling Simulations

The solidification range was predicted using two different types of modeling software, JMatPro and Thermocalc. Using the Scheil solidification module in the Thermocalc® software a plot which showed the temperature ranges when each phase formed under non-equilibrium solidification conditions was created.

A step profile calculation was performed with the JMatPro simulation software. This calculation predicted the amount of each phase which would be present at a given temperature. This software can also predict the amounts of each element which would be present in each phase. This is extremely useful in understanding how the addition of a single element to the weld deposit can affect all the phases which may be present, and would thereby affect the mechanical or corrosion properties.

4.10 Susceptibility to Solidification Cracking by Cast Pin Tear Test

The procedure for the cast pin tear test was the same standard procedure which was developed by The Ohio State University Metallurgy Group and reference is section 2.2.2. In this procedure buttons are produced according to Table 4.6 using the same equipment in shown Figure 2.10. The buttons were cast with the GTAW torch in the cast pin testing apparatus at an amperage setting of 250 amps.

pin length inches	2	1.875	1.75	1.625	1.5	1.375	1.25
button weight grams	16	15.5	15	14.5	14	13.5	13
pin length inches	1.125	1	0.875	0.75	0.63	0.5	
button weight grams	12.5	12	11.5	11	10.5	10	

Table 4.6 pin lengths and button masses for CPTT

The sample material was taken from the all weld metal multi-pass deposits three button for each pin size were made, see Figure 4.4 for the locations. The pins were cast at an amperage setting of 150 amps. The only modification to the standard test was starting with the two-inch length pin because ENiCrMo-4 and ENiMo-10 are not prone to solidification cracking. If the sample showed any signs of cracking, the test was repeated using a shorter pin length. This was repeated until there were two consecutive pin lengths for which no cracks were visible using an American Optics model 570 stereoscope and a Bausch and Lomb Stereozoom 7 stereoscope. The pins were held in a custom built holder which allows the pin to rotate and take a radial measurement. The fixture and stereoscope setup that was used is illustrated in Figure 4.6

Figure 4.6 Cast pin evaluation system

4.11 Metallurgical Characterization Optical Microscopy, SEM, and EDS

The samples which were prepared for optical microscopy were first mounted using a Leco PR-32 mounting press and Leco Bakelite. The samples were then ground from a 240 grit SiC paper down to an 800 grit SiC paper. Finally they were polished with a 3 micro diamond paste and an ethyl alcohol lubricant. Samples were cleaned in an ultra-sonic bath between each grinding and polishing step. The weld metal microstructure was then observed using a Nikon Epiphot metallograph to observe the general features and soundness of the welded microstructure. The metallurgical characterization was to ensure that the weld metal was free from discontinuities such as inclusions or cracking which could be caused by the variations in the flux coating.

The metallography samples that were to be analyzed by the SEM were mounted in a conductive Bakelite and went through the same polishing sequence as the other metallography samples, but they spent and additional 12 hours on an Beuhler Vibromet 2 polisher using a non-crystallizing 0.05 micron colloidal silica. The samples were then electro-etched with a solution of 15g CrO_3, 150ml of H_3PO_4, and 20ml H_2SO_4 the sample was submerged and held at a potential of 6 volts for 30 seconds. A Quanta 200 scanning

electron microscope was then utilized to determine if the weld metal had multiple phases and search for any evidence of gamma prime. Any secondary phases were then identified using energy dispersive spectroscopy analysis or EDS.

4.12 Tensile Testing

Tensile samples were machined from the all weld metal multi-pass deposits. The electrodes of interest were alloyed with titanium, aluminum, and unalloyed baseline electrodes. These samples were chosen because the additions of aluminum and titanium promote the formation of gamma prime which can increase the tensile strength of the nickel based alloys. According to the literature, even small additions of aluminum and titanium can increase the tensile strength.(15) These elements have a high affinity for oxygen and are known as deoxidizers. They are very effective at removing oxygen from the weld pool; this results in less porosity in the weld deposit. It also makes it very difficult to transfer aluminum and titanium into the weld deposit.

The tensile samples were T3 tensile samples commonly referred to as a “252” or T3. The reduced cross section is 0.252 inches and the gauge length is 1.60 inches. The samples were tested with a 20,000 lb tensile machine at an extension rate of 0.25 inches per minute. The allowable extension rate for the tensile testing according to the AWS code is between 0.05 inches per minute and 0.5 inches per minute. When pulling tensile samples a slow extension rate, 0.05 inches per minute, will result in better yield strength and lower ultimate tensile strength. A fast extension rate will result in lower yield strength and higher ultimate tensile strength. In order to average this affect the middle of the AWS allowable range was chosen.

Chapter 5 Results

5.1 Effect of Alloying Additions on Arc Stability and Electrode Operating Characteristics

To keep the arc length and welding voltage constant for the electrodes with varying amount of alloying elements in the coating, the feed speed was adjusted. There was only slight variance in the electrode feed rate over the entire range of coating compositions. The alloying elements had little effect on melt off rate of the electrode. Since the arc length is relatively constant, the rate that the electrode is fed in to the weld pool is equal to the rate at which the electrode is melting. The dominating factor in the melt off rate appears to be the core wire which was used to make the electrode. The graphs of average melting rate for the baseline coating compositions ENiCrMo-4 and ENiMo-10 are illustrated below in Figure 5.1. These baseline graphs illustrated how the composition of the core wire of a welding electrode influences the melt off rate.

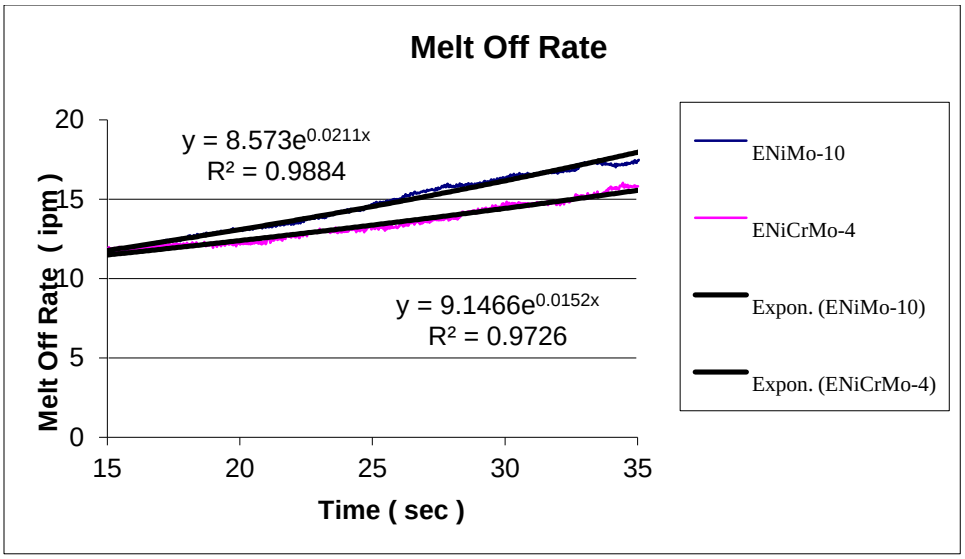

Figure 5.1 The melt off rate of ENiMo-10 and ENiCrMo-4 electrodes

An exponential trend line has been added and is a very good fit (notice the high R-squared values). The exponential trend line was chosen because the resistance heating of the electrode is the current squared times the resistance. This heating increases the melt off rate of the electrode; hence, the increase in feed rate to maintain a constant arc length. The trend lines have been calculated for all coating compositions of the ENiCrMo-4 electrodes and are given in Table 5.1 and the graph is illustrated in Figure 5.2.

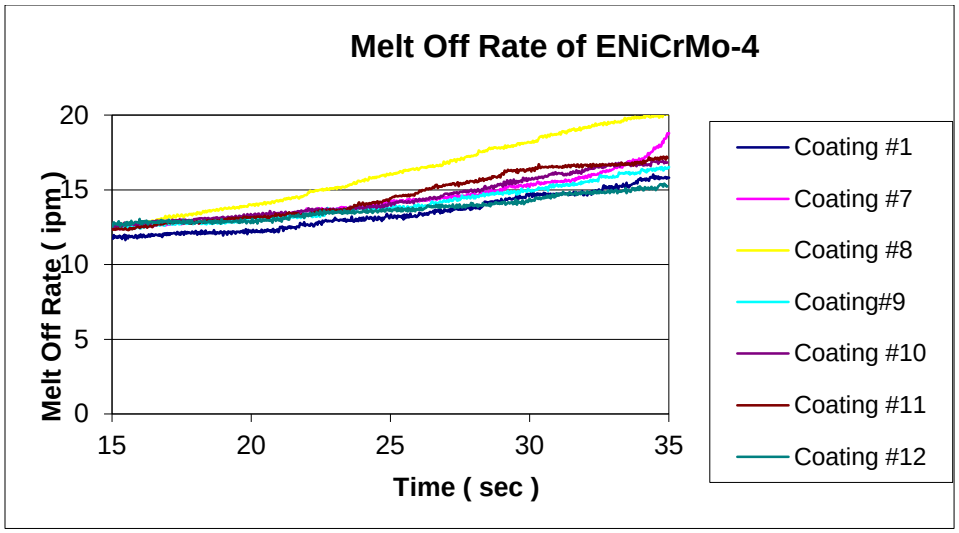

Figure 5.2 Comparison of the melt off rates for all ENiCrMo-4 electrodes.

If the welding arc was perfectly smooth and calm it would produce a melt off rate which increased exponentially and as the electrode heated up from resistance heating. Therefore, the R squared values represent how close a predicted exponential trend line is to the actual melt off rate. Thus, the lower the R squared value the more variation which would be caused by inconsistences in the welding arc. Since the only difference among these electrodes are the coating ingredients then the lower the R squared, is value the greater the influence of a coating ingredient. All of the R squared values and the equations for the exponential trend line are listed in Table 5.1.

Mix Number	Alloying Additions	Exponential Trend line Of Average Melt Off Rate	R-Squared Value
1	None	$y = 9.1466e^{0.0152x}$	0.9726
7	Al	$y = 9.4815e^{0.0164x}$	0.9564
8	Ti	$y = 8.5337e^{0.0251x}$	0.9967
9	Nb, Fe	$y = 9.846e^{0.0141x}$	0.9746
10	Mo	$y = 9.7145e^{0.0157x}$	0.9708
11	Ni	$y = 9.169e^{0.0185x}$	0.9734
12	Zr, Fe, Si	$y = 10.825e^{0.0095x}$	0.9615

Table 5.1 Equations for the exponential trend line of average melt off rate for the ENiCrMo-4 electrodes

These calculations were used to analyze the ENiMo-10 electrodes as well. In the baseline electrodes the ENiMo-10 electrodes had a slightly higher melt off rate. However the effect of the coating had opposite effects from the additions of alloying elements. In the ENiCrMo-4 electrodes the alloying additions generally increased the melt off rate. In the ENiMo-10 electrodes the alloying additions generally decreased the melting rate.

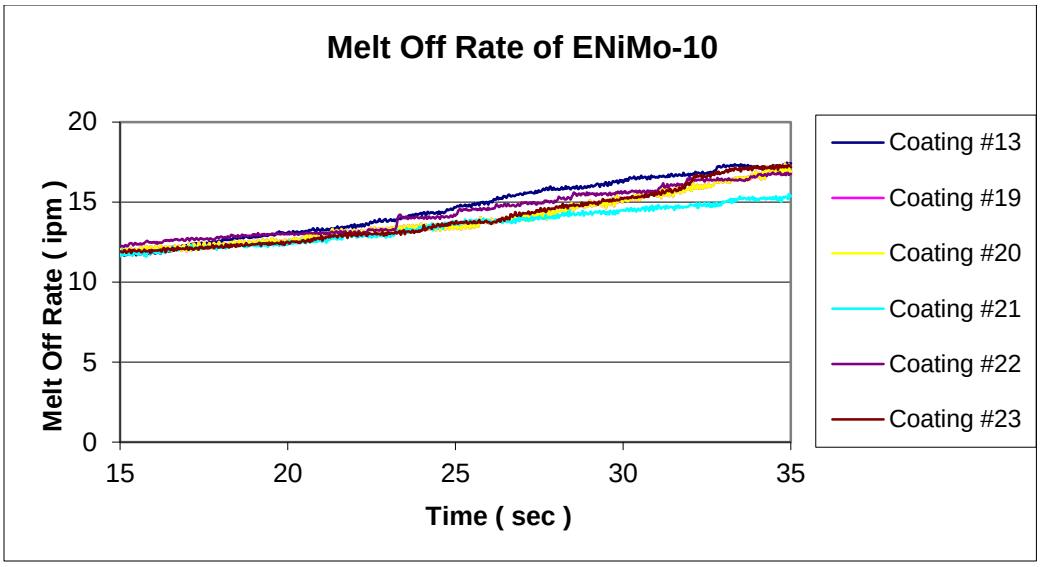

Figure 5.3 Comparison of the melt off rates for ENiMo-10 electrodes

The higher melt off rate is likely due to the fact that the ENiMo-10has a higher resistivity which increases the I^2R heating. Table 5.2 reinforces the claim that the melt off rate of the electrodes is closely modeled by an exponential trend line because the R-squared values are very close to one.

ENiMo-10			
Coating Number	Alloying Additions	Exponential Trend line Of Average Melt Off Rate	R-Squared Value
13	None	$y = 8.573e^{0.0211x}$	0.9884
19	Al	$y = 8.8994e^{0.0178x}$	0.9669
20	Ti	$y = 8.8994e^{0.0178x}$	0.9669
21	Nb, Fe	$y = 9.4948e^{0.014x}$	0.9858
22	Mo	$y = 9.3538e^{0.0169x}$	0.976
23	Ni	$y = 8.4591e^{0.0199x}$	0.9682

Table 5.2 Equations for the exponential trend line of average melt off rate for the ENiMo-10 electrodes

5.1.2 Arc Analysis Voltage and Current Histogram

The stability of the electric arc which is produced by a SMAW electrode is very important to creating sound welds. If the welding electrode melts inconsistently, it will cause sporadic metal transfer which leads to increased defects and discontinues. The arc stability and the metal transfer of a SMAW electrode have been very difficult to quantify because of inability to obtain raw numerical data in real time. When this data was available it was only pertinent to the specific welding operator. However, the automatic stick welding machine removes the operator from the equation. The data acquisition system was designed to be able to capture the true amperage and voltages of welding in real time.

The key indication of a stable and smooth operating welding arc is the metal transferring smoothly into the weld pool. This is a function of both the welding voltage and the welding current. Welding voltage is created from the gap between the electrode and the base metal. However, the end of the electrode is melted and is constantly forming and releasing droplets of molten metal. If the droplets are the same size and are grown and released similarly, the voltage should decrease and increase with the droplets of molten metal as well. The more concentrated the particular voltage instances are to the average welding voltage the more consistent the droplets are. Traditional knowledge states that the transfer mode in SMAW is globular. However, when the percentages of the current instances are examined in the same graph as the voltage, it becomes apparent that the metal transfer is actually a combination of transfer modes. Figure 5.4 is a three dimensional plot of the baseline, non-alloyed ENiCrMo-4 electrode which was welded with the automated SMAW system. The largest peak which is close to the average voltage and amperage is most likely globular transfer. However, the spike which is at three to five volts appears to be short circuit metal transfer. This spike suggests that the voltage in SMAW goes to zero. However, the automated SMAW system cannot be used to determine this because in order to function it generated a background voltage of about the three to four volts. Therefore, this spike suggests the voltage goes to zero, but it is

impossible to be sure in this case. The midsized spike which is around the 150 amperage range represents when the metal was in a transitional transfer mode somewhere between short circuit and globular. This transfer mode was close to the average voltage, but much higher current. This suggests that in this transfer mode the arc gap was at the average length, but the arc had very low resistance.

The plot for the ENiMo-10 was very similar and is illustrated in Figure 5.5. The main different is that the peaks on the graph which represent the different transfer modes are more concentrated. This may be due to the fact that the molten metal at the tip of an ENiMo-10 welding electrode has a higher surface tension which allows for a larger droplet of metal to form under the same welding conditions.

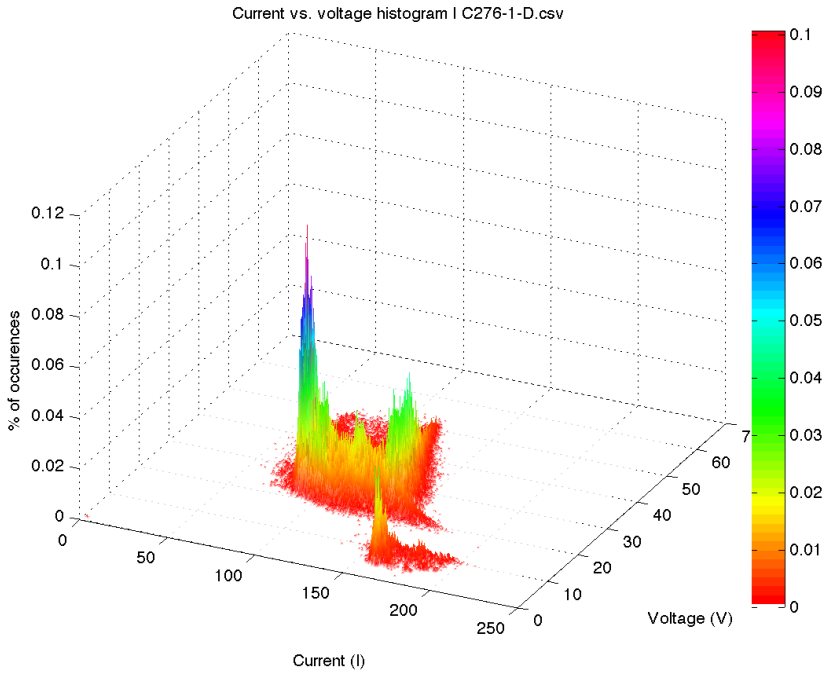

Figure 5.4 ENiCrMO-4 current and voltage histogram

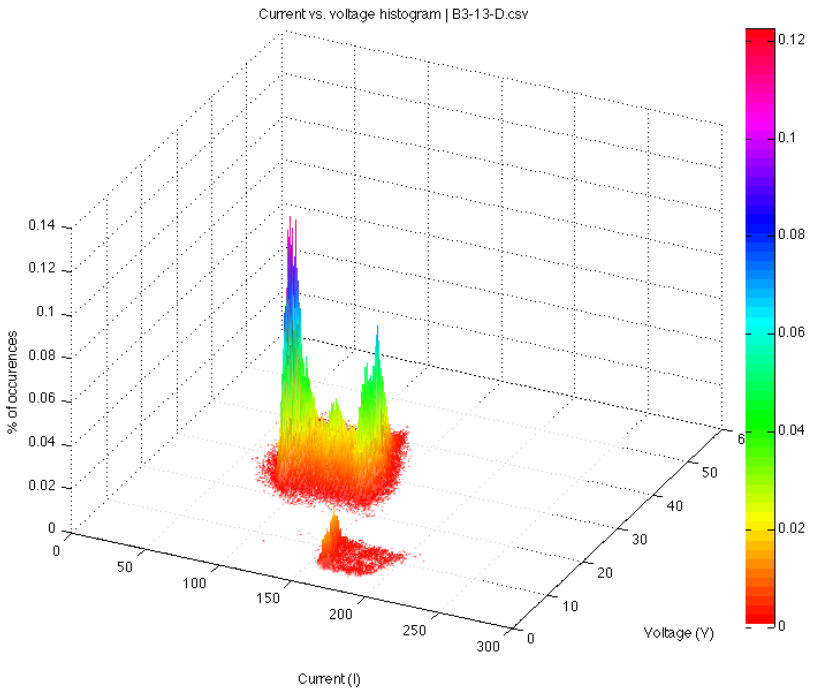

Figure 5.5 ENiMo-10 current and voltage histogram

When comparing the arc stability of the ENiCrMo-4 to the ENiMo-10 it is apparent that Figure 5.5 does not have as much scatter in the low voltages which means that the metal transfer is more constituent and focused. On that criteria it can be stated that ENiMo-10 is more stable than ENiCrMo-4.

Comparing the effect of coating additions within a specific electrode class is not as straight forward. The histogram of the current and voltage makes in too difficult to interpret the difference. However if the histograms of the voltage are examined without the current it becomes clearer. Figures 5.6 through 5.8 are the voltage histograms for the ENiCrMo-4 electrodes the red line is at 25 volts the setting of the automatic SMAW machine. Figures 5.9 through 5.11 illustrate the voltage histograms of the ENiMo-10 electrodes.

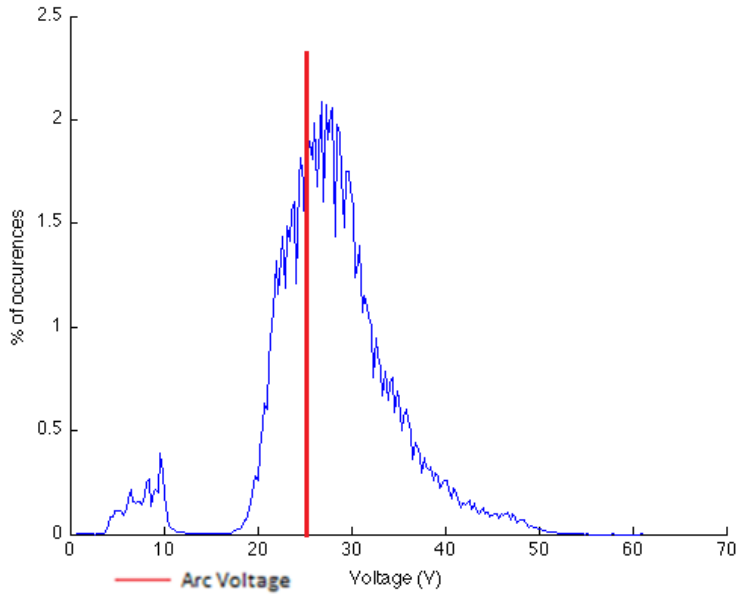

Figure 5.6 ENiCrMo-4 unalloyed coating

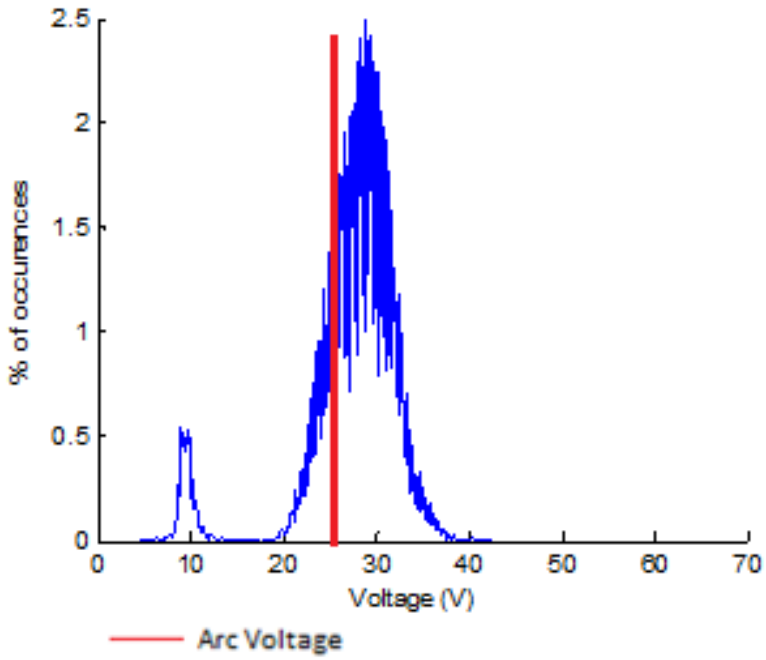

Figure 5.7 ENiCrMo-4 5 wt% aluminum in coating

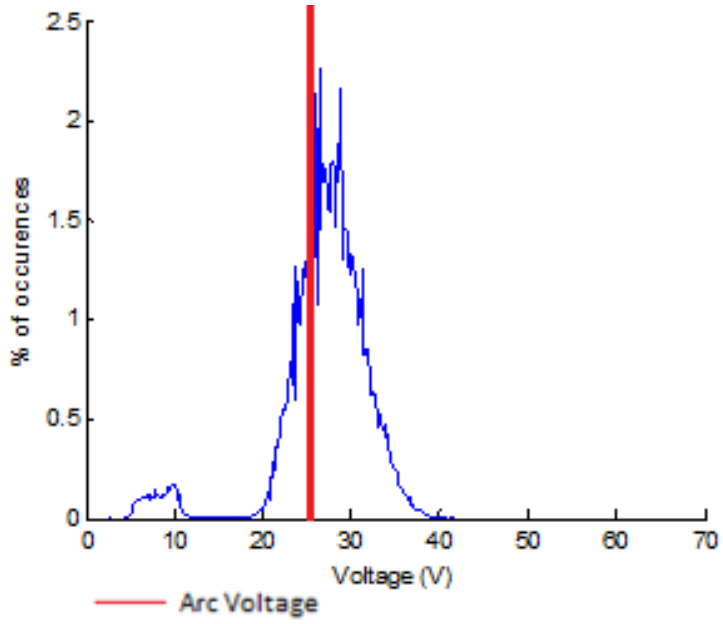

Figure 5.8 ENiCrMo-4 5 wt% titanium in coating

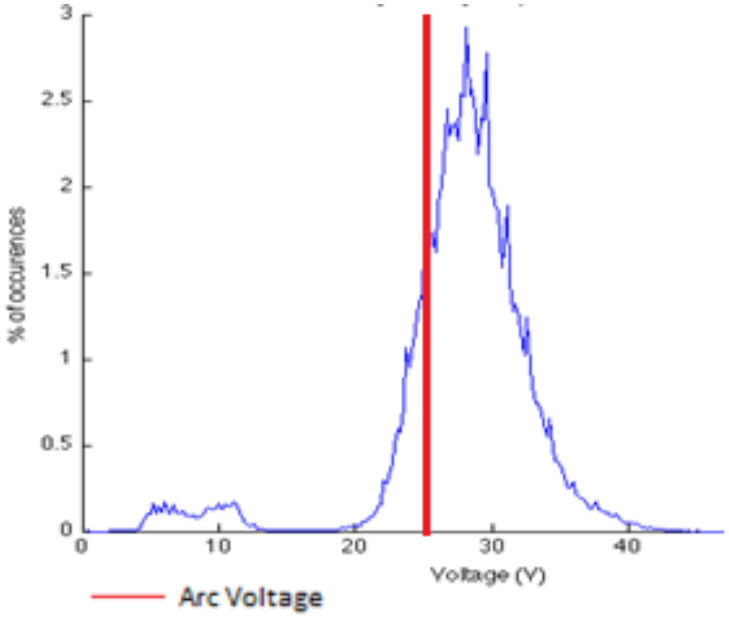

Figure 5.9 ENiMo-10 unalloyed coating

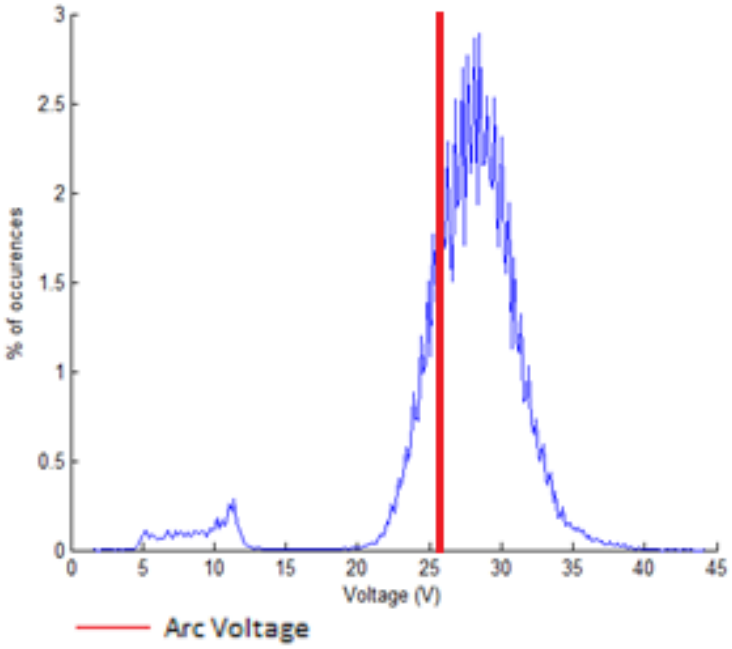

Figure 5.10 ENiMo-10 5 wt% aluminum in coating

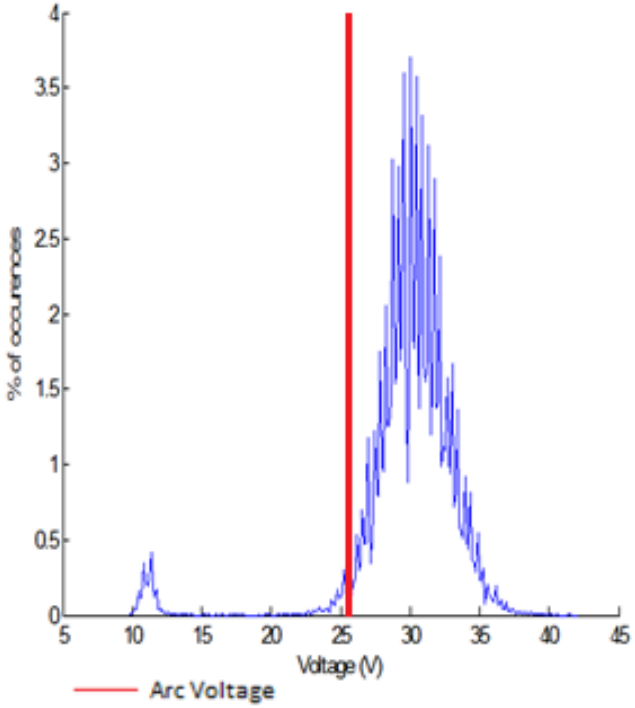

Figure 5.11 ENiMo-10 with 5 wt% titanium in coating

Analyzing the data for the true average voltage and standard deviation the subtle differences of the alloying additions become apparent. The true average voltage and the standard deviation are listed in Table 5.3

Electrode Type	Coating Addition	True Average Voltage	Standard Deviation
ENiCrMo-4	unalloyed	30.38	7.19
ENiCrMo-5	5 wt% Al	26.15	5.11
ENiCrMo-6	5 wt% Ti	26.93	5.08
ENiMo-10	unalloyed	26.24	5.49
ENiMo-11	5 wt% Al	26.57	4.56
ENiMo-12	5 wt% Ti	27.14	4.21

Table 5.3 Arc stability comparison

Using this method it is clear that the additions of aluminum and titanium help to stabilize the arc by smoothing out the metal transfer and titanium is slightly more effective than aluminum. Table 5.3 also reaffirms that welding arc of anENiMo-10 electrode is more stable than the ENiCrMo-4 electrode. It can also be stated that the ENiMo-10 has a more stable metal transfer.

5.2 Effect of Coating Composition on the Recovery Rate of Alloying Elements

Below are Tables 5.4 and 5.5 which lists the weld deposit composition of each ENiCrMo-4 and ENiMo-10 electrodes which was determined using optical emission spectroscopy or OES.

Chemical Composition of ENiCrMo-4 Undiluted Weld metal							
Element	#1	#7	#8	#9	#10	#11	#12
Carbon	0.020	0.029	0.018	0.018	0.017	0.013	0.016
Manganese	0.29	0.40	0.37	0.32	0.29	0.29	0.36
Phosphorus	0.012	0.013	0.014	0.016	0.013	0.012	0.014
Sulfur	0.009	0.009	0.009	0.009	0.009	0.010	0.008
Silicon	0.14	0.56	0.59	0.22	0.13	0.15	0.88
Nickel	56.39	55.07	55.56	55.66	55.09	59.43	55.30
Chromium	14.98	16.32	15.93	15.23	15.21	14.23	15.74
Molybdenum	16.240	15.820	15.770	15.650	17.590	14.760	15.660
Vanadium	0.117	0.141	0.138	0.126	0.121	0.108	0.136
Niobium	0.020	0.040	0.040	0.730	0.020	0.020	0.040
Titanium	0.044	0.094	0.128	0.048	0.041	0.044	0.082
Cobalt	1.240	1.200	1.210	1.216	1.218	1.180	1.200
Copper	0.15	0.14	0.14	0.14	0.14	0.14	0.14
Aluminum	0.054	0.067	0.049	0.057	0.049	0.052	0.068
Boron	0.0010	0.0010	0.0010	0.0010	0.0011	0.0010	0.0010
Tungsten	4.04	3.92	3.90	3.90	3.89	3.73	3.90
Zirconium	0.006	0.005	0.004	0.005	0.005	0.005	0.035
Iron	6.20	6.11	6.06	6.61	6.11	5.77	6.36

Table 5.4 the weld deposit chemical composition of all ENiCrMo-4 electrodes

Chemical Composition of ENiMo-10 Undiluted Weld metal						
Element	#13	#19	#20	#21	#22	#23
Carbon	0.011	0.016	0.011	0.011	0.015	0.011
Manganese	0.35	0.52	0.50	0.41	0.30	0.34
Phosphorus	0.008	0.008	0.008	0.011	0.008	0.008
Sulfur	0.009	0.008	0.008	0.008	0.008	0.009
Silicon	0.03	0.61	0.52	0.14	0.01	0.03
Nickel	67.94	67.40	67.37	67.18	64.61	69.78
Chromium	1.27	1.44	1.41	1.35	1.25	1.21
Molybdenum	31.130	30.490	30.680	30.267	34.890	29.390
Vanadium	0.043	0.052	0.050	0.046	0.046	0.039
Niobium	<0.01	0.020	0.010	0.620	<0.01	<0.01
Titanium	0.042	0.170	0.208	0.050	0.040	0.042
Cobalt	0.121	0.118	0.118	0.118	0.116	0.124
Copper	0.05	0.05	0.05	0.05	0.05	0.05
Aluminum	0.061	0.070	0.066	0.066	0.068	0.066
Boron	0.0021	0.0021	0.0021	0.0020	0.0023	0.0021
Tungsten	0.06	0.06	0.06	0.06	0.06	0.06
Zirconium	0.007	0.007	0.007	0.007	0.009	0.007
Iron	1.18	1.09	1.11	0.44	1.50	1.21

Table 5.5 the weld deposit chemical compositions of the ENiMo-10 electrodes

5.2.2 Recovery Rates of Selected Alloying Elements

The data from Tables 5.3 and 5.4 was then used with equation 4.1 in order to calculate the amount recovered of selected alloying elements. The result of equation 4.1 is to be considered a unit less number. It is purely a tool to compare one flux coating to another. It is now important to remember the work of VanBemsta (47) who noted that alloying elements will recover much higher percentages when they are present in the core wire then when they are present in the coating. This is because as the fine metallic particles melt and are transferred through the arc, a much larger amount of surface area per volume exposed and thus they experience a higher rate of oxidation when compared to the larger volume droplets of molten core wire.

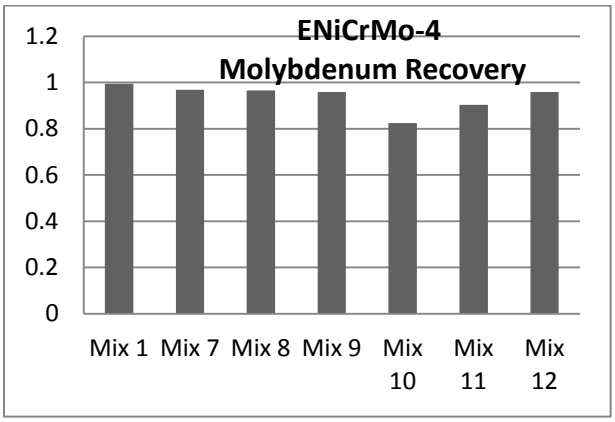

Figure 5.12 ENiCrMo-4 molybdenum recovery

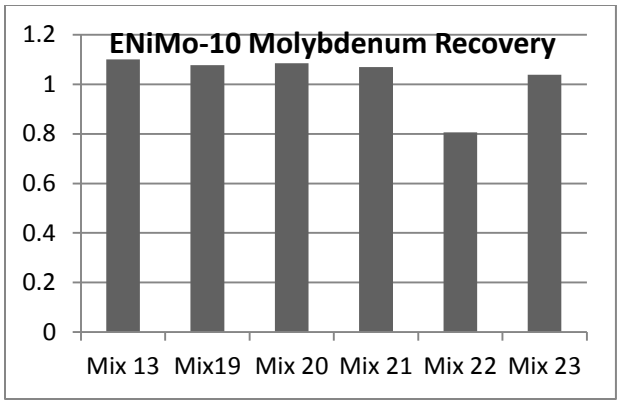

Figure 5.13 ENiMo-10 molybdenum recovery

Molybdenum is an alloying addition which is very important as a sold solution strengthener and for corrosion resistance. Molybdenum recovery is fairly steady in the ENiCrMo-4 electrodes; the only minor variation is in the ENiMo-10 mix 10 which had a five percent addition of pure molybdenum powder in the coating. The recovery for the molybdenum goes over 100 percent in the ENiMo-10, but these are unit less numbers and are valid for comparison. The same type of occurrence was apparent in ENiMo-10 in mix 22 which had 15wt% molybdenum powder added to the coating. These observations validate the work of VanBemsta.(47)

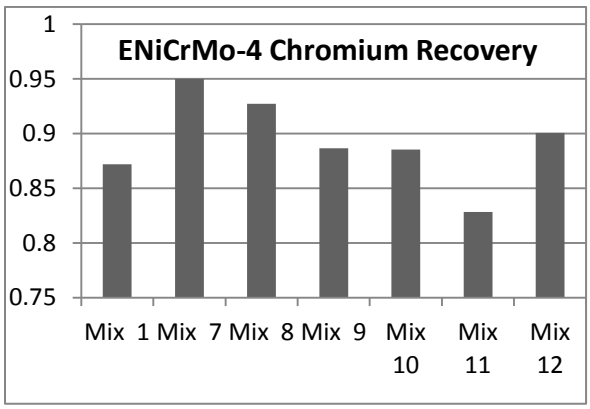

Figure 5.14 ENiCrMo-4 chromium recovery

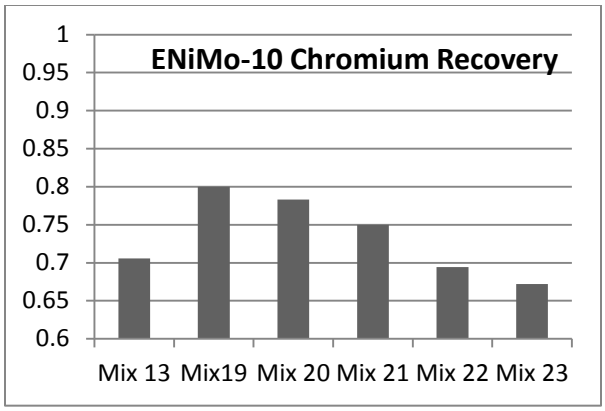

Figure 5.15 ENiMo-10 chromium recovery

The chromium oxidizes more easily than the molybdenum which is very apparent when comparing the recovery rates of the baseline coatings, mixes 1 and 13. Chromium is another element which is very important as sold a solution strengthener and for corrosion resistance. The chromium levels within a specific alloy can vary from heat to heat, which is why chromium is the element most often adjusted in an electrode coating. Graphs of the recovery rates for chromium are illustrated in Figures 5.14 and 5.15. Notice how the addition of deoxidizers, mixes 7, 8, 12, 19, and 20 increase the amount of recovery of chromium over the baseline recovery.

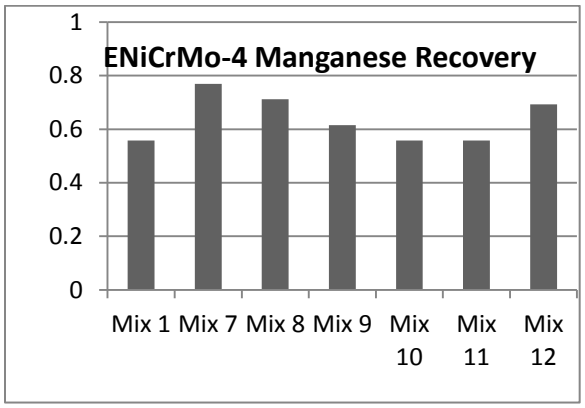

Figure 5.16 ENiCrMo-4 manganese recovery

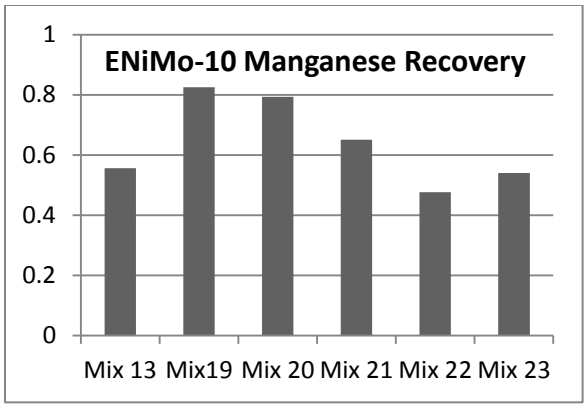

Figure 5.17 ENiMo-10 manganese recovery

Manganese is another element which increases the high temperature strength in nickel base alloys. However, it also has a relatively high affinity for oxygen and sometimes it has poor recovery when alloyed to the weld deposit through the flux coating. One way to improve the amount of recovery is to add additional deoxidizers.

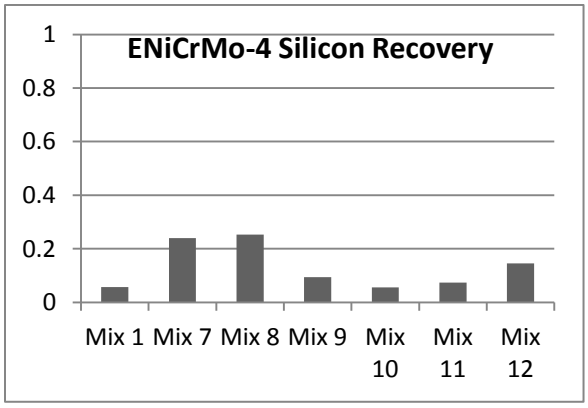

Figure 5.18 ENiCrMo-4 silicon recovery

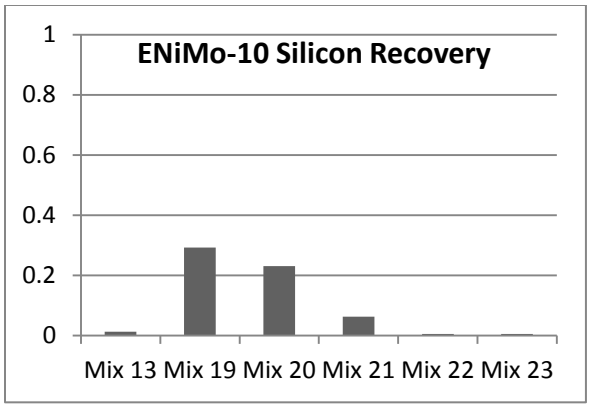

Figure 5.19 ENiMo-10 silicon recovery

The recovery rate of the silicon is much higher in the coating iterations which contained additional deoxidizers. The recovery rate of the silicon is also inflated because the binder is made of silicates which also contain silicon. The percent recovery for the deoxidizers is illustrated in Figures 5.20 through 5.23. Notice that the recovery rates are much lower than those of the other alloying elements due to extremely high affinity for oxygen of these deoxidizing elements.

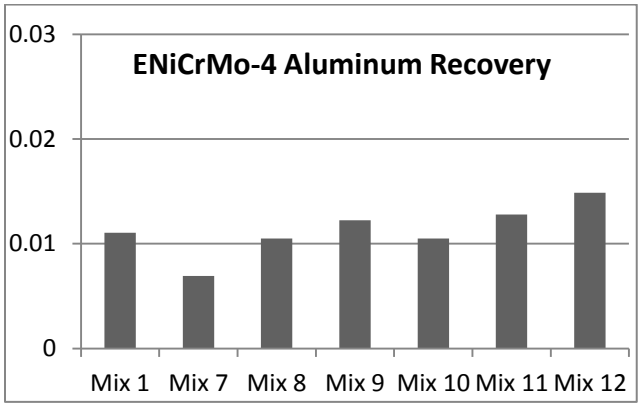

Figure 5.20 ENiCrMo-4 aluminum recovery

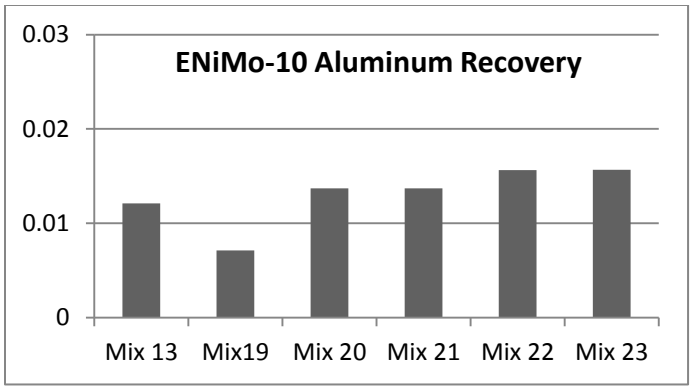

Figure 5.21 ENiMo-10 aluminum recovery

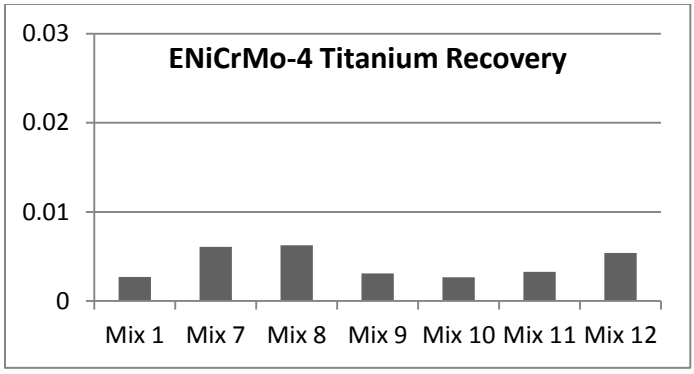

Figure 5.22 ENiCrMo-4 titanium recovery

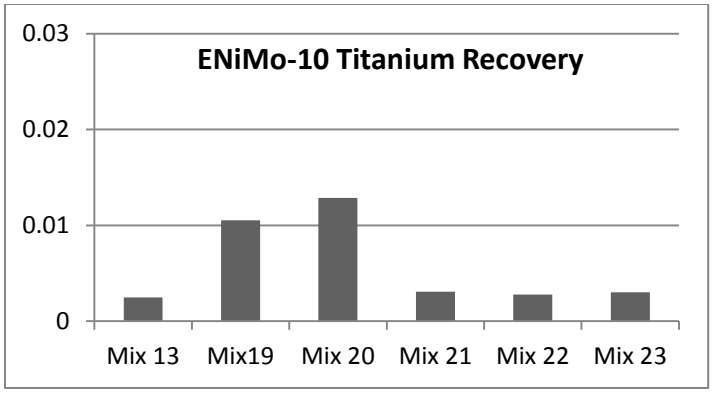

Figure 5.23 ENiMo-10 titanium recovery

The percent recovery can also be calculated for iron, niobium, and carbon in the same manner. Iron is only seen as an alloying element to reduce cost if there is concern for long range ordering, which is not a typical in these alloys. The niobium levels in these electrodes are very low which often renders these calculations somewhat meaningless because the levels are too close to the detection limits for OES which results in unpredictable readings. Carbon is another element which OES analysis is not recommended due to the rapid vaporization of carbon during the OES arc analysis.

5.3 Weld Solidification Behavior in ENiCrMo-4 and ENiMo-10 Electrodes

The SS DTA samples for the ENiCrMo-4 were welded on C-276 base metal and are illustrated below in Figure 5.24 the red arrows indicate the location of the thermocouple plunge. The SS DTA samples for the ENiMo-10 electrodes are illustrated in Figure 5.25

Figure 5.24 SS DTA samples for ENiCrMo-4 electrodes

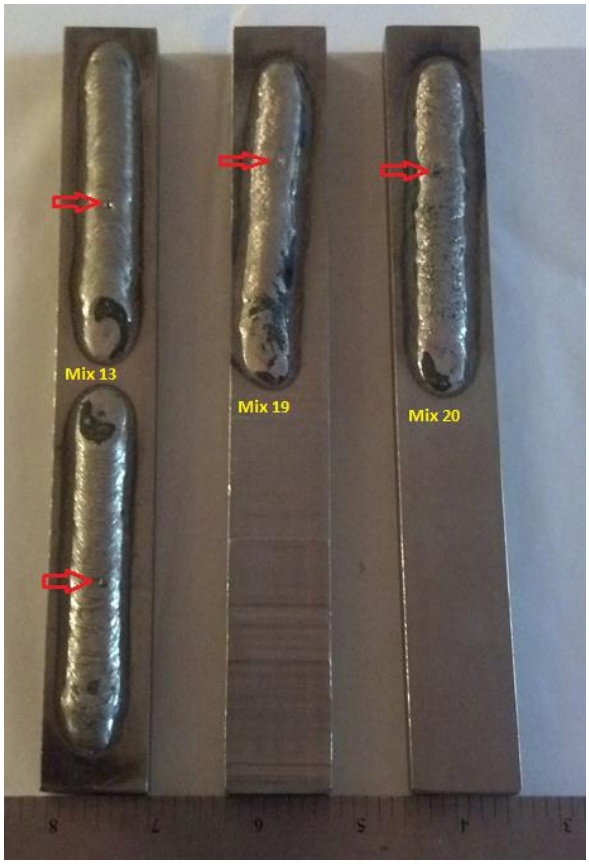

Figure 5.25 SS DTA samples for the ENiMo-10 electrodes

5.3.1 Additional noise from the welding arc

A thermocouple was plunged into the weld pool in order to determine the temperature range at which the liquid metal solidifies. The welding arc and SMAW machine produced a lot of background noise which caused some difficulty with the data. The traditional welding method of data collection for the SS DTA process is to use a GTAW torch to melt the metal over the sensor or plunge the sensor into a weld metal button as it solidifies. In both situations the arc is extinguished before the thermocouple is plunged into the molten metal. A comparison between using the SMAW machine and the GTAW with a weld metal button is illustrated in Figures 5.26 and 5.27. These graphs are both

from unalloyed ENiCrMo-4. Figure 5.24 used an all weld metal button and the GTAW welding process. Figure 5.25 used the mechanized SMAW and a pneumatic actuator controlled by an electromagnetic value, operated by a limit switch. This mechanism was used to plunge the thermocouple into the molten weld metal as the arc passed by.

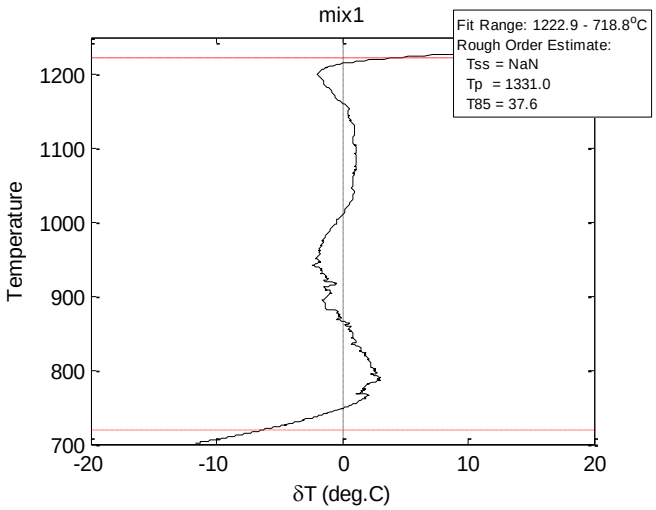

Figure 5.26 ENiCrMo-4 noise generated GTAW & button method

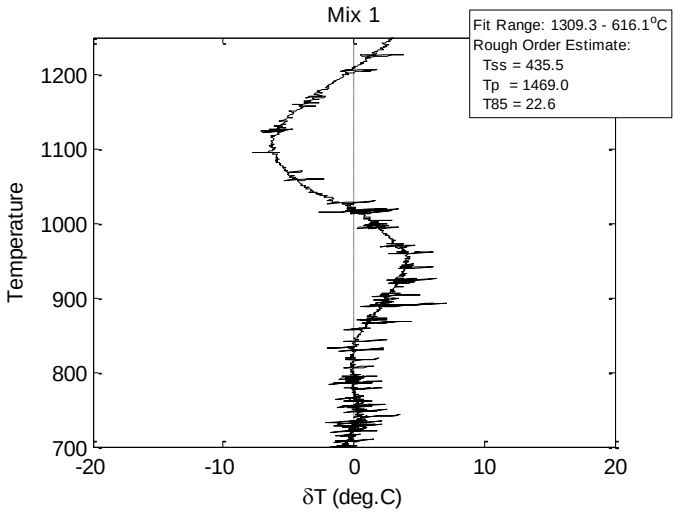

Figure 5.27 ENiCrMo-4 noise generated by automatic SMAW

The amount of noise which was created by the automatic SMAW machine made the data very difficult to interpret and the liquidus temperature which was not attainable because the welding arc was so close to the thermocouple at the time of the plunge.

5.3.2 Solidus temperature from SS DTA

The solidus temperature was measure for the ENiCrMo-4 and ENiMO-10 electrodes with unalloyed coating, 5 wt% aluminum and 5 wt% titanium. Figures 5.28, 5.29, and 5.30 represent the point at which solidification is complete in the ENiCrMo-4 electrodes.

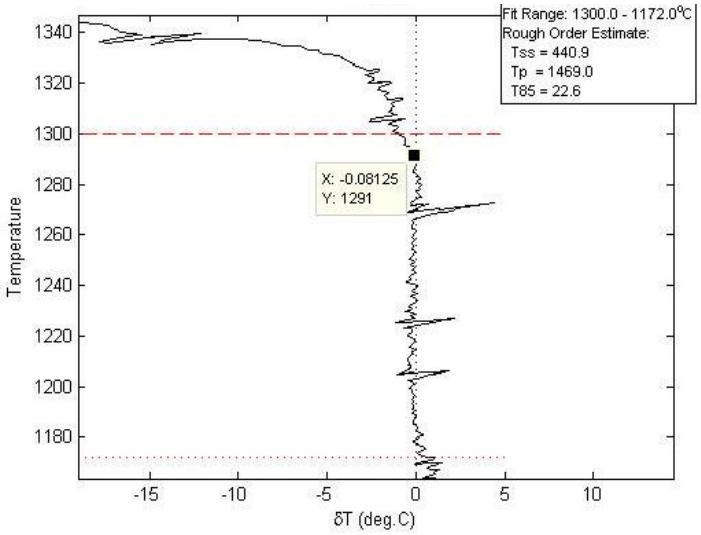

Figure 5.28 SS DTA plot for ENiCrMo-4 unalloyed coating

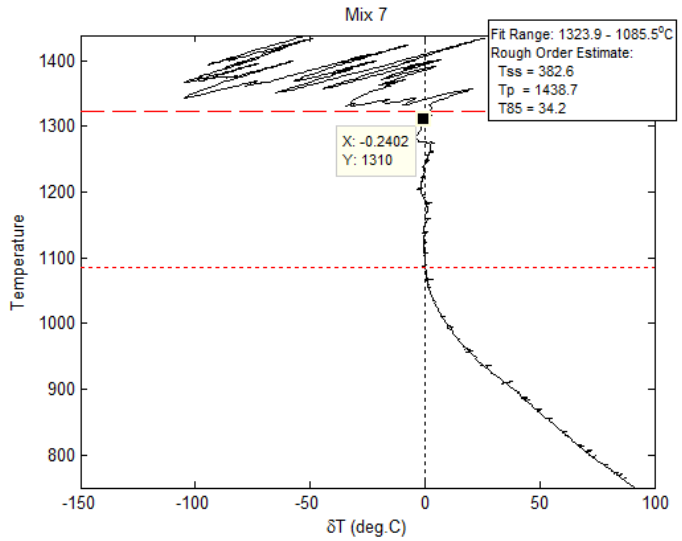

Figure 5.29 SS DTA plot of ENiCrMo-4 with 5wt% Al

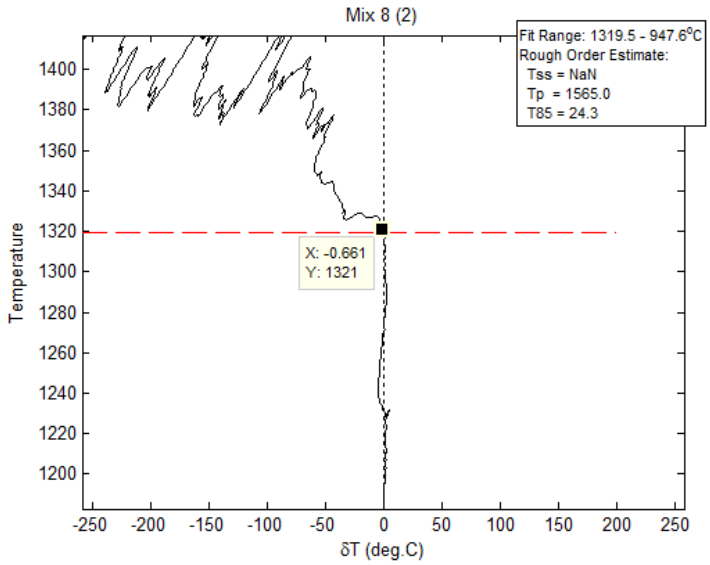

Figure 5.30 SS DTA plot of ENiCrMo-4 with 5wt% Ti

The overall results for the solidus temperature for the ENiCrMo-4 electrodes are listed in Table 5.6.

Electrode	Mix #	Alloying Addition	Solidus Temperature
ENiCrMo-4	Mix 1	None	1291°C
ENiCrMo-4	Mix 7	5 wt% Al	1310°C
ENiCrMo-4	Mix 8	5 wt% Ti	1321°C

Table 5.6 SS DTA solidus temperature SS DTA measurements

The results for the ENiMo-10 electrodes were processed in the same manner. However, the SS DTA plot for ENiMo-10 with unalloyed coating was made with data taken using a 20 gram button and GTAW torch to plunge the thermocouple because of an error in the data collection process using the SMAW process.

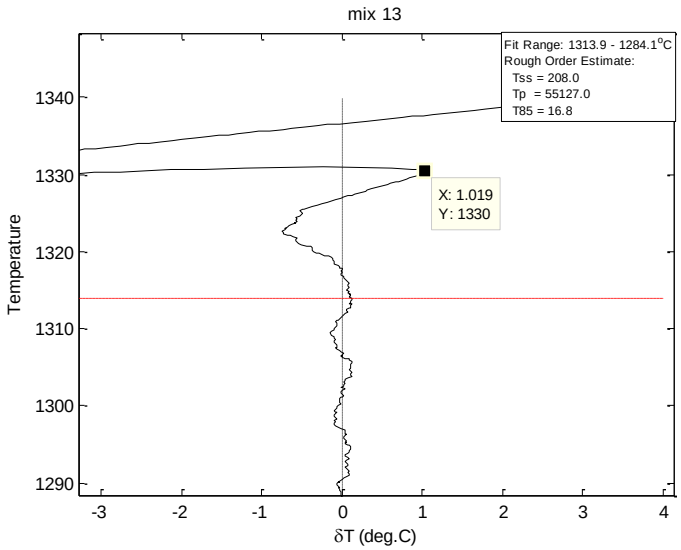

Figure 5.31 ENiMo-10 unalloyed coating GTAW button method

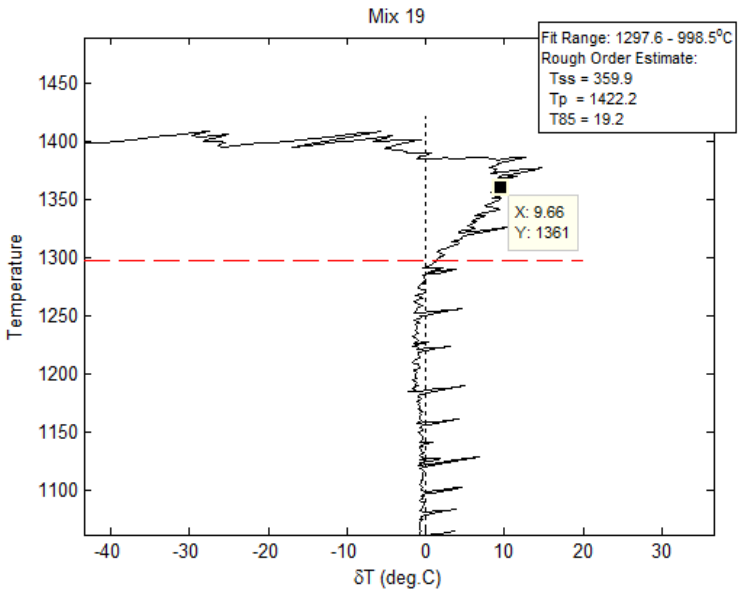

Figure 5.32 ENiMo-10 with 5wt% Al

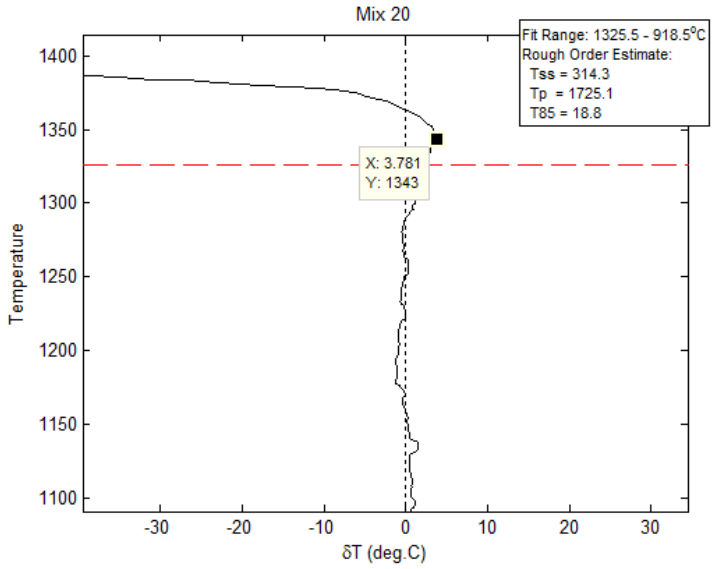

Figure 5.33 ENiMo-10 with 5wt% Ti

The overall results for the solidus temperature for the ENiMo-10 electrodes are listed in Table 5.7

Electrode	Mix #	Alloying Addition	Solidus Temperature
ENiMo-10	Mix 13	None	1330°C
ENiMo-10	Mix 19	5 wt% Al	1361°C
ENiMo-10	Mix 20	5 wt% Ti	1343°C

Table 5.7 SS DTA solidus temperature measurements for ENiMo-10

ENiMo-10 with the unalloyed coating was done with GTAW and button method. These results exhibited significantly lower solidus temperature than the plunges which were done with the automatic SMAW process. The difference of method appears to be the major factor in the 103 degree difference between the unalloyed coating and the coating with 5wt% Ti as an alloying addition. This dramatic difference was not observed in the ENiCrMo-4 electrodes which suggest that the process variation was the dominating factor.

5.3.3 JMatPro Simulation Step Temperature profiles

In order obtain reference points for comparison with SS DTA data. JMatPro software was used to identify phases and their relative abundance percent at a given temperature. The calculations were made using the chemical composition data taken from Tables 5.4 and 5.5, for mixes 1, 7, 8, 13, 19, and 20. The temperature range was from 1500°C down to 200°C with 50 degree steps. This simulation assumes equilibrium conditions at solidification. An example of these plots for the unalloyed ENiCrMo-4 is illustrated in Figures 5.34 and Figure 5.35 illustrates the unalloyed ENiMo-10.

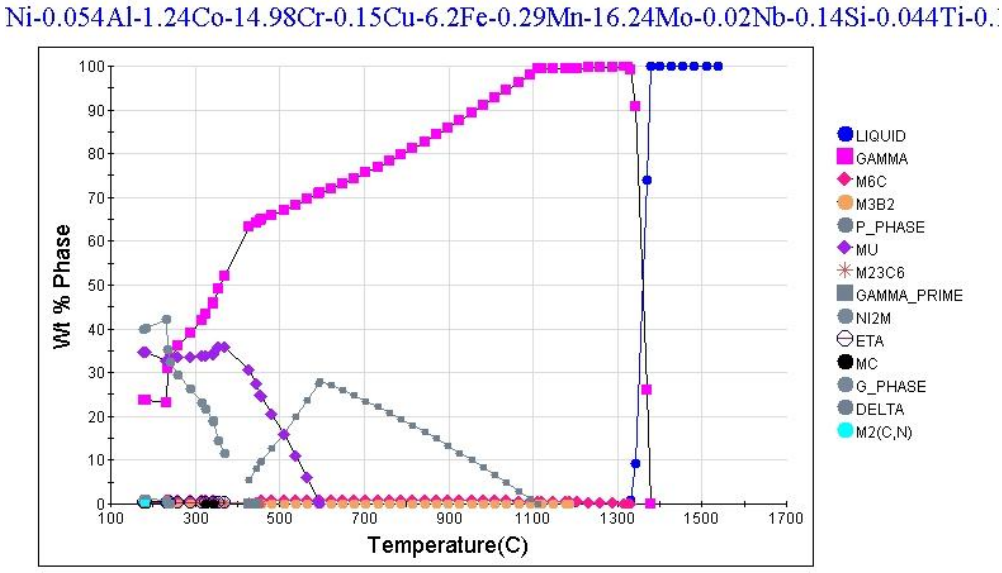

Figure 5.34 Step temperature profile for ENiCrMo-4

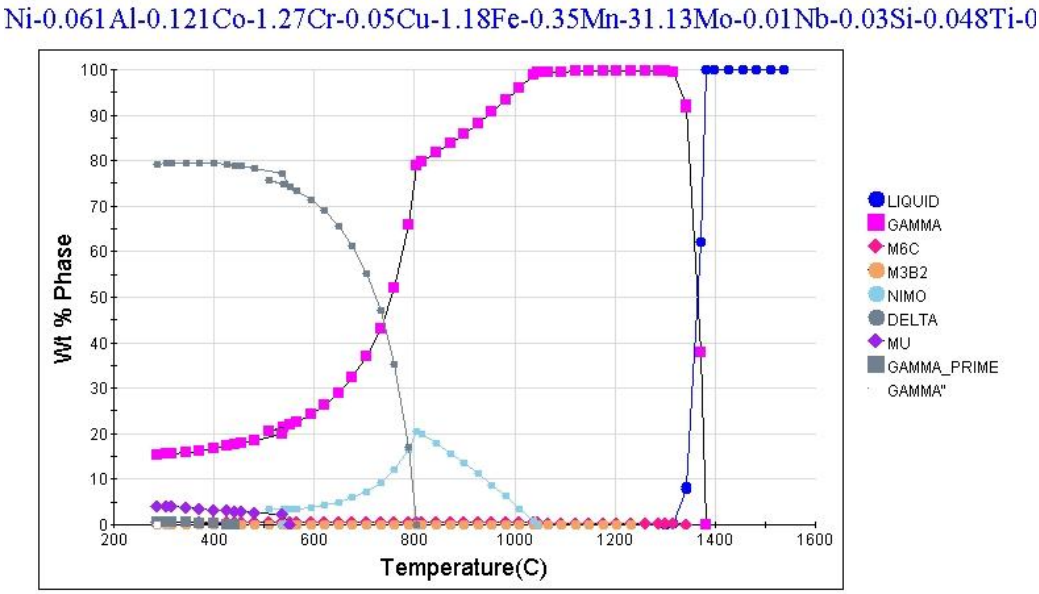

Figure 5.35 step temperature profile for ENiMo-10

These step profiles predict intermetallic phases which may not necessarily be present in the actual weld metal. The solid state transformations which are listed in these plots are all made assuming equilibrium conditions. The chemical compositions for both the ENiCrMo-4 and the ENiMo-10 had only minor differences and the step plots did not vary significantly.

5.3.4 Thermocalc Scheil Simulation

The scheil calculation was developed to predict the solidification range in a non-equilibrium condition, which is ideally suited to welding because the fast solidification rate. The Thermocalc® software includes a program which was designed to calculate the scheil solidification range under non-equilibrium conditions. The terminal solidification takes in to account the formation of carbides which may or may not form in reality this tends to depress the solidification range below what is typically measured. This calculation works very well, however the phases and elements must be limited in order to get reasonable results. For this work the tramp elements such as sulfur, phosphorus, and boron were omitted from the calculation. The only phases which were to be reported by the program were: Gamma phase, P phase, Mu phase, M6C carbide, NiMo, sigma, gamma prime, and delta prime. Figures 5.36 and 5.37 illustrate the base line plots.

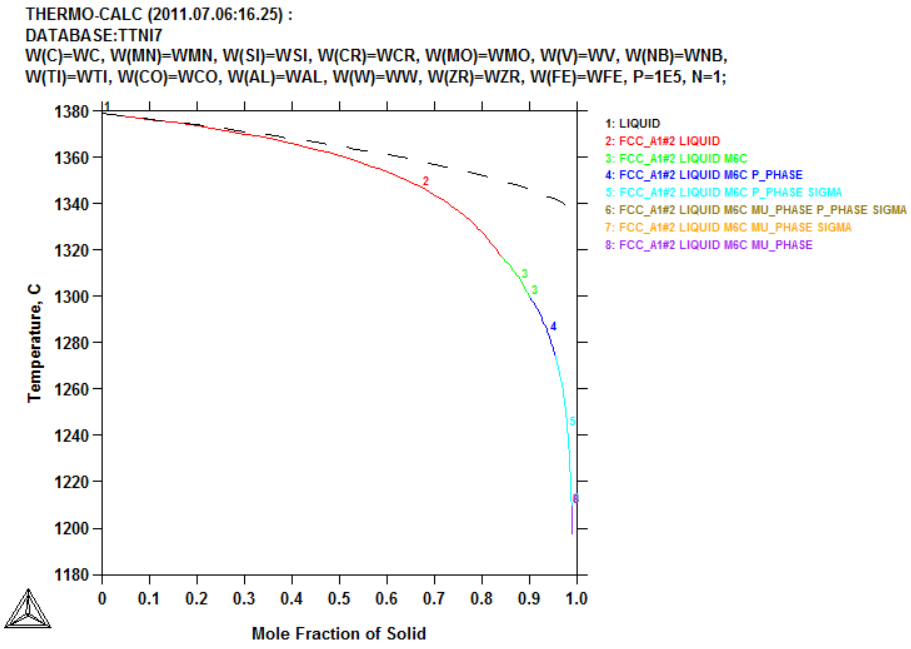

Figure 5.36 Scheil non-equilibrium solidification of ENiCrMo-4

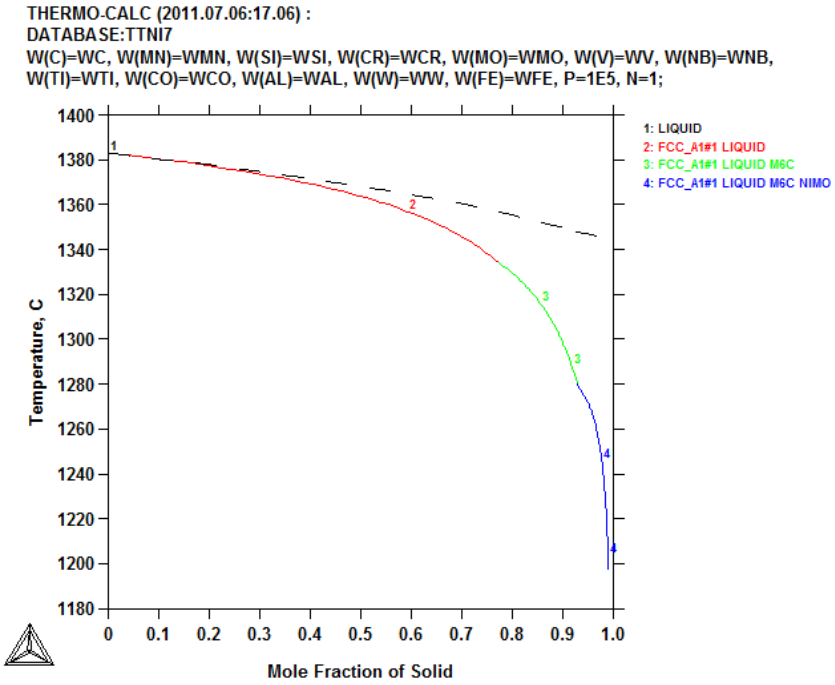

Figure 5.37 Scheil non-equilibrium solidification of ENiMo-10

5.3.5 Comparison of modeling software to SS DTA

The SS DTA results were then compared to both the JMatPro step results, which is equilibrium solidification and the Scheil simulation results, which is the solidification of the gamma phase along with the solidification for any terminal carbides which may form in the liquid. These results for the ENiCrMo-4 are listed in Table 5.8 and the ENiMo-10 listed in Table 5.9.

Solidus Temperature				
		JMatPro	Scheil	SSDTA
ENiCrMo-4	unalloyed	1325°C	1317°C 1197°C	1291°C
ENiCrMo-4	5wt% Al	1291°C	1304°C 1097°C	1310°C
ENiCrMo-4	5wt% Ti	1290°C	1292°C 1096°C	1321°C

Table 5.8 Comparison of solidus predictions and measurements for ENiCrMo-4

Solidus Temperature				
		JMatPro	Scheil	SSDTA
ENiMo-10	unalloyed	1301°C	1333°C 1197°C	1330°C
ENiMo-10	5wt% Al	1228°C	1314°C 1085°C	1361°C
ENiMo-10	5wt% Ti	1234°C	1304°C 1093°C	1343°C

Table 5.9 Comparison of solidus predictions and measurements for ENiMo-10

The modeling software predicted a decline in solidus temperature for all the alloyed coating weld metal compositions. The Scheil simulation lists two temperatures.

The first is the temperature in which the gamma phase solidifies the second is the terminal solidification of all the carbides. These carbides may not necessarily form and depress the solidification range, which is way both values are listed. The opposite trend was observed it the SS DTA measurements. This may be due to dilution effects from the base metal, even though this would be considered a matching weld metal the composition would not be the same as the undiluted weld metal. The solidus measurement for the baseline ENiMo-10 was significantly lower than the solidus temperature measurements on the other two ENiMo-10 electrodes. This is due to difference in the methods of data collection.

The method for taking SS DTA measurements using the automatic SMAW machine was moderately successful. However, the amount of background noise which was caused by the machine and welding arc made interpreting the solidus points very difficult. The liquids temperature could not be determining due to the close proximity of the welding arc. The temperature trends which were predicted from the modeling software did not follow the trend which was observed by the SS DTA measurements. It is undeterminable whether it was due to the amount of noise form the automatic SMAW machine or if it was due to dilution effects from the base metal.

5.4 Solidification cracking susceptibility in ENiCrMo-4 and ENiMo-10

The cast pin tear test has traditionally been used for base metals and specially prepared weld metal compositions. Using multi-pass all weld metal deposits can be somewhat problematic because the weld metal is not homogeneous. Each weld bead is a small cast structure which is comprised of dilution from previous beads and the electrode. Each of these weld beads is also segregated due to rapid solidification and cooling. Each sample was cut up from the multi-pass all weld metal deposit; therefore the chemical composition may not be identical from sample to sample. Refer to Figure 4.1 for the location of the CPTT samples.

5.4.1 Cast Pin Tear Test ENiCrMo-4

The results of the Cast Pin Tear for select mixes of the ENiCrMo-4 electrodes are listed below in Figure 5.38. There were a few anomalies in the maximum cracking response curves. In mix seven there were two pin lengths 1.625 and 2.00 which did not follow the trend because the samples were cast multiple times and were not necessarily homogenous due to the weld metal microstructure.

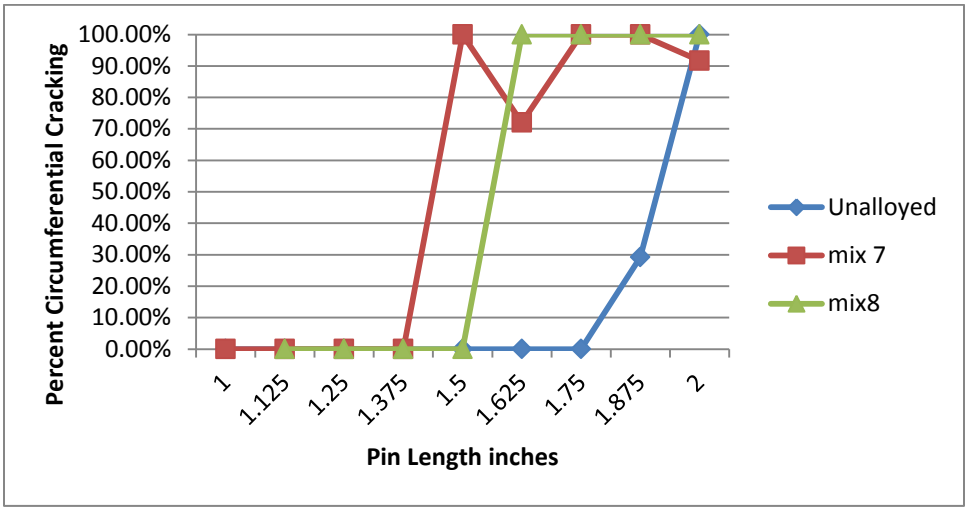

Figure 5.38 CPTT results for ENiCrMo-4 electrodes

In order to compare the results of one electrode to another in is useful to use the maximum pin length with no cracking, the minimum pin length with 100% cracking, and by subtracting the two lengths the zero to 100% cracking length range can be calculated. Each of these values can be used to compare the cracking susceptibility of one electrode to another. ENiCrMo-4 generally exhibits good resistance to solidification cracking which is why it did not have 100% cracking in all samples at the 2 mold length. The cast pin rankings for the ENiCrMo-4 electrode are listed below in Figure 5.39

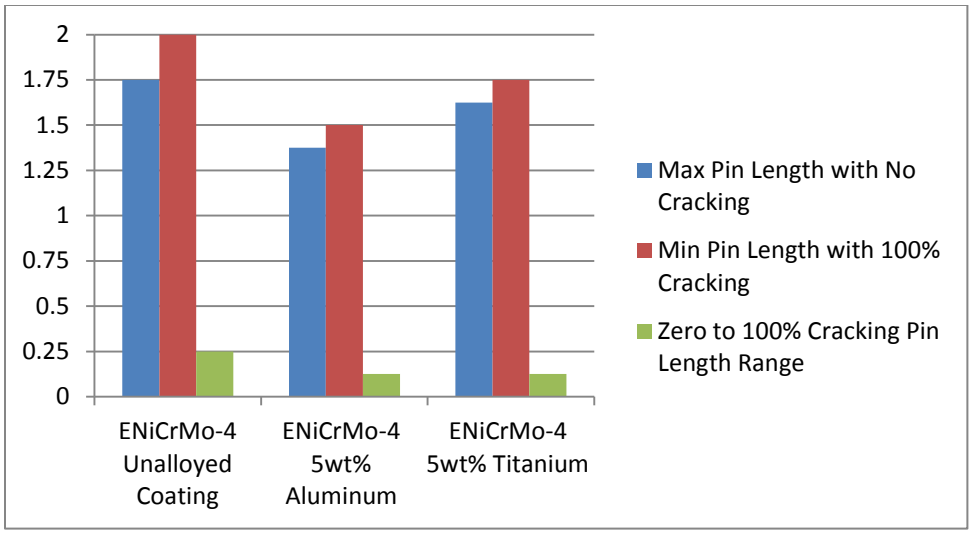

Figure 5.39 ranking results for ENiCrMo-4

5.4.2 Cast Pin Tear Test Results ENiMo-10

The results for the ENiMo-10 can be interpreted in the same manner as the ENiCrMo-4 and are listed below in Figure 5.40. The ENiMo-10 electrode demonstrated the same anomalies as the ENiCrMo-4 for same reason, the weld metal microstructure.

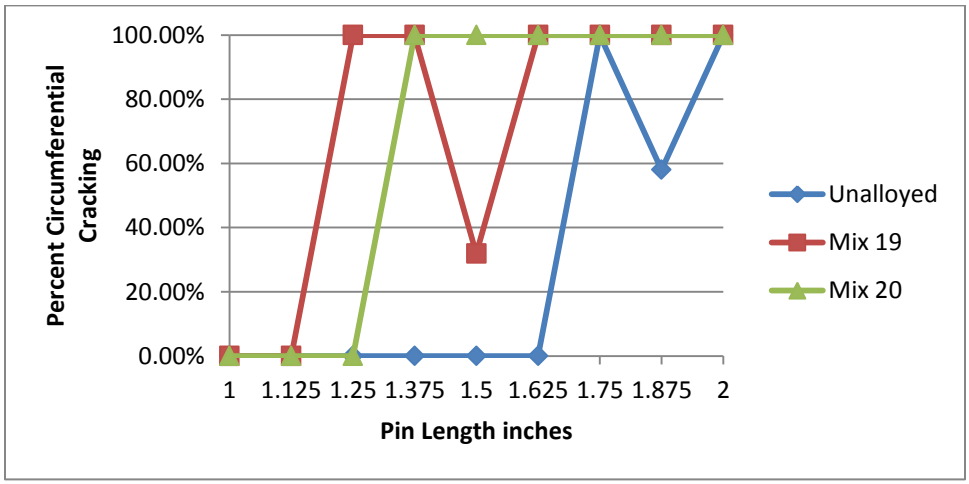

Figure 5.40 CPTT results for ENiMo-10

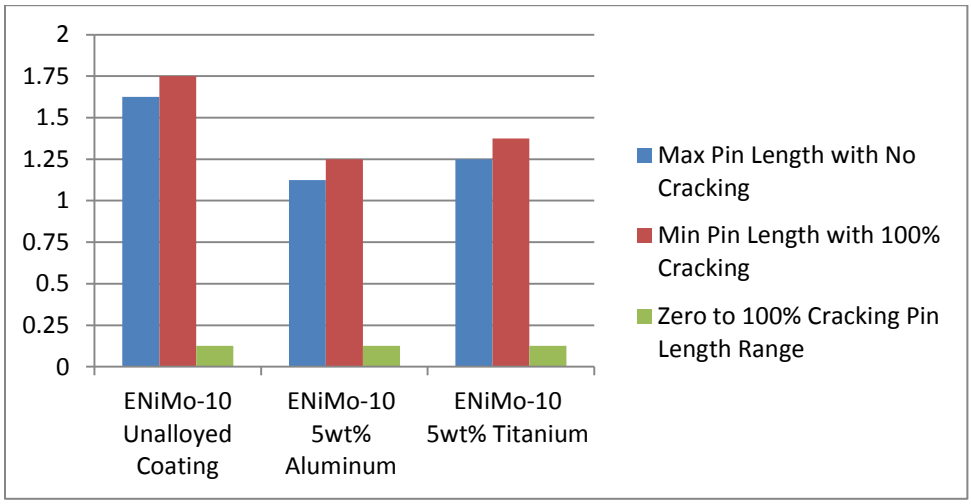

Figure 5.41 CPTT ranking results for ENiMo-10

5.4.3 Summary of cast pin tear test results

The cast pin tear test results are somewhat inconclusive. It can be stated according to this test ENiCrMo-4 is less susceptible to cracking than ENiMo-10, however, that goes against the literature.(11) It is also clear that in the ENiMo-10 additions of aluminum and titanium increase the cracking susceptibility of the electrode. However, when looking at Figures 5.38 and 5.40 it is obvious that the cracking range is not linear. There are two possible explanations for this behavior: the most likely is that the samples were taken from real weld metal build ups which are not homogeneous. Each weld bead is actually a small cast structure which allows for elements to segregate to dendrite cores and interdendritic regions. The samples were cut from larger pieces of weld metal and were not identical. Using the average value of three cast pins may not have been enough samples to statically smooth the trend lines created by the actual data points.

The second factor which may have altered the chemical composition is that many of the pins had to be cast multiple times due to inconsistences with the cast pin apparatus.

Both electrodes contained carbon which does burn in an electric arc. The copper molds are cleaned with alcohol between uses; any residue which may have been left in the mold may have added carbon and hydrogen which could affect the castability of the sample. Multiple castings may have burned out the carbon or added carbon which can form with niobium to from a low melting temperature eutectic which could result in the non-liner results which were observed.

The cast pin tear test has been proven to be an effective tool for comparing the cracking susceptibility of one alloy to another. However, it is less effective at comparing the subtle differences which can be caused by variations in the flux coating. This is primarily because of the lack of uniformity in the samples which are taken from all non-diluted weld metal samples. Inconsistences may also arise from multiple castings of the same sample. Three samples were not sufficient to statistically support this data and overcome these variations.

It may be possible to cast enough pins in order to get smooth trend lines and compare the variations in flux coatings. However, it would be more practical to create samples with a base line chemical composition and modify them individually with one alloying element sequentially order to determine the effect of each alloying element on the cracking response of the baseline compositions. Once the limit of each alloying element was found, tighter guidelines could be made in order to ensure that any variation which was caused by the flux coating would have known effects on cracking susceptibility.

5.5 Metallurgical Characterization of ENiCrMo-4 and ENiMo-10 Welds

The macro and micro structures of the weld metal were observed to insure that there are no negative metallurgical affects from the variations in the flux coating. The basic structures were first observed under the Nikon Epiphot metallograph.

5.5.1 Optical Microscopy of ENiCrMo-4

The macrostructure of the weldments made with the ENiCrMo-4 were typical of any nickel base welding consumables. The macro-structure of a weld deposit made with Mix 7 is illustrated in Figure 5.42

Figure 5.42 Macrostructure of ENiCrMo-4 mix 7

The structure is normal with larger grains growing from the center of the weld beads. These are not always visible in each cross-section, but are seen when the grains were oriented parallel to the cut surface. There is also some visible porosity which is not uncommon for nickel base weld metal. The AWS code 5.11 discounts any porosity which is smaller than 0.015 inch in diameter. Over all the cross section macro-structure of the ENiCrMo-4 electrode did not show any anomalies.

In mixes 7 and 8 which contained additions of aluminum and titanium respectively, when etching these samples to observe them for gamma prime phase, small inclusions of titanium were found. These inclusions appear red when the metal is etched at 6 volts in a solution of 15g CrO_3, 150ml of H_3PO_4, and 20ml H_2SO_4.

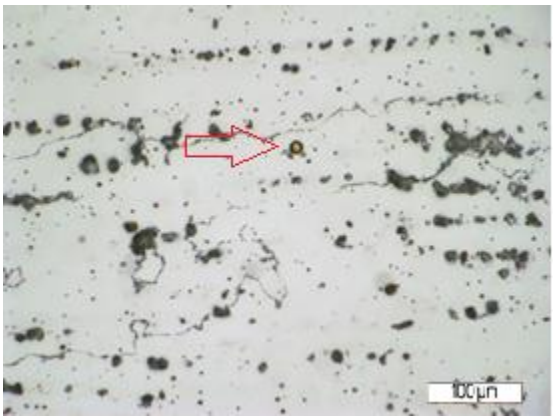

Figure 5.43 Titanium inclusion ENiCrMo-4 weld metal with the addition of Al

Figure 5.44 Titanium inclusion ENCrMo-4 weld metal with additions of Ti

These inclusions are quite small and will not cause any major problem when welding or with the mechanical properties. However, they may become problematic if they occur too often or become too large.

5.5.2 Optical Microscopy of ENiMo-10

Again there was nothing unusual observed in either the macro-structure of the ENiMo-10 weld metal. However, the ENiMo-10 baseline had a small crack in the unalloyed coating that where not observed in any of the samples.

Figure 5.45 Macrostructure of the ENiMo-10 weld metal

Looking at the macrostructure there is the presents of a center line crack which then grew into the bead above it. There were other small micro cracks which were observed in the ENiMo-10 weld metal with the unalloyed coating, illustrated in Figure 5.45

Figure 5.46 ENiMo-10 crack

Figure 5.47 ENiMo-10 slag inclusion and crack

Figure 5.46 illustrated another crack which started from a slag inclusion. Like the ENiCrMo-4 additions of aluminum and titanium in mixes 19 and 20 resulted in titanium

inclusion which became evident once the weld metal was with etched at 6 volts in a solution of 15g CrO_3, 150ml of H_3PO_4, and 20ml H_2SO_4. The inclusion are illustrated in Figures 5.48 and 5.49.

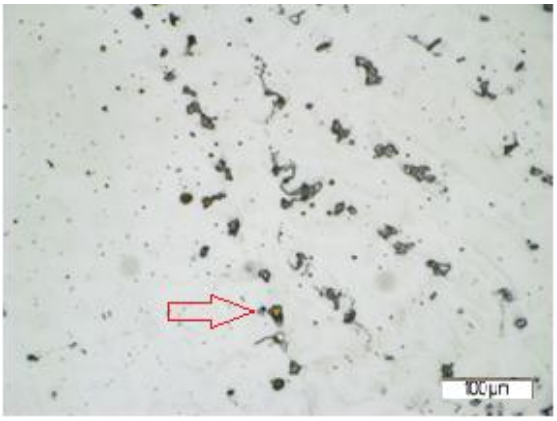

Figure 5.48 Ti inclusion in ENiMo-10 with additions of Al to coating

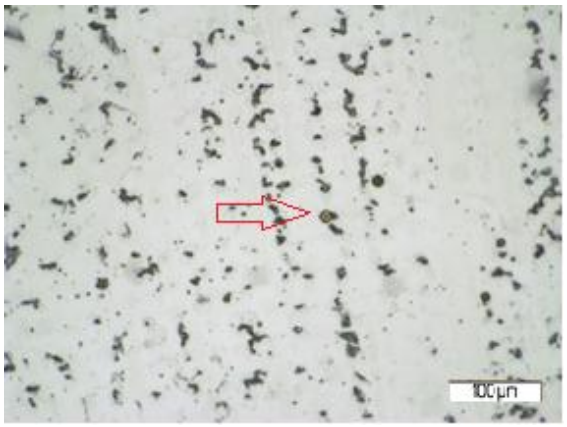

Figure 5.49 Ti inclusion in ENiMo-10 with additions of Ti to coating

5.5.3 SEM and EDS Analysis

A Quanta 200 scanning electron microscope utilizing XEDS was used in combination with the EDAX software in order to look for any gamma prime or other second phases. In the weld metal from the ENiCrMo-4 electrode which was coated with unalloyed flux there was no evidence of gamma prime phase. This was not surprising because the baseline ENiCrMo-4 electrode only had 0.044 wt % titanium and 0.054 wt% aluminum. There was evidence of a second phase which appears to have a higher concentration of molybdenum than the gamma matrix. The composition of the matrix and the precipitate are listed in Table 5.10. The locations of each point that was scanned are illustrated in Figure 5.50.

Mix1	Si	Error	Mo	Error	Cr	Error	Fe	Error	Ni	Error
Matrix 1	1.84	3.36	17.2	1.04	15.9	0.75	6.17	5.61	58.9	0.5
Matrix 2	1.32	3.08	15.9	2.01	14.5	1.48	6.84	2.59	61.3	0.91
Precipitate 3	2.68	3.87	38.8	1.06	14.3	1.42	4.73	3.16	39.5	1.07
OES Bulk	0.14		16.24		14.98		6.20		56.39	

Table 5.10 ENiCrMo-4 EDS results

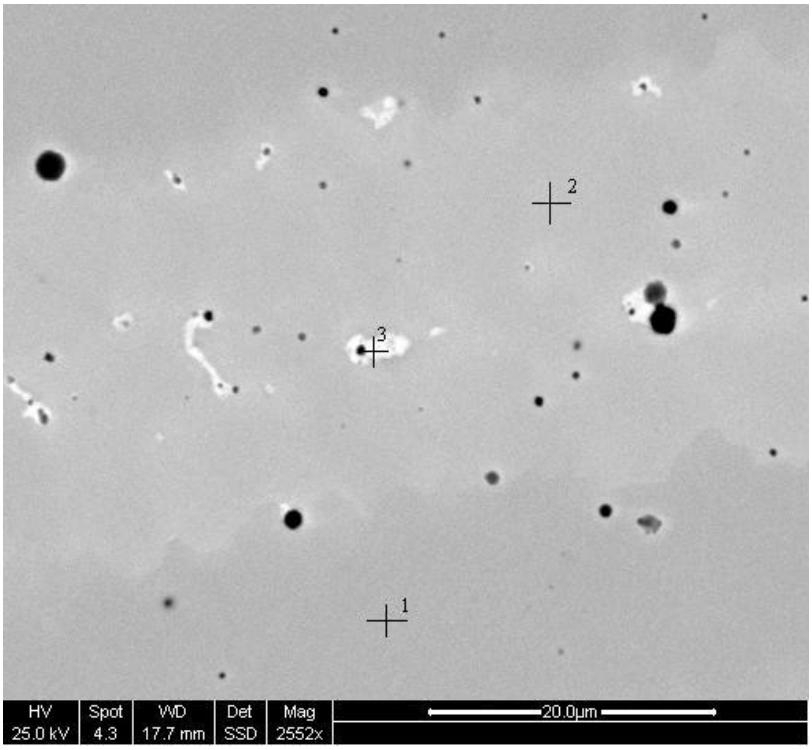

Figure 5.50 XEDS scan of ENiCrMo-4 with unalloyed coating

The process was repeated on the weld metal samples from mix 7 and 8 with similar results. No evidence of gamma prime phase was found and a precipitate which was higher in molybdenum than gamma matrix was obseverveed. The composition of all the percipitates is listed in Table 5.11.

	Si	Error	Mo	Error	Cr	Error	Fe	Error	Ni	Error
Baseline	2.68	3.87	38.8	1.06	14.3	1.42	4.73	3.16	39.5	1.07
5 wt% Al	3.93	1.88	36.6	0.68	14.1	0.87	4.32	2.02	41.1	0.63
5 wt% Ti	3.89	1.75	40.6	0.59	13.8	0.81	4.04	1.96	37.8	0.60

Table 5.11 The compositions of the precipitates in ENiCrMo-4

According to the literature the second phase which is persent at the end of solidifaction is the P phase which is the nueclation site for μ phase. The composition of these percipitates agrees with both the literature (6) and the JMatPro simulations. This is most likely a mixture of P phase and μ phase. Due to the fine scale of these percipitates varification of this would require a SEM which was capible of higher resolutuion.

The Quanta 200 was also used to examine the ENiMo-10 weld metal. The entire sample was examined using XEDS under high magnification. The composition of the only precipitate or second phase observed is listed in Table 5.12 along with the matrix composition of the ENiMo-10 electrode with a unalloyed coating. The locations of the EDS scan are illustrated in Figure 5.51.

	Al	Error	Mo	Error	Cr	Error
Precipitate 1	0.0	0.0	42.73	0.92	1.44	5.49
Matrix 2	0.31	21.96	24.44	1.30	1.15	6.48
Matrix 3	0.16	46.21	32.26	1.10	1.25	6.52
OES Bulk	0.061		31.13		1.27	
	Fe	Error	Ni	Error	Ti	Error
Precipitate 1	1.68	5.20	52.30	0.79	0.20	29.51
Matrix 2	1.97	4.55	70.33	0.68	0.1	55.93
Matrix 3	1.67	5.56	63.36	0.72	0.16	38.62
OES Bulk	1.18		67.40		.042	

Table 5.12 The EDS results for ENiMo-10 weld metal with unalloyed coating

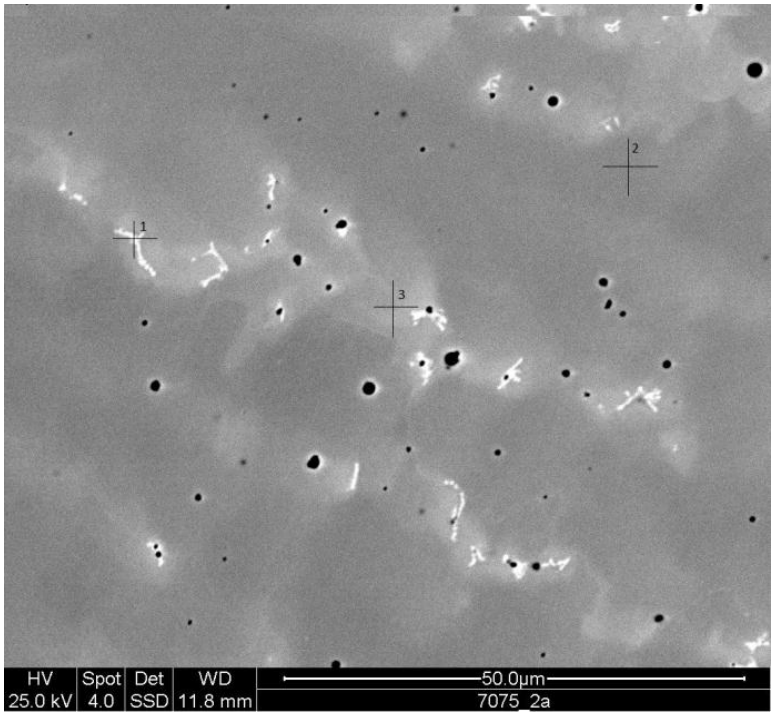

Figure 5.51 XEDS scan of ENiMo-10 with unalloyed coating

All of the precipitates from the ENiMo-10 weld metal are listed in Table 5.13. The terminal solidification sequence of the matching Hastelloy® B-3®was not published in the literature. The precipitates in the ENiMo-10 show elevated levels of molybdenum, but do not match any single phase which is predicted by JMatPro. The precipitates must be some combination of the predicted phases. In order to determine components of these precipitates a scanning electron micro scope which is capable of higher resolution is required.

	Al	Error	Mo	Error	Cr	Error
Baseline	0.0	0.0	42.73	0.92	1.44	5.49
5 wt% Al	0.43	69.03	39.86	4.58	2.13	17.91
5 wt% Ti	0.28	38.57	40.01	1.54	1.52	7.80
	Fe	Error	Ni	Error	Ti	Error
Baseline	1.68	5.20	52.30	0.79	0.20	29.51
5 wt% Al	2.04	20.55	48.71	3.85	0.60	42.69
5 wt% Ti	2.04	8.38	50.76	1.26	0.54	16.71

Table 5.13 The compositions of the precipitates in ENiMo-10

5.6 Tensile Results

Tensile testing is one of the most important tests for the evaluation of the modifications to the flux coating. In addition to the bend and X-ray soundness tests which are required by AWS 5.11. The tensile test is the only test that verifies the strength of the weld metal. The tensile test is an important test because weld strength is the one of the most important properties in the selection of a weld metal. The tensile samples were cut from completely undiluted weld metal see Figure 4.1 and were machined to and tested to the specifications of the AWS. The 0.250 inch round samples were extended a strain rate of 0.25 inches per minute, again within the specifations of the AWS A5.11.

Electrode	Sample #	Alloying Addition	UT (ksi)	Elongation
ENiCrMo-4	1	None	103.98	23.7%
ENiCrMo-4	7	Al	105.44	22.4%
ENiCrMo-4*	8	Ti	109.6	10.6%
ENiMo-10	13	None	92.7	15.0%
ENiMo-10	19	Al	108.0	14.6%
ENiMo-10	20	Ti	112.8	25.8%

Table 5.14 The ultimate tensile strength and elongation of selected electrodes

*Sample number eight had additional cold working due to a malfunction in the tensile testing machine. The test cycle was unintentionally started which stretched the sample upon which the machine then aborted the test and returned the machines jaws to the home position. Observation of the sample showed that the machine applied enough force to the sample to cause plastic deformation. This is evident by the instability of the sample at the yield point which is evident in Figure 5.55. The elongation of this sample is irrelevant due to this occurrence, but the ultimate tensile strength is still valid for comparison purposes only.

The data from the tensile machine was recorded and a plot was made comparing the stress and the strain, which is illustrated in Figure 5.52

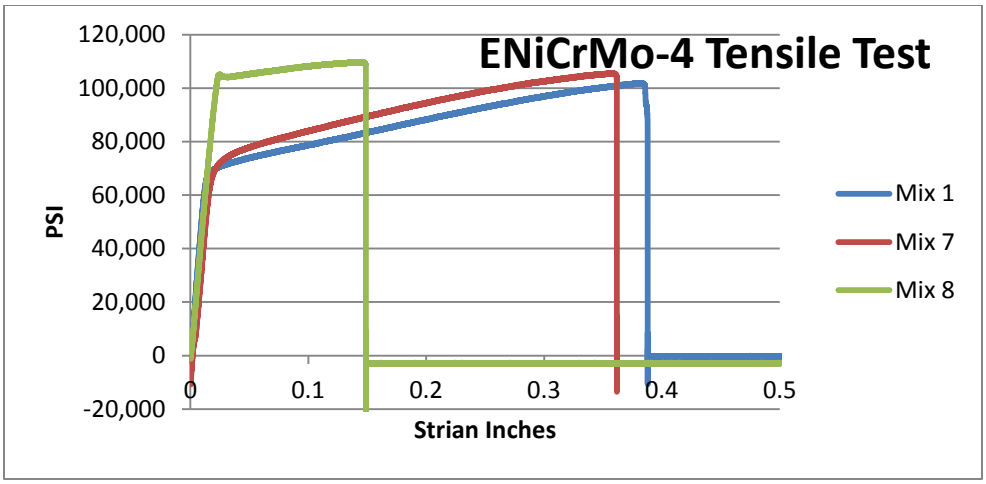

Figure 5.52 Stress VS strain for ENiCrMo-4 electrodes

In the ENiCrMo-4 electrodes the result of the additions of aluminum and titanium caused increases in the ultimate tensile strength and decreases in the elongation or ductility. With the 5wt % additions of aluminum and titanium to samples seven and eight respectively it could be assumed that this was due to the formation of gamma prime phase. However, looking back to the data on the element recovery in section 5.2 and the composition of the weld metal from mix 7 and 8 the aluminum and titanium in these coating formulations add up to more than 0.2 wt% (Al + Ti) in the weld deposit. The low levels in the weld deposit along with the results in section 5.5.3 allude to the fact that the increase in tensile strength was not due to the formation of gamma prime phase.

The test was done in the same manner for the ENiMo-10 electrodes and the plot comparing the stress and strain of the ENiMo-10 weld metal tensile samples is illustrated in Figure 5.53. These tests were performed under the same conditions as the ENiCrMo-4 electrodes. An ENiMo-10 has to meet a minimum requirement of 25% elongation to qualify under AWS A5.11; the baseline composition fell short at only 15% elongation. This is because the baseline coating was missing many of the alloying elements which would normally be added to the coating in a standard ENiMo-10 electrode. The absence of additional deoxidizers causing an increase in oxygen content in the weld metal is the likely cause. The addition of aluminum or titanium will greatly reduce the levels of

oxygen in the weld metal. This is illustrated by mix 20 in Figure 5.53, however the additions of aluminum should have produced similar results, but mix 19 had very poor elongation as well. To explain this, a detailed examination of the chemical composition was made. Mixes 7 and 19 which contained additions of aluminum also have elevated levels of carbon when compared to the other coating iterations. In the literature there were no published reactions in nickel base weld metal between aluminum and carbon which would explain this increase. It is possible that even though the aluminum was considered commercially pure in may have contained a trace amount of carbon which would explain the elevated carbon in the weld metal of mixes 7 and 19. In the ENiMo-10 electrodes the amount of carbon is extremely critical in order to meet the elongation. Mix 19 contained nearly 50 wt% more carbon then mix 20. This increase in carbon also greatly increased the amount of M_6C carbides in the weld metal which resulted in a dramatic loss in ductility.

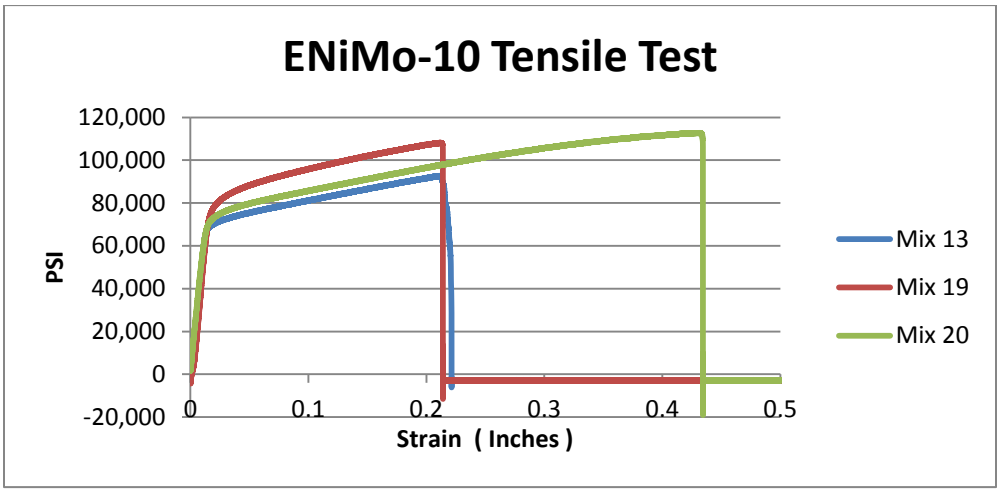

Figure 5.53 Stress VS strain for the ENiMO-10 electrodes

Chapter 6 Conclusions

6.1 Arc Stability

6.1.1

Using histograms to plot the distribution of the welding amps and volts produces a quantifiable way to measure the stability of a SMAW welding arc. Three dimensional plots can be used for visual comparison if there are large amounts of scatter such as in the comparison of the ENiMo-10 and the ENiCrMo-4.

6.1.2

To compare minor variations such as differences in coating composition, statistical tools such as standard deviation can be used. According to this method, additions of aluminum and titanium increase arc stability in both electrodes, with additions of titanium being slightly more effective.

6.2 Recovery of alloying elements added via the flux coating

6.2.1

It can be concluded from this work, which also reaffirms the work of VanBemsta, that alloying additions which are supplied through the flux coating do not have as potent an effect on the weld deposit as alloying elements which are present in the core wire.

6.2.2

It can also be concluded that the percent recovery of alloying elements can be influenced by the addition of other alloying elements. The aluminum and titanium

sacrificially scavenged oxygen in order to protect the other alloying elements which have a lower affinity for oxygen.

6.3 SS DTA solidus temperature measurements

6.3.1

The SS DTA measurements for both electrodes with the unalloyed coatings closely modeled the Scheil simulation for the solidification of the gamma phase and the equilibrium solidus predicted by JMatPro. But, the SS DTA measurements did not show the amount of solidification depression suggested by the formation of all the secondary phases.

6.3.2

The electrodes with aluminum and titanium additions did not follow the same trend as the modeling predicted. This implies that there were additional effects from the coating additions which were not captured in the testing. A possible cause may have been due to the interference from the molten slag. More work is needed to discover the effect of plunging the thermocouple through the molten slag in the SS DTA process.

6.4 Cast pin tear test to rank cracking susceptibility

The cast pin tear test was used to evaluate the ENiCrMo-4 and ENiMo-10 weld metal with three variations of the flux coating. The test revealed that additions of aluminum and titanium increased the cracking susceptibility in both the ENiCrMo-4 and the ENiMo-10, with aluminum affecting the susceptibility slightly more than the titanium. This is due to the additional silicon which was recovered in the weld deposit because of the addition of the deoxidizers. The effects of silicon on solidification cracking has been well documented in the literature.(11, 16, 18, 19, 20)

6.5 Tensile strength with respect to the gamma prime phase

In both the ENiCrMo-4 electrodes and the ENiMo-10 electrodes the ultimate tensile strength was increased by additions of aluminum and titanium. But, no evidence of the gamma prime phase was found in any of the weld metal samples.

Chapter 7 Future Work

7.1 Arc Stability

Further investigation is needed understand how the operation of the electrode will affect the voltage and power histograms. Experiments involving variations in voltage and current variations need to be performed and the results analyzed. This work was limited to two nickel base SMAW electrodes trials need to be conducted with a wide variety of both iron base and nickel base SMAW electrodes before this method can be used to rank SMAW electrodes.

7.2 SS DTA solidus temperature measurements

Comparison work needs to be preform to investigate the effect of plunging the thermocouple through the molten slag into a SMAW weld pool. If this is to be done using automatic SMAW, additional work must be done to eliminate the additional noise caused by the welding arc and the machine.

7.3 Tensile strength with respect to the gamma prime phase

This work revealed that the increase in tensile strength was not due to the formation of gamma prime phase. The reason for this increase is most likely due to a decreased level of oxygen in the weld metal. However, additional testing is needed to verify this; unfortunately all of the sample weld metal was consumed by the cast pin tear testing.

There was an additional anomaly in the ENiMo-10 electrodes which was unexpected. The addition of the deoxidizers should have produced similar results as far as the effect on the elongation. However, the electrode which had a 5 wt % of titanium had a substantial increase in elongation which was not observed in the electrode with 5 wt % aluminum in the coating. The electrode which had the addition of 5 wt % aluminum also had an increase in the amount of carbon which may have led to an increase M6C carbide formation which can reduce the elongation of the weld metal. Further investigation into this anomaly is needed.

References

1) Welding Handbook Volume 2 Welding Processes. Eighth Edition 1991

2) Eagar, T.W. Mitra, U "Slag Metal Reactions during Submerged Arc Welding of Alloy Steels" Metallurgical Transactions A vol 15A 1984 pg 217

3) Jackson C.E. "Fluxes and Slags in Welding" WRC Bulletin 1973

4) AWS A 5.11 2011 Specification for Nickel and Nickel-Alloy Welding Electrodes for Shielded Metal Arc Welding. American Welding Society

5) Haynes Wire Company, "HASTELLOY® B-3® Welding Data" Mountain Home NC

6) Frick, J. Woldman's Engineering Alloys. Ninth Edition 2000 ASM International, Materials Park, Oh 44073

7) Cieslak, M.J. Headley, T.J. Romig, A.D. "The welding metallurgy of Hastelloy alloys C-4 C22 and C276" Metallurgical Transactions A Vol. 17a 1986 pg 2035

8) Turchi P.E.A., Cr-Mo-Ni Phase Diagram, ASM Alloy Phase Diagrams Center, P. Villars, editor-in-chief; H. Okamoto and K. Cenzual, section editors; http://www1.asminternational.org.proxy.lib.ohio-state.edu/AsmEnterprise/APD, ASM International, Materials Park, OH, 2006.

9) Agarwal, D. C. "Nickel Alloy Meet Corrosion Challenges" Advanced Materials & Processes Issue 8 Vol. 159 2001 pg 48

10) Scheil, Erich US patent #3203792 "Highly Corrosion resistant Nickel-Chromium-Molybdenum alloy with improved resistance to intergranular corrosion" 1965

11) DuPont, John N., Lippold, John C., and Kiser, Samuel D. "Welding Metallurgy and Weldability of Nickel-Base Alloys." John Wiley & Sons, Inc. 2009

12) R. B. Leonard, "Thermal Stability of Hastelloy Alloy C-276", Paper No. 35, National Association of Corrosion Engineers, 1968 Cleveland, Ohio

13) Dieter, George E. Mechanical Metallurgy Macgraw Hill 1988

14) Fuchs, G.E. "The strength and stability of super alloys" Sripta Metallurgica vol.19 issue 3 pg 275-278 1985

15) Turchi P.E.A., Ni-Mo Phase Diagram, ASM Alloy Phase Diagrams Center, P. Villars, editor-in-chief; H. Okamoto and K. Cenzual, section editors; http://www1.asminternational.org.proxy.lib.ohio-state.edu/AsmEnterprise/APD, ASM International, Materials Park, OH, 2006.

16) Clausing, R. E. Patriarca, P. Slaughter, G. M. "Welding of Nickel-Molybdenum Alloys" Welding Journal vol. 38 issue 10 pp 393-400 1959

17) Jordan, D. E "Welding of High-Molybdenum nickel-based alloys" Welding in the World 41. 1998 pp 1-9

18) Agarwal, D. C. "Chronological developments in "B" and "C" family nickel alloys (part one)" Stainless Steel World Issue 12 Volume 15 2003 pp 31-37

19) Lienert, T. J., Robino, C. V., Hills, C. R., and Cieslak, M. J. 1990 A welding metallurgy study of Hastelloy alloys B-2 and W, Trends in Welding Research I, ASM International, Material Park, OH, pp 159-165

20) Crook, Paul. Corrosion Resistant Nickel Alloys. Parts 1 – 4. Advanced Materials & Process. June, July, August, and September 2007

21) Lippld, J. C., Clack, W. A. T., and Tumuluru, M. 1992. An investigation of weld metal interfaces. *The Metal Science of Joining*, published by Metals, Minerals and Materials Society, Warrendale,Pa, pp. 141-146

22) Kou, Sindo, *Welding Metallurgy.* Second Edition. Hoboken, NJ: John Wiley & Sons, Inc. 2003

23) Cieslak, M. J., Headley, T. J., Kollie, T., and Romig, A. D. 1998 A melting and solidification study of alloy 625, *Metallurgical Transactions* , 19A: 2319-2331.

24) Cieslak, M. J., Stephens, J. J., and Carr, M. J. 1988. A study of the weldability and weld-related microstructure of Cabot Alloy 214, Metallurgical Transactions A, 19A: 657-667

25) Kou, T. Y., Lee H. T., and Tu, C. C. Evaluation of effects of niobium and manganese additions on nickel base weldments. *Science and Technology of Welding and Joining*, vol 8 No 1 2003

26) DuPont, J. N., Robino, C. V., Marder, A. R., Notis, M. R., and Michael, J. R. 1988. "Solidificatio of Nb-bearing Superalloys: Part I. Reaction Sequences", *Metalurgical and Material transactions A*, 29A: 2785-2796

27) Design, Fabrication, and Welding. The Nickel Institute. http://nickelinstitute.org/NickelUseInSociety/MaterialsSelectionAndUse/DesignFabricationAndWelding

28) Lippold, J. C. Ramirez, A. J. "High temperature behavior of Ni-base weld metal Part I Ductility and microstructural characterization)" Materials Science and Engineering 2004 pp 259-271

29) Ramirez, A. J., Lippold, J. C., "High temperature behavior of Ni-base weld metal Part II - Insight into the mechanism for ductility dip cracking" *Material Science and Engineering* A 380 (2004) pp 245-258

30) Capobianco, T. E., McGee, J. J., Morris, B. W., Penik, M. A., Young, G. A. "The Mechanism of Ductility Dip Cracking in Nickel-Chromium Alloys" The Welding Journal vol.87 issue 2 pp 31s-43s 2008

31) Lippold, J.C. and Nissley, N. E. 2008 Ductility dip cracking in high-Cr Ni-base filler metals, *Hot Cracking Phenomena in Welds II,* Springer, ISBN 978-3-540-78627-6 pp. 409-426

32) Nissley, N.E., Collins, M.G. Guaytima, G., and Lippold, J. C. 2002 Development of the Strain-to-Fracture Test for Evaluating Ductility-Dip Cracking in Austenitic Stainless Steels and Ni-base Alloys, Welding in the world, pp 32-40

33) Thompsom, R.G. and Genculu, S. 1983. "Microstuructual evolution in the HAZ of Inconel 718 and correlation with the hot ductility test," Welding Journal, 62: 337s-346s.

34) Morrison, T. J., Shira, C. S., and Weisenberg, L. A., 1969. The influence of minor elements on alloy 718 weld microfissuring. The Welding Research Council Bulletin, pp. 47-67

35) Lippold, J. C., Koteccki, D. J., Welding Metallurgy and Weldability of Stainless Steels. John Wiley and Sons Inc. 2005

36) Brien, R. E., Legrand, P. E., Pease, G.R., "The Control of Porosity In High-Nickel-Alloy Welds" Welding Journal vol. 37 issue 8 pp 354-360 1958

37) Milner, D. R. "Porosity in Nickel Welded by the Argon-Arc Process" British Welding Journal vol. 3 issue 11 pp 542-545 1956

38) Agarwal, D.C., Hoberg, B "The Fabrication Practices & Impact Of Welding On Corrosion Resistance of High Ni-Cr-Mo Alloys" Corrosion 2006 paper 06208

39) DuPont, J. N. Solidification of an alloy 625 weld overlay. *Metallurgical and Materials Transactions A*, Volume 27, issue 11 (November 1996), p. 3612 - 3620

40) Alexandrov, B.T., Lippold, J.C. A new methodology for studying phase transformations in high strength steel weld metal. *ASM Proceedings of the International Conference: Trends in Welding Research*, v 2005, p 975-980, 2005, *Trends in Welding Research - Proceedings of the 7th International Conference*

41) Electrode Engineering Inc. Archives 1940-2009

42) Alexandrov, B. T., Lippold, J. C., Further Development of the Cast Pin Tear Test for Evaluating Solidification Cracking in Ni-base Alloys. 2011, Hot Cracking Phenomena in Welds III, Part 3, Pages 317-331

43) M. L. Gallagher and John Lippold, Weld Cracking Susceptibility of Alloy C-22 Weld-Metal. 2011, Hot Cracking Phenomena in Welds III, Part 3, Pages 367-391

44) Alexandrov, B. T., Lippold, J. C., Nissley, N. E., Evaluation of Weld Solidifiaction Cracking in Ni-Base Superalloys Using the Cast Pin Tear Test. 2008, Hot Cracking Phenomena in Welds II, Part II, Pages 193-213

45) Chai C.S. Eagar T.W. "Slag-metal equilibrium during Submerged Arc welding" Metallurgical Transactions B vol 12B 1981 pg 539

46) Tanaka J., Element transfer behavior during submerged arc welding. Weld pool Chemistry and metallurgy. The WI Cambridge, UK, 1980, pp 279-288.

47) VanBemsta, "Contribution to the study of slag/metal reactions during the arc welding of nickel and copper base alloys" Weld Pool Chemistry and Metallurgy, Proceedings, International Conference, London Session V, paper 36. 1980 pp 382-383

48) Ellingham, H. J. T. (1944), *J. Soc. Chem. Ind. (London)* 63: 125

49) Natalie, C.A. and Olson, D.L. "Physical and Chemical Behavior of Welding Fluxes." Center for Welding Research, Colorado School of Mines, 1985.

50) Liu, S. " Arc Welding Consumables: Covered and Cored Electrodes - A Century of Evolution." ASM Intl./AWS, Pine Mountain, Georgia, June 1998, and published in "Trends in Welding Research", pp. 505-516, ASM Intl./AWS, August 1999

51) Allen, J. W., Olson, D. L., Frost, R. H. Exothermically Assisted Shielded Metal Arc Welding. The Welding Journal 1998 vol. 77 pp 277- 285

52) Liu, S., Sham, K. "Flux System Optimization for Shielded-Metal Arc Welding Electrodes for High Nickel Alloys" Materials Science and Technology (MS&T) 2008

53) Yakobashvili, S. B., Adhesion of Certain Welding Slags to Nickel-Base Alloys. Svar. Proiz. 1963, No. 4. pp 17-19

54) Barsoum, M. "Fundamentals of Ceramics" McGraw-Hill Materails Science and Engineering Series. 1997

55) Sokolov, Y. and Shordhorov, M. "Modifiled Halide Fluxes Used in the Welding of Nickel Alloys" *Welding Production* issue 3 1961

56) Kang, Daein. "Development Of An Arc Voltage Control Mechanism For Underwater Wet SMAW Process" The Ohio State University. 1996

57) Eduardo Jose´ Lima II, Alexandre Queiroz Bracarense. "Trajectory generation in robotic shielded metal arc welding during execution time" Industrial Robot: An International Journal vol. 36 November 1 2009 pp 19-26

58) Chen, B., Han, F., Huang, Y., Lu, K., Liu, Y., Li, L., "Influence of Nanoscale Marble (Calcium Carbonate $CaCO_3$) on Properties of D600R Surfacing Electrode" Materials Science and Technology, Pittsburgh Pennsylvania 2008

59) Mil-E-22000G. Military Specification Electrodes, Welding, Covered: General Specification For. 1989 AMSC

60) Carter, D., Reinnmuller, M., Tomich, B. Effect of Welding Power Supply Design on SMWA Weld deposits. OSU Welding Engineering Capstone Project 2010